



Republic of Iraq
Ministry of Higher Education and Scientific
Research
University of Kerbala /College of Medicine
Department of Chemistry and Biochemistry



The role of some biomarkers in evaluation of renal tubular damage in patients with autosomal dominant polycystic kidney disease

A thesis

Submitted to the Council of the College of Medicine, University of Kerbala, in Partial Fulfillment
of the Requirements for the Degree of Master in Clinical Chemistry and Biochemistry

By

Ayat Khidhir Ali

B.Sc. Chemistry sciences/ University of Karbala (2019-2020)

Supervised By

Assist Prof. Dr. Rana Majeed Hameed

Ph.D. Biochemistry

Department of Biochemistry

College of Medicine - University of
Kerbala

Prof. Dr. Riyadh Muhi Abbood Al-Saegh

Professor of Nephrology and Kidney
Transplantation

Department of Internal Medicine

College of Medicine - University of
Kerbala

2024 A.D

1446 A.H.

بِسْمِ اللَّهِ الرَّحْمَنِ الرَّحِيمِ

وَكَيْفَ تَصْبِرُ عَلَىٰ مَا لَمْ تُحِطْ بِهِ خَيْرًا

{68}

صدق الله العلي العظيم

سورة الكهف - الآية 68

Supervisor's Certification

We certify that this thesis " **The role of some biomarkers in evaluation of renal tubular damage in patients with autosomal dominant polycystic kidney disease** " was prepared under our supervision at the Department of Biochemistry, College of Medicine /University of Kerbala, in a partial fulfillment of the requirement for the Master degree in Clinical Chemistry.



Assist. Prof.

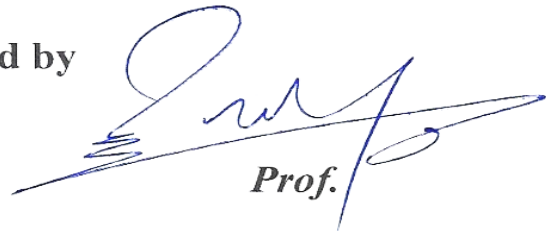
Dr. Rana Majeed Hameed

Ph.D. Biochemistry

Department of
Biochemistry

College of Medicine

Supervised by



Prof.

Dr. Riyadh Muhi Abbood Al-Saegh

Professor of Nephrology and Kidney
Transplantation
Department of Internal Medicine
College of Medicine
University of Kerbala

In view of the available recommendation, I forward this M.Sc. thesis for debate by the examining committee.



Assist. Prof.

Dr. Atheer Hamid Al-Ghanimi

Head of Chemistry Department

College of Medicine

University of Kerbala

/ / 2024

Examining Committee Certification

We, the examining committee certify that we have read this M.Sc. thesis entitled: **(The role of some biomarkers in evaluation of renal tubular damage in patients with autosomal dominant polycystic kidney disease)**

We have examined the postgraduate student **(Ayat Khidhir Ali)** in it M.Sc. thesis content and in our opinion, it meets the standard for the master degree in

(Clinical Chemistry)

Signature: 

Assist. Prof. Dr. Suzanne Jubair Abass
College of pharmacy
University of kerbala
Date: 17/9 /2024
(Member)

Signature: 

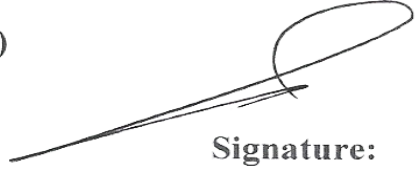
Lecturer dr. Ammar Gany Yassin
College of medicine
University of kerbala
Date: / /2024
(Member)

Signature : 

Assist. Prof. Dr. Rana Majeed Hameed
College of Medicine
University of kerbala
Date: / /2024
(Member/Supervisor)

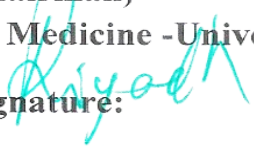
Signature: 

Prof. Dr. Riyadh Muhi Al-Saegh
College of Medicine
University of Kerbala
Date: / /2024
(Member/Supervisor)

Signature: 

Assist. Prof. Dr. Haider Abd Jabbar Alammar
College of Medicine
University of Al-Qadisiyah
Data: / /2024
(Chairman)

Approved by the College of Medicine -University of Kerbala

Signature: 

Prof. Dr. Riyadh Dayhood Al-Zubaidi
Dean of the College of Medicine

DEDICATION

To the experiences we never expected, and the paths that were redirected. To myself who faced all this. To the friends and family we found along the way.

Acknowledgments

First, and above all, thanks to the Great Merciful Allah who gives me health, strength, patience and perseverance and facilitated the ways for me to accomplish this work.

also, I would like to thank the autosomal dominant polycystic kidney disease (ADPKD) patients for their cooperation and all staffs in the research laboratory of the Department of Chemistry and Biochemistry, College of Medicine, University of Kerbala. Additionally, I would like to thank the medical staffs in the laboratories of “, Al Hasan Al-Mujtaba Teaching Hospital ,and Al-Saegh Center for Nephrology and Kidney Transplantation” , Karbala health directorate, without their precious support it would not be possible to conduct this research.

In addition, I would like to express my sincere gratitude to my supervisor Dr. Rana Majeed Hameed professor of biochemistry, Department of Chemistry and Biochemistry, College of Medicine, University of Kerbala for her continuous support, patience, motivation, Reassurance, and immense knowledge. Her guidance helped me in all the time of my research and writing of this thesis. I couldn't have imagined having a better advisor and mentor for my M.Sc. study.

Special thanks then go to my supervisor Dr. Riyadh Muhi Abbood Al-Saegh, professor of nephrology and kidney transplantation, College of Medicine, University of Kerbala for his support in patients collection, suggestion, support, guidance, encouragement.

Thanks are due to Dean Prof. Dr. Riyadh Dayhood Al-Zubaidi Dean the College of Medicine ,University of Kerbala, and Assist. prof. Dr. Atheer Hameed Odda Head of the Department of Chemistry and Biochemistry.

Moreover, I would like to express my deep thanks to Prof. Dr. Fadhil Jawad Al-Tu'ma, Dr. Maher Abbood Mukheef for their valuable help and advice.

Ayat

Summary

PKD is a disorder characterized by the development of numerous bilateral kidney cysts. Cyst growth plays an important role in autosomal dominant polycystic kidney disease progression, and the degree of compression that enlarging cysts exert on the neighboring renal tubules may upregulate *kidney injury molecule 1* (KIM-1) expression. Urinary KIM-1 may therefore signal a higher risk of kidney disease progression in ADPKD. *chitinase 3-like protein 1* (CHI3L1) is highly expressed in healthy kidney tissue and is freely filtered by the glomerulus. CHI3L1 is also secreted by activated macrophages in the kidney upon stress or damage. *Neutrophil gelatinase-associated lipocalin* (NGAL) from tubular epithelial cells occurs following damage. The level of NGAL expression correlates with the degree of kidney injury and may help to discriminate patients who are at higher risk of faster decline in kidney function. New prognosis markers need to be developed, either alone or in combination with conventional markers, which can predict the rate of disease progression in ADPKD, therefore, the main aim was to determine whether serum tubular & proximal damage and inflammation markers have association with progression of polycystic kidney patients or not.

A cross-sectional study included eighty-five participants aged between 7 and 84 years. All patients were diagnosis with ADPKD progression was expressed as changes in their GFR or total kidney volume (htTKV). The study was conducted at the Al-Hassan Al-Mujtaba teaching hospital & Al-Saegh Center for Nephrology and Transplantation outpatient clinics in Karbala city from September / 2023 to August / 2024. At baseline, inflammatory (Neutrophil gelatinase-associated lipocalin (NGAL)), and tubular damage markers (Kidney Injury Molecule-1 (KIM-1), and Chitinase Levels) were measured in serum using enzyme-linked immunosorbent assay (ELISA), while the serum lipid profile was analyzed using

an Abbott Laboratories device. Mean differences analyses were performed to assess the biomarkers with ADPKD and progression. The efficiency of the predicting value was assessed using the receiver operating characteristic (ROC) curve. The mean KIM-1 level progressively increases across GFR stages, with the highest level observed in G4 (4.3 ± 1.5) and the lowest in G1 (1.7 ± 0.5). This suggests a potential association between higher KIM-1 levels and more severe kidney dysfunction (lower GFR). Similar to KIM-1, NGAL shown that the highest level was in G4 (5.2 ± 2.6), but there is a substantial drop to G3b (1.8 ± 0.6). For CHI3L1, results were shown that the levels appear to be relatively increased across all GFR stages (around 1.7 - 4.7). Both KIM-1 and NGAL have good AUC values, indicating reasonable overall performance in discriminating between patients with stage 4 CKD among ADPKD. NGAL has a slightly higher AUC (80.5%) compared to KIM-1 (79.1%). NGAL has a higher sensitivity (71.4%) than KIM-1 (57.1%). This means NGAL is more likely to correctly identify patients with stage 4 CKD in ADPKD. While KIM-1 has a much higher specificity (99%) compared to NGAL (91%). Specificity indicates the likelihood of correctly identifying patients without stage 4 CKD in ADPKD. Both KIM-1 and NGAL could be valuable tools for monitoring kidney function in ADPKD patients, particularly as GFR declines. By tracking changes in KIM-1 and NGAL levels, healthcare professionals might gain insights into the progression of kidney damage in ADPKD. While CHI3L1 might have some utility, a weaker association with GFR in ADPKD suggests it might be less suitable for monitoring kidney function in this specific context.

List of content

List of content:

Summary	I-II	
List of contents	III- VI	
List of tables	VII-VIII	
List of figures	IX-X	
List of Abbreviation	XI-XII	
Chapter One: Introduction and Literature Review		
Subject number	Subject	Page
1	Introduction	1
1.1	Polycystic Kidney Disease	1
1.2	Types of Polycystic Kidney Disease	1
1.3	Epidemiology	2
1.4	Autosomal Dominant Polycystic Kidney Disease	3
1.5	Pathophysiology of autosomal dominant polycystic kidney disease	3
1.6	ADPKD Proteins: Structure and Functions	4
1.7	Mechanism of Cyst Formation	7
1.8	Diagnosis and screening of autosomal dominant polycystic kidney disease	13
1.9	Treatment of autosomal dominant polycystic kidney disease	15
1.10	Progression Biomarkers of ADPKD	16
1.10.1	Proximal Tubular Damage Marker	18
1.10.2	Distal Tubular Damage Marker	21

List of content

1.10.3	Marker of progression of Kidney Inflammation	23
1.11	Knowledge Gap	28
1.12	Aims of the study	29
Chapter Two: Subjects, Materials and Methods		
Subject number	Subject	Page
2	Subjects, Materials and Methods	30
2.1	The study Design	30
2.2	Ethical approval	30
2.3	Blood Sample Collection and Storage	30
2.4	The Sample Size	31
2.5	Inclusion criteria	32
2.6	Exclusion criteria	32
2.7	Diagnostic Criteria for ADPKD	32
2.8	Ultrasound criteria for htTKV measurement	33
2.9	Ultrasound Diagnostic Criteria for ADPKD TKV, and htTKV	34
2.10	Measurement of Kidney Cysts and Biomarker Levels	35
2.11	Measurement of eGFR	36
2.12	Classification of eGFR and Biomarker Measurement.	36
2.13	Patient Evaluation	38
2.14	Measurement of the Body Mass Index Group	38
2.15	Measurement of the Atherogenic Indices	39

List of content

2.16	The Materials & Tools	40
2.17	The Laboratory Kits	42
2.18	The Instruments	42
2.19	The Methods	43
2.19.1	Measurement of Serum Cholesterol	43
2.19.2	Measurement of Serum Triglyceride	44
2.19.3	Measurement of Serum High-Density Lipoprotein	45
2.19.4	Measurement of Serum Very Low-Density Lipoprotein-Cholesterol	46
2.19.5	Measurement of Serum Low-Density Lipoprotein-Cholesterol	46
2.19.6	Determination of Serum Creatinine Level	46
2.19.7	Determination of Serum Urea Level	47
2.19.8	Measurement of Serum CHI3L1	49
2.19.9	Measurement of Serum KIM 1	53
2.19.10	Measurement of Serum NGAL	58
2.20	Statistical Analysis	62
Chapter Three: Results and discussion		
Subject number	Subject	Page

List of content

3	Results and Discussion	63
3.1	Demographic of patients group with (ADPKD)	63
3.2	Medical history of the study group	65
3.3	Study the Kidney Characteristics ADPKD	68
3.4	Study of Lipid Profile in ADPKD	72
3.5	Study the Atherogenic Indices in ADPKD	73
3.6	Study the Kidney damage Biomarkers in ADPKD	76
3.7	Study the Kidney damage Biomarkers based on the eGFR Stage in ADPKD	81
3.8	Study the Kidney damage Biomarkers based on Left Kidney cyst Size in ADPKD	85
3.9	Study the Kidney damage Biomarkers by Right Kidney Cyst Size in ADPKD	88
3.10	Receiver operating characteristics (ROC) curve	92
	conclusions	103
	Recommendations	103
	Future work	103
	References	Page
	References	104
	Appendixes	

List of Tables

List of Tables:

No.	Title	Page
1-1	Ultrasound-based criterion for the diagnosis or exclusion of ADPKD	14
2-1	BMI WHO classification	38
2-2	The Materials, Tools, and Their Suppliers used in This Study	41
2-3	The Laboratory kits used in this study	42
2-4	Instruments and tools used in this study	42
2-5	Reactive ingredients of serum creatinine level (Abbott, USA).	47
2-6	Reactive ingredients of serum urea level (Abbott, USA).	48
2-7	Serial dilution of Standard CHI3L1	50
2-8	The standard curve of Human CHI3L1	52
2-9	Serial dilution of Standard KIM 1	54
2-10	The standard curve of Human KIM 1	57
2-11	Serial dilution of Standard NGAL	59
2-12	The standard curve of Human NGAL	61
3-1	Demographic characteristic of the study group	64
3-2	Medical history among 85 patient with Autosomal Dominant Polycystic Kidney Disease (ADPKD)	67
3-3	Categories of patients based on their htTKV	69
3-4	The relation between eGFR and normal, increased ,and decreased htTKV	71
3-5	Mean \pm Standard deviation of the lipid profile of the studied patients	72

List of Tables

3-6	Mean differences of atherogenic indices Levels among the studied patients	74
3-7	Mean differences of KIM-1, NGAL and CHI3L1 Levels among the studied patients	78
3-8	Mean differences of KIM-1, NGAL and CHI3L1 Levels among the studied patients of ADPKD based on their sex	78
3-9	Mean differences of KIM-1, NGAL and CHI3L1 Levels among the studied patients of ADPKD based on their GFR.	82
3-10	Mean differences of KIM-1, NGAL and CHI3L1 Levels among the studied patients of ADPKD based on their the largest size of Left Kidney cysts	86
3-11	Mean differences of KIM-1, NGAL and CHI3L1 Levels among the studied patients of ADPKD based on their largest size of right Kidney cysts	89
3-12	AUC, optimal threshold, Sensitivity and specificity of KIM-1 and NGAL levels for predicting stage 4 of CKD among the studied patients of ADPKD	93
3-13	AUC, optimal threshold, Sensitivity and specificity of KIM-1 and NGAL levels for predicting stage 3 of CKD among the studied patients of ADPKD	96
3-14	AUC, optimal threshold, Sensitivity and specificity of CHI3L1 levels for predicting stage 3 of CKD among the studied patients of ADPKD	98
3-15	AUC, optimal threshold, Sensitivity and specificity of KIM-1 and ,NGAL levels for predicting stage 2 of CKD among the studied patients of ADPKD	100

List of figures:

List of figures:

No.	Title	Page
1-1	Structures of polycystin-1 and polycystin-2	6
1-2	Broad routes that contribute to the development of PKD	9
1-3	Diagrammatic representation of the beginning and development of cyst formation	10
1-4	Biomarkers in various nephron segments	17
1-5	structure of KIM-1	19
1-6	Human and mouse CHI3L1 crystal structures.	22
1-7	Crystal structure of NGAL	24
1-8	Molecular structure of NGAL	25
2-1	Flow chart of study design	37
2-2	Serial dilution of Standard CHI3L1	51
2-3	The standard curve of Human CHI3L1	53
2-4	Serial dilution of Standard KIM 1	55
2-5	The standard curve of Human KIM 1	57
2-6	Serial dilution of Standard NGAL	59
2-7	The standard curve of Human NGAL	61
3-1	Mean Differences of the eGFR in patients groups of ADPKD based on their height adjusted total kidney volume.	71
3-2	Violin boxplot to demonstrated the density of Lipid profile Levels among the studied patients	73
3-3	Violin boxplot to demonstrated the density of atherogenic indices among the studied patients	74
3-4	Mean differences of (KIM-1), (NGAL) and (CHI3L1) Levels among the studied patients of ADPKD based on their sex	79

List of figures:

3-5	Mean differences of (KIM-1), (NGAL) and (CHI3L1) Levels among the studied patients of ADPKD based on their (GFR)	83
3-6	Mean differences of (KIM-1), (NGAL) and (CHI3L1) Levels among the studied patients of ADPKD based on their largest size of Left Kidney cysts	87
3-7	Mean differences of (KIM-1), (NGAL) and (CHI3L1) Levels among the studied patients of ADPKD based on their largest size of right Kidney cysts	90
3-8	ROC curves for KIM-1 and NGAL among the studied patients of ADPKD to analyze the optimal diagnostic points for predicting disease progression (stage 4) based on the eGFR.	94
3-9	ROC curves for KIM-1 and NGAL among the studied patients of ADPKD to analyze the optimal diagnostic points for predicting disease progression (stage 3) based on the eGFR	97
3-10	ROC curves for CHI3L1 among the studied patients of ADPKD to analyze the optimal diagnostic points for predicting disease progression (stage 3) based on the eGFR	99
3-11	ROC curves for KIM-1 and NGAL among the studied patients of ADPKD to analyze the optimal diagnostic points for predicting disease progression (stage 2) based on the eGFR	101

List of Abbreviation:

List of Abbreviation:

Abbreviation	Meaning
AC	Atherogenic coefficient
ADPKD	Autosomal dominant polycystic kidney disease
AIP	Atherogenic index of plasma
AKI	Acute kidney injury
ARPKD	Autosomal recessive polycystic kidney disease
BMI	Body Mass Index
cAMP	Cyclic adenosine monophosphate
CHI3L1	Chitinase-3-like protein 1
C-index	Cholesterol index
CKD	Chronic kidney disease
Cr	Creatinine
CRI-I	Castelli's risk index 1
CRI-II	Castelli's risk index 2
eGFR	Estimated glomerular filtration rate
ELISA	Enzyme linked immune sorbent assay
ER	Endothelium reticulum
ESKD	End-stage kidney disease

List of Abbreviation:

HDL	High-density lipoproteins
HtTKV	Height adjusted total kidney volume
KIM 1	kidney injury molecule-1
LDL	Low-density lipoproteins
NGAL	Neutrophil gelatinase-associated lipocalin
O.D	Optical density
PC1	polycystin-1
PC2	polycystin-2
PKD	Polycystic kidney disease
PKD1	polycystic kidney disease 1
PKD2	polycystic kidney disease 2
ROC	Receiver operating characteristics
SD	Standard deviation
TG	Triglyceride
TKV	Total kidney volume
TRPP	Transient Receptor Potential channel
VLDL	Very-low-density lipoproteins

Chapter one

Introduction

And

Literature review

1. Introduction

1.1 Polycystic kidney disease.

Polycystic kidney disease (PKD) is a condition where numerous fluid-filled sacs (cysts) develop in the kidneys. The most common form, called autosomal dominant polycystic kidney disease (ADPKD), is inherited. These cysts grow gradually over time. As they enlarge, they damage healthy kidney tissue. This progressive decline in kidney function can eventually lead to permanent kidney failure (Schirrer, 2021).

1.2 Types of Polycystic Kidney Disease

There are two main types of pol PKD distinguished by how they are inherited from parents: Autosomal dominant PKD (ADPKD) and Autosomal recessive PKD (ARPKD) (Horie, 2016), both linked to problems with tiny structures in cells called cilia. The ADPKD type is the more common. It often shows up in adults, even though people are born with the faulty gene. ARPKD is a less frequent but more serious type.

Both types involve the development and uncontrolled growth of fluid-filled cysts in the kidneys. This progressive cyst growth damages the kidneys and reduces their function over time. While the main problem is in the kidneys, these can be severe "multisystem" disorders, meaning they can affect other organs as well. (Vasileva, 2021) The main difference between ARPKD and ADPKD is that ARPKD is a recessive condition. It needs two copies of the faulty gene (one from each parent) to develop the disease. while ADPKD is a dominant condition. only need one copy of the faulty gene (from one parent) to develop the disease. Even though both diseases involve cyst formation in kidneys and livers due to abnormal genes, the way they're

inherited and the timing/location of cyst development differ significantly. (Besse, 2020).The ADPKD and ARPKD, are the top genetic culprits for adult and childhood kidney problems, respectively. Mutations in two genes, PKD1 and PKD2, are responsible for ADPKD. These genes create proteins called polycystin-1 (PC1) and polycystin-2 (PC2) that work together in structures on cells called primary cilia. Most ARPKD cases stem from mutations in the polycystic kidney and hepatic disease 1 (PKHD1) gene, which codes for the protein Fibrocystin/Polyductin (FPC). This protein plays a crucial role in kidney function. In a smaller number of ARPKD cases, mutations in the DAZ interacting zinc finger protein 1 like (DZIP1L) gene are the cause. (Ma, 2021)

1.3 Epidemiology

ADPKD is one of the most frequent genetic kidney diseases. It affects an estimated 1 in every 1,000 to 2,500 people. (Cornec-Le Gall, 2019). It's important to note that the prevalence of ARPKD is actually much lower than 1:20,000 in Europe. (Bergmann, 2018) The most common monogenic cause of end stage kidney disease (ESKD) is ADPKD (Lanktree, 2021) about 4%–10% of ESKD worldwide. (avu, 2020) and about 50% of the cases going hidden (undiagnosed) through the population.

1.4 Autosomal dominant polycystic kidney disease

The ADPKD is a genetic disorder passed down through families, and is a major reason for ESKD in the United States. It can cause high blood pressure (hypertension), progressive chronic kidney disease (CKD), and scarring (fibrosis) in the kidneys (Colbert, 2020). Even though ADPKD primarily targets the kidneys, it's a systemic disease because the proteins involved (polycystins) are present in many tissues throughout the body (Reiterová, 2022).

Cystogenesis begins in specific locations within the kidney tubules, often even before birth (in utero) (Cornec-Le Gall, 2019). In severe cases, ADPKD can eventually lead to ESKD, where the kidneys can no longer function on their own. Up to 70% of people with ADPKD will reach this stage by age 70 (Neumann, 2013), About 10% of patients in dialysis and transplantation programs are ADPKD patients. (Spithoven, 2014)

1.5 Pathophysiology of autosomal dominant polycystic kidney disease

Cysts gradually grow due to abnormal cell proliferation, fluid secretion and production of extracellular matrix. Glomerular filtration rate remains normal for years because of maladaptive glomerular filtration in the remaining nephrons. Some patients suffer from chronic pain because of cyst enlargement, acute pain can be caused by cyst infection or colic pain by nephrolithiasis. Arterial hypertension is present in 75% of patients with normal renal function from an early age. Cyst expansion is associated with intrarenal ischemia leading to the activation of renin-angiotensin-aldosterone system. On the other hand, angiotensin contributes to cyst expansion, increases oxidative stress, tubulointerstitial fibrosis, endothelin and

sympathetic activity. Increased left ventricle mass was reported even in young normotensive ADPKD patients which is associated with higher cardiovascular mortality. ADPKD is a systemic disease because polycystins are expressed in many tissues. The systemic and multi-organ nature of ADPKD manifests by the occurrence of cysts in extra-renal organs such as the liver, pancreas and spleen, as well as by other affected organs such as cardiovascular abnormalities and brain vessel aneurysms. Polycystic liver disease is the most common extra-renal comorbidity accompanying ADPKD. Cyst volume of liver is frequently higher in females after multiple pregnancies and/or use of hormonal replacement therapy. The abnormality of connective tissues can be associated with hernias, diverticulosis and heart valve abnormalities in ADPKD patients. (Reiterová, 2022)

1.6 Autosomal dominant polycystic kidney disease proteins: structure and functions

The PKD1 and PKD2 genes, while crucial for preventing cysts in ADPKD, also play a broader role in cellular functions. Structures of polycystin-1 and polycystin-2 was presented in Figure (1.1), are involved in regulating important processes within cells, Such as Fluid movement (transport) across cell membranes, Cell development (differentiation), Cell growth (proliferation), Cell death (apoptosis), Cell attachment (adhesion). (Reiterová, 2022). The PKD1 gene creates a large protein called PC1 that sits on the outer surface of the cell membrane (plasma membrane). The PC1 has a long, extended part that reaches outside the cell (extracellular domain). Scientists believe PC1 might act like a special type of receptor that interacts with molecules outside the cell and triggers responses inside (atypical G protein-coupled receptor). PKD2 gene produces PC2, a protein that acts as a

channel for ions (charged particles) to flow across cell membranes. The PC2 belongs to a larger family of ion channels called Transient Receptor Potential (TRPP) channels. (Hardy, 2020).The PC1 is like a potential docking station for a molecule, It has three key structural regions, the N-terminal domain, the 11 transmembrane domains and the C-terminal domain. (Wilson, 2004),The PC2,is also known as TRPP2, shares similarities with other proteins in the Transient Receptor Potential (TRP) channel family. Both PC2 and TRP channels are constructed with six transmembrane segments, which act like anchors that hold them within the cell membrane. A special loop domain separates the first two transmembrane segments. This loop is crucial for forming a passage (pore) that allows ions to flow through the channel. Both PC2 and TRP channels have N-terminal and C-terminal domains at their ends, located inside and outside the cell respectively. These terminal domains can interact with other molecules and play a role in channel function. (Hofherr, 2011)

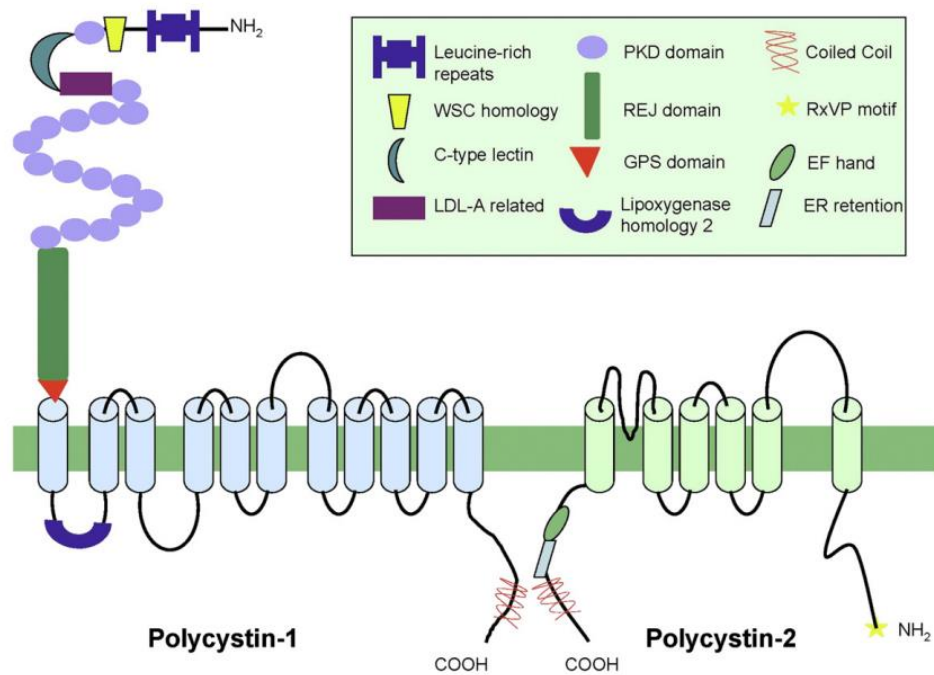


Figure (1.1) Structures of polycystin-1 and polycystin-2. (Gallagher, 2010)

WSC: water soluble concentrate, LDL-A: low density lipoprotein-A, PKD: polycystic kidney disease, REJ: receptor for egg jelly, GPS: G protein-coupled receptor proteolytic site, EF: a motif that consists of an α -helix “E,” a loop that may bind calcium, and a second α -helix “F”, ER: endoplasmic reticulum.

The membrane bilayer is shown by the thick green line. The boxed figure caption lists the protein motifs. The cylinders that are light blue and green are thought to be transmembrane segments. The size of structures is not depicted. (Gallagher, 2010)

Cyst development occurs only in 1-4 percent of tubes due to deficiencies in the proteins polycystin-1 and polycystin-2. Unfortunately, the condition often advances to ESKD. This is mostly due to the mechanism of compression/obstruction of the interstitial tissue and surrounding tubular structures, which results in ischemia, inflammation, and progressive fibrosis. (Halvorson, 2010). A clear link between disruption of polycystin function and hypertension is suggested by the expression of PC1 and PC2 in vascular smooth muscle and endothelium, as well as heightened vascular smooth muscle contractility and reduced endothelium-dependent vasorelaxation in ADPKD. (Johnson, 2014) Although expressed in the proximal tubules, PC1 and PC2 are more noticeable in the collecting ducts and distal tubule. (Ong, 1999) .Transmembrane proteins called polycystins combine to produce a nonselective, Ca^{2+} permeable cation channel that may play a role in epithelial differentiation of ductal structures and the preservation of intracellular Ca^{2+} homeostasis. (Blazer-Yost, 2020)

1.7 Mechanism of cyst formation:

Cysts are thought to be clonal (formed from a single cell), originating from cells with heterozygous germline mutations that are inherited and in which (1) a somatic mutation renders the remaining normal allele inactive (two-hit model), (Pei, 2001) or (2) an as-yet-unidentified non-genetic factor that lowers the PKD protein's function or quantity below a threshold that is crucial (threshold model) (Rossetti, 2009) According to a "threshold mechanism" that has been hypothesized, the cystogenic process of clonal growth is initiated when PC levels within a particular tubular epithelial cell drop below a crucial level (10 to 30 percent). (Lanktree, 2021)

Disease pathobiology has been informed by genetic studies from patients and animal models, which strongly support a "threshold model" in which somatic mosaicism, germline and somatic PKD1 and/or PKD2 mutations, gene mutations in the endoplasmic reticulum protein biosynthetic pathway, or reduced functional polycystin dosage below a critical threshold within individual tubular epithelial cells are the trigger for cyst formation. (Lanktree, 2021) The majority of cases are caused by mutations in either of the two genes, PKD1 or PKD2, which code for proteins thought to be part of a receptor/channel complex. According to studies, cyst initiation is caused by a loss of complex function below an unknown threshold. This leads to the deregulation of several metabolic processes and downstream pathways, which in turn causes the cyst to expand. (Jiahe, 2023) A mutant cell will finally begin to proliferate when PC1/PC2 function in an epithelial cell along the nephron falls below threshold. Rather of congealing into a solid ball of cells, this clonal growth will begin as an out pouch from the tubule surrounded by a single layer of mutant cells, which will eventually split off to create a cyst (Jiahe, 2023), the routes that contribute to the development of PKD was presented in Figure (1.2) & the development of cyst formation was presented in Figure (1.3)

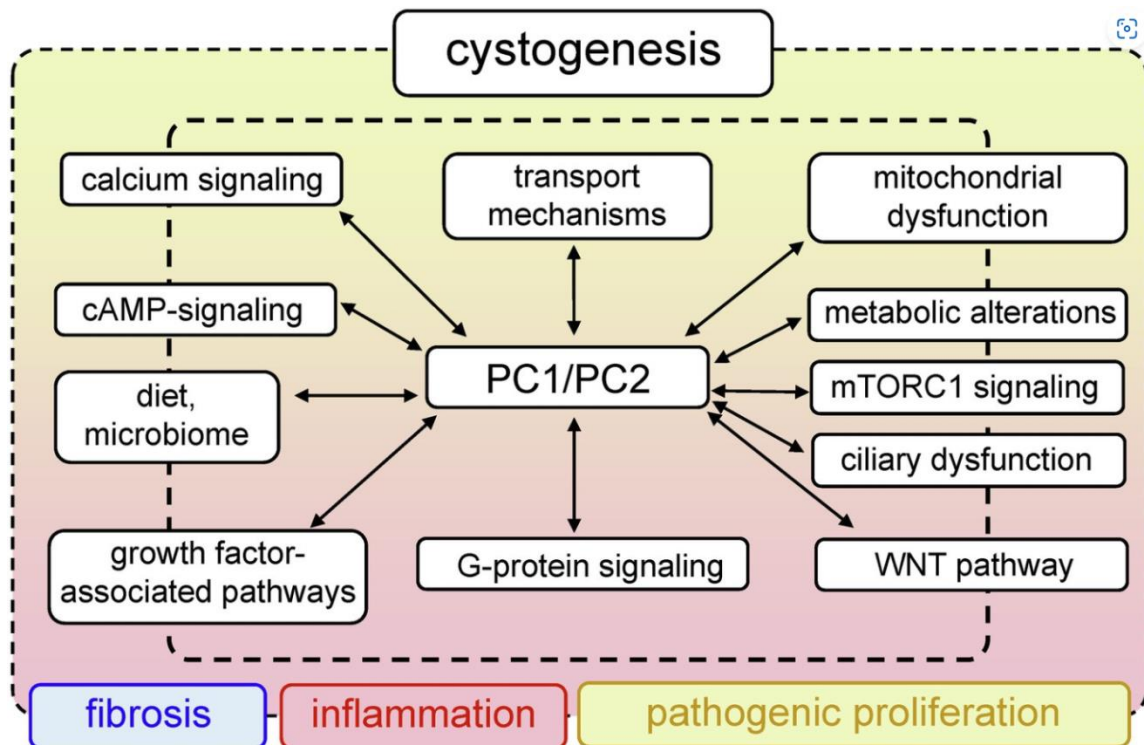


Figure (1.2). Broad routes that contribute to the development of PKD. (Vasileva, 2021). A number of interrelated signalling pathways work abnormally when PKD1/PKD2 mutations occur, and this can cause aberrant proliferation, fibrosis, and inflammation that accompany cystogenesis (Vasileva, 2021). Camp: cyclic adenosine monophosphate, PC1: polycystin-1, PC2: polycystin-2, mTORC1: mammalian target of rapamycin complex 1, WNT: Wingless-related integration site.

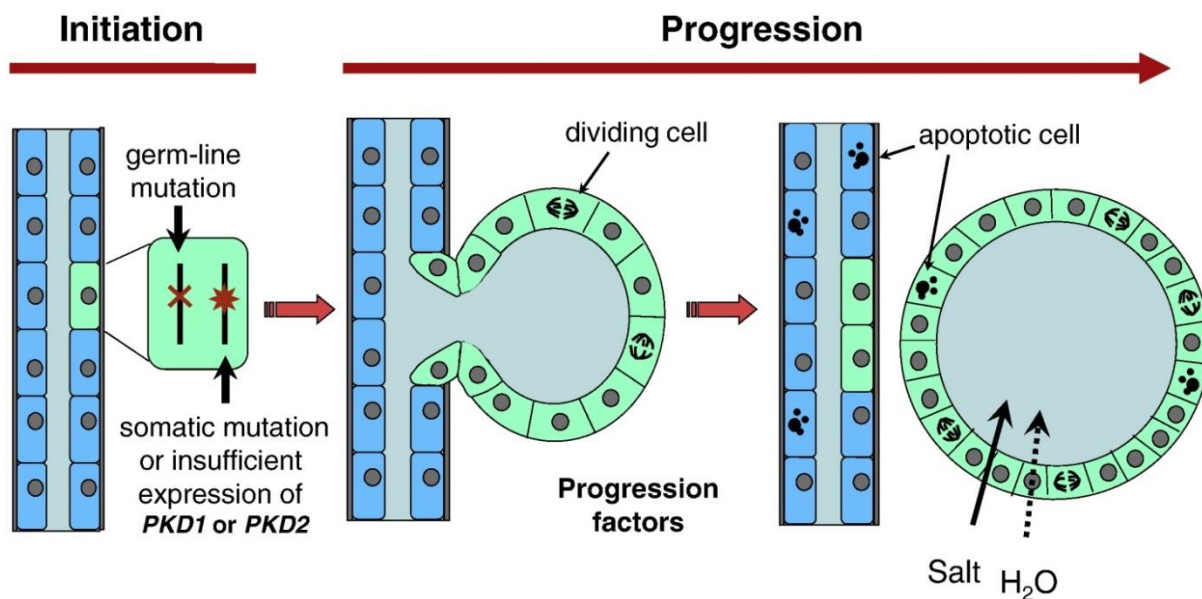


Figure (1.3) Diagrammatic representation of the beginning and development of cyst formation. (Grantham, 2015) Pathogenesis of cyst formation and growth. In a single tubule cell bearing a germ-line mutation of PKD1 or PKD2, a second “hit”, shown here as a somatic mutation, renders the cell PKD1 or PKD2 recessive. In the presence of progression factors, including vasopressin, cell proliferation is stimulated, and the increased mural area forms an ecstatic bulge into the interstitium. With further enlargement, the cyst separates from the parent tubule to create an isolated sac and a blocked tubule. Salt is pumped into the cyst via a chloride-dependent secretion mechanism stimulated by vasopressin, and water follows osmotically. The original tubule undergoes atrophy and apoptosis. PKD1, PKD2 Polycystic kidney disease type 1, type 2 genes. (Grantham, 2015)

Saccular diverticula from the tubule wall, which grow and break continuity with the tubule lumen, are the precursors of cysts. Epithelial proliferation and trans-epithelial solute and water secretion drive the formation of cysts. Renal epithelial cells proliferate excessively, resulting in cysts that eventually replace the majority of normal tissue. An increase in the overall size of the kidney is typically seen along with cyst expansion, and this

characteristic helps distinguish ADPKD from ordinary kidney cysts. (Turner, 2015).

It is believed that abnormal tubule epithelial cell growth results in the expansion of the tubule wall, creating a mural pocket. The fluid that fills the tiny cyst as it becomes larger comes from unreabsorbed glomerular filtrate; nevertheless, most cysts separate from the parent tubule at a diameter of about 2 mm and form isolated fluid sacs that are bordered by a layer of epithelial cells. (Grantham, 1987) Uncontrolled cell proliferation and fluid production into the cyst lumen cause cystic bodies to expand unabated. (Grantham, 2003) , secondary due to the second-hit somatic mutation. (Szánthó, 2020) Cyclic adenosine monophosphate (cAMP) mediated activities that cause aberrant cell proliferation and cyst-filling fluid secretion are both started by activating the cystic fibrosis transmembrane conductance regulator (CFTR) chloride channel and increasing the Ras/mitogen-activated protein kinase (MAPK) pathway (Calvet, 2008), and transmembrane protein 16 (TMEM16) A (anoctamin 1), which causes the production of trans epithelial chloride (Benedetto, 2019). Significant changes in intracellular metabolism, some of which include mitochondria, an essential organ for storing Ca^{2+} and a crucial player in cellular Ca^{2+} signalling, are responsible for stimulating cystic development. By modifying mitochondrial shape, suppressing miR-17, controlling calcium signalling, lowering cAMP levels, and preserving the copy number of mitochondrial DNA (mtDNA). Polycystin proteins have the ability to both directly and indirectly control mitochondrial function (Magayr, 2020) .As these cysts enlarge, they compress the renal parenchyma, resulting in tubulointerstitial injury. In 50% of patients, this causes ischemic impairment and eventually progressive

renal failure (Norman, 2011). According to recent research, deficiencies in the processes that concentrate urine and the neurohypophysis's resultant dysregulation of vasopressin excretion are the hallmarks of PKD.

Preclinical research revealed the function of arginine vasopressin-mediated cAMP as a driver of fluid release into the cysts in ADPKD (Torres, 2012).

The fluid build-up inside hundreds or thousands of cysts, which significantly increases the overall kidney volume. Cysts fill with glomerular filtrate-derived fluid in the early stages, although most cysts bigger than 2 mm in diameter are unrelated to the nephron segment from which they originated (Grantham, 1987). A number of transcription factors and signalling pathways regulate how cystogenesis develops and progresses (Harris, 2014). When it comes to PKD, one of the most researched mechanisms is calcium signalling. The Endoplasmic Reticulum (ER) is a major site of expression for PC2, a calcium permeable non-selective cation channel that interacts with other calcium channel proteins (Köttgen, 2008). By binding to the inositol 1,4,5-trisphosphate receptor (IP3R), it controls the activity of ryanodine receptors as well as Ca^{2+} homeostasis (Anyatonwu, 2007). The PC1 increases ER calcium absorption, which, in contrast to PC2, speeds up the decay of the intracellular calcium response to ATP. All of these points to polycystins playing a significant role in intracellular calcium homeostasis (Gallagher, 2010). The abnormal interaction between intracellular calcium and cAMP signalling is shown in cystic epithelial cells, where increased cAMP levels cause cyst fluid production and increase protein kinase A activity (Sussman, 2014). It is not yet fully known how decreased polycystin signalling in tubular epithelial cells' primary cilia causes cystic illness (Harris, 2014).

1.8 Diagnosis and screening of autosomal dominant polycystic kidney disease

The diagnosis of ADPKD is dependent on the stage of the disease. When the disease is fully established, the diagnosis is clinically based on patient's history and physical examination. (Pei, 2006)

Physical examination commonly reveals large, irregular kidneys and possibly hepatomegaly. However, definitive diagnosis can be difficult due to other disorders having overlapping symptoms. Therefore, complementary approaches such as diagnostic imaging or genetic tests are necessary to confirm the diagnosis. Imaging techniques, including ultrasound, computed axial tomography, or nuclear magnetic resonance, allow for the detection of cysts in the kidney, liver, or pancreas. (Mosetti, 2003) The magnetic resonance technique has proven to be more sensitive than ultrasound, allowing measurements of height-adjusted total kidney volume (htTKV) and better definition of the cysts without the use of contrast agents. However, these imaging tests are expensive (Irazabal, 2015). and are often not performed on a subset of the ADPKD population including those who are young individuals at risk or patients with atypical or *de novo* renal cystic disease (Pei, 2006). Definitive diagnosis is established by ultrasound examination (Feather, 2020). Ultrasonography criteria for diagnosing ADPKD are based on the number of visible cysts, the patient's age, and a family history of ADPKD. (Alguire, 2006)

Table (1.1) Ultrasound-based criterion for the diagnosis or exclusion of ADPKD (Mei, 2020)

<i>Age, years</i>	15-39	40-59	>60
<i>Diagnostic confirmation</i>	At least 3 cysts (unilateral or bilateral)	At least 2 cysts in each kidney	At least 4 cysts in each kidney
<i>Disease exclusion</i>	No recommendation	<2 cysts in each kidney	<2 cysts in each kidney

Although inexpensive and low-risk, ultrasonography has limitations, with ultrasound-criteria only described for those with a family history of ADPKD, thus excluding the 10–15% with de novo disease and those unaware of their family history. (Iliuta, 2017). Abdominal-MRI can be used, but is less readily available and more expensive (Mallawaarachchi, 2021). Patients with ADPKD can present with hypertension, hematuria, proteinuria, or kidney function impairment. Flank pain, due to kidney hemorrhage, obstructive calculi, or urinary tract infection, is the most common symptom reported by patients. (Torres, 2020)

Genetic testing is not consistently used in the management of individuals with ADPKD, although it can provide invaluable information regarding disease progression and prognosis. (Noce, 2022)

1.9 Treatment of autosomal dominant polycystic kidney disease

In ADPKD, the loss of renal function may remain undetected until the fourth decade of life, when renal cystic development is advanced and most nephrons have been destroyed. (Chapman, 2015) Thus, it is important to find variables to identify patients who are at higher risk of disease progression, especially since there is evidence that treatment with tolvaptan—a vasopressin V₂-receptor antagonist—may slow the deterioration of renal function. (Torres, 2016) Experimental therapies targeting increased cAMP, activation of the mammalian target of rapamycin complex 1 (mTORC1), and reduced 5'-AMP-activated protein kinase signaling have been shown to slow cystic disease progression. (Harris, 2014) Studies of animal models implicate the antidiuretic hormone arginine vasopressin and its second messenger adenosine-3',5'-cyclic monophosphate (cAMP) as promoters of kidney-cyst cell proliferation and luminal fluid secretion. The suppression of vasopressin release by means of high water intake, genetic elimination of vasopressin, and vasopressin V₂-receptor blockade all reduce the cyst burden and protect kidney function. Such preclinical studies justify studying the effects of tolvaptan, in human ADPKD. Vasopressin V₂ receptor signaling has also been shown to be a potent inducer of cAMP, and in 2015, Tolvaptan, was approved to slow the progression of cyst development and eGFR decline in patients with ADPKD (Torres, 2012) but due to a relatively unfavorable side effect/benefit ratio it has been suggested to limit therapy with tolvaptan to patients at risk of rapidly progressing ADPKD. (E., 2016)

Healthy lifestyle and diet, maintenance of optimal weight, regular cardiovascular exercise and avoidance of smoking are generally recommended in ADPKD. High water intake is used as a prevention of

nephrolithiasis but also leads to the suppression of vasopressin which could lead to an increase of fluid secretion into cysts. However, the results of trials with increased water intake were not conclusive. Salt intake should not exceed 5 g per day as all patients with other renal diseases. (Reiterová, 2022)

1.10 Progression Biomarkers of ADPKD

An increasing number of studies have recently discovered new serum and urine biomarkers of the disease's progression, which are less expensive and easier to dose from the early stages of the disease, in addition to the conventional factors (PKD1 mutation, hypertension, proteinuria, and total kidney volume) (Pana, 2023) .There are now a number of factors that may be used to predict how quickly ADPKD will advance. In the early stages of this illness, when cysts are gradually forming and GFR can stay within the normal range, GFR indexed for age is a powerful predictor but less sensitive (Grantham, 2006).

Therefore, total kidney volume (TKV) has received a lot of attention as a predictor of early-stage illness (Irazabal, 2015) .However, TKV and genotype evaluation is time-consuming and costly, and there is no evidence linking these factors to the rate at which a patient's condition progresses. Consequently, it is necessary to create new indicators that can forecast the rate at which ADPKD illness progresses, either by itself or in conjunction with traditional risk markers (Messchendorp, 2019).

The concentration of molecules in urine that express more when there is an ischemic state or tubular injury may serve as a predictor of the decline in renal function that is specifically linked to ADPKD and its mechanism of impaired renal function. These include tubular injury-related molecules

including β 2-microglobulin, liver fatty acid-binding protein (L-FABP), neutrophil gelatinase-associated lipocalin (NGAL), and kidney injury molecule-1 (KIM-1) and many others which were mentioned in Figure (1.4) (Nauta, 2013).

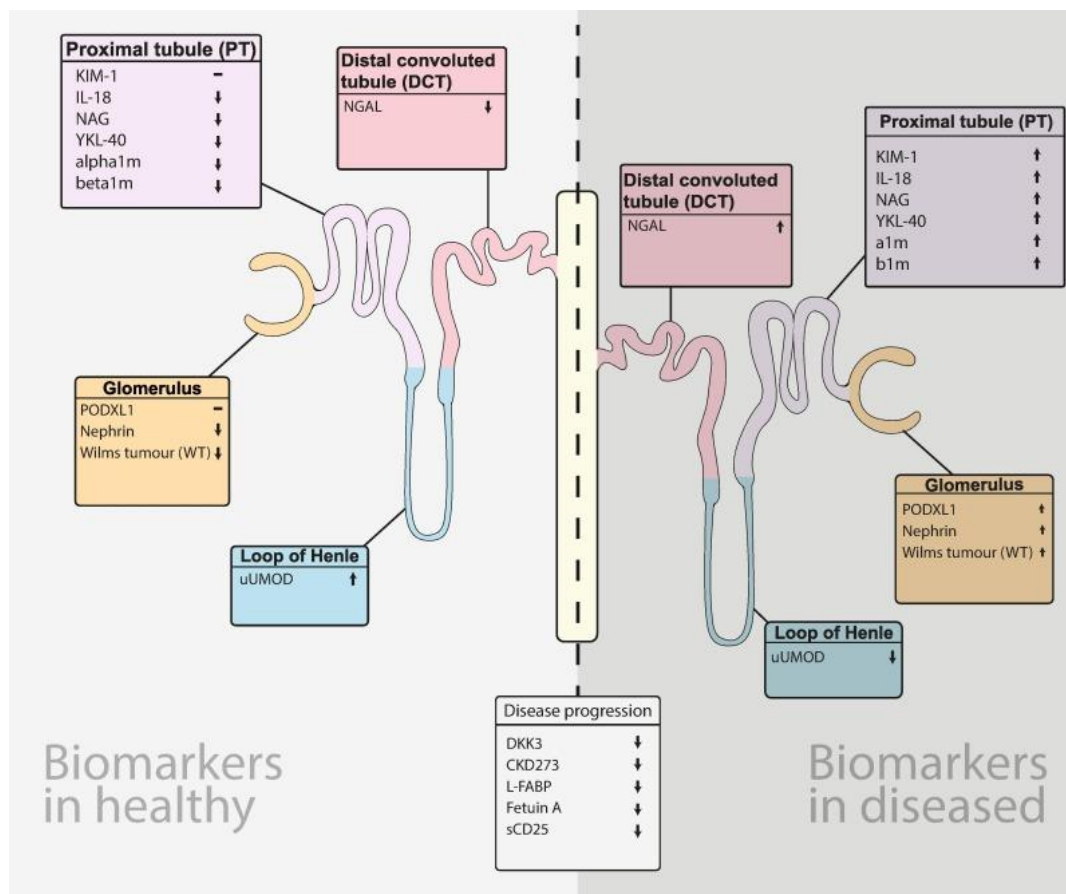


Figure (1.4) biomarkers in various nephron segments. (Canki, 2024) The biomarker level in relation to the opposite condition (i.e., healthy versus sick) is shown by the arrows. A decline is indicated by ↓, and an increase is shown by ↑. indicates that in that state there is no detection of the biomarker. (Canki, 2024). *NGAL: neutrophil gelatinase associated lipocalin, KIM-1: kidney injury molecule 1, IL-18: interleukin-18, NAG: N-acetylglucosaminidase, YKL-40: derived from the three N-terminal amino acids - tyrosine (Y), lysine (K), and leucine (L), also known as chitinase-3-like protein 1, PODXL1: Podocalyxin-like protein 1, uUMOD urinary uromodulin, DKK3: Dickkopf 3, CKD273: a panel of 273 urinary peptides, L-FABP: Liver fatty acid-binding protein.*

1.10.1 Proximal tubular damage marker

kidney injury molecule 1:

Kidney injury molecule-1(KIM-)1 is a 104-kDa transmembrane glycoprotein that is also referred to as HAVcr-1 and TIM-1, *as shown in Figure (1.5)*. These proteins are members of the T-cell immunoglobulin and mucin domain family (TIM). immunological cells display TIM glycoproteins, which are involved in controlling immunological responses. Kidney injury molecule -1 is distinct from other members of its family in that epithelial cells as well as immunocompetent cells express it. Kidney injury molecule -1-mediated cellular and humoral effects are implicated in several physiological and pathological processes. The processes governing KIM-1's involvement in viral invasion, immune response control, adaptive responses of the kidney epithelium to acute ischemia or toxic insult, progression of chronic renal disorders. (Karmakova, 2021)

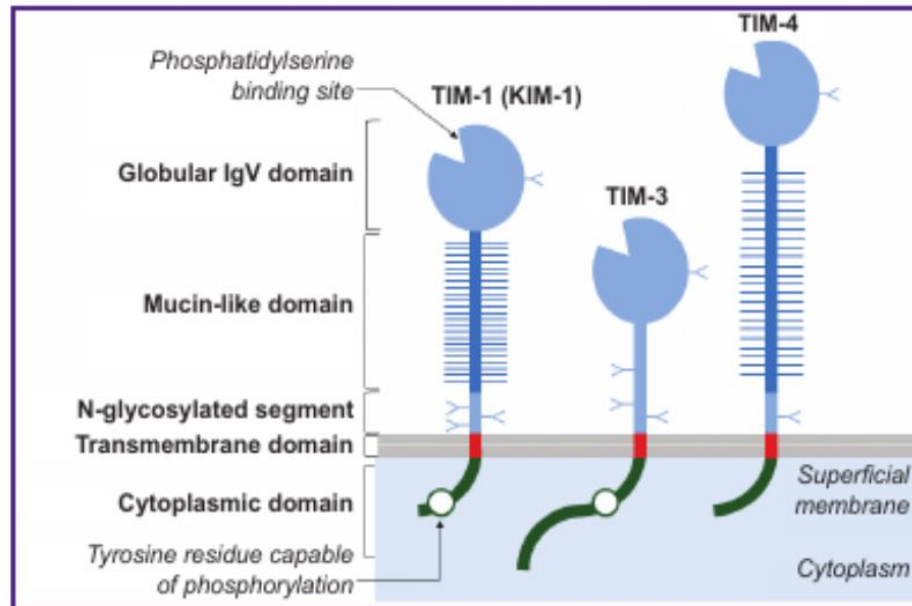


Figure (1.5) structure of KIM-1 (Karmakova, 2021) TIM-1: T cell immunoglobulin mucin 1, KIM-1: Kidney Injury Molecule-1/T

A transmembrane glycoprotein produced by proximal tubular cells, KIM-1 is known to be an early, sensitive, and particular urine biomarker for kidney damage. Recently linked to the severity of acute and chronic kidney injury (Brilland, 2023).

In the first human investigation, biopsies taken from the proximal tubules of individuals who had acute tubular necrosis showed high urine KIM-1 (u-KIM-1) levels and widespread expression of this protein (Han, 2002). Conversely, lower levels have been linked to the type 1 diabetes microalbuminuria regression (Vaidya, 2011). ADPKD is influenced by cyst compression of renal tubules, which can also cause KIM-1 to be expressed. It is unclear if u-KIM-1 indexed for creatinine (uKIM-1/Cr) is a predictive indicator of ADPKD disease progression (Griffin, 2020).

The development of ADPKD is significantly influenced by cyst formation, and the degree of compression that growing cysts place on surrounding renal tubules may increase the expression of KIM-1. Therefore, in ADPKD,

While KIM-1 is not expressed in healthy kidneys, it is expressed in many different kidney disorders in humans, primarily in the proximal tubular cells' apical membrane (Van Timmeren, 2007). New research indicates that KIM-1 could also be helpful in forecasting the course of CKD (Schulz, 2020).

In a healthy kidney, KIM-1 levels are undetectable, but when ischemia or renal tubular cell disruption occur, they sharply rise (Vaidya, 2006), particularly when there has been drug-induced harm (Griffin, 2019).

Kidney injury molecule -1 has been demonstrated to be able to predict the onset of CKD in addition to its function in the diagnosis of AKI (Schulz, 2020). The loss of kidney function in ADPKD is believed to be primarily caused by cystic compression of tubular cells. thus, it follows that it is conceivable that KIM-1 expression would be similarly elevated in PKD and that KIM-1 may, like height adjusted TKV (HtTKV), be used to forecast the course of the illness (Grantham, 2011). Patients with ADPKD showed higher uKIM-1/Cr levels; however, there was no correlation between the values and cyst development or size. Elevated uKIM-1/Cr indicates the disruption of tubular cells and might indicate many cysts. It is not related to the initial HtTKV (Griffin, 2020). It is yet unknown how KIM-1 contributes to cellular damage or the development of illness (Gauer, 2016).

1.10.2 Distal tubular damage markers

Chitinase-3-like protein 1:

Chitinase-3 like-protein-1 (CHI3L1) is a 40 kDa non-enzymatic member of the glycoside hydrolase family, *structure was presented in Figure (1.6)*. It is controlled by cytokines, growth factors, medications, extracellular matrix alterations, and stress. It binds to chitin, heparin, and hyaluronic acid. Many different types of cells, such as neutrophils, chondrocytes, smooth muscle cells, fibroblast-like cells, tumor cells, and synoviocytes, produce and release CHI3L1. It is important for remodelling reactions, inflammation, tissue healing, and tissue damage (hao T, 2020).

The secondary structural components of each of the four chains in CHI3L1 are shown by colour. Chain C has been tinted in grey to emphasize the dispersion of the mutations that have been found within a single chain. We distinguish between mutations that are heterozygous (orange) and homozygous (pink) (Backes, 2015).

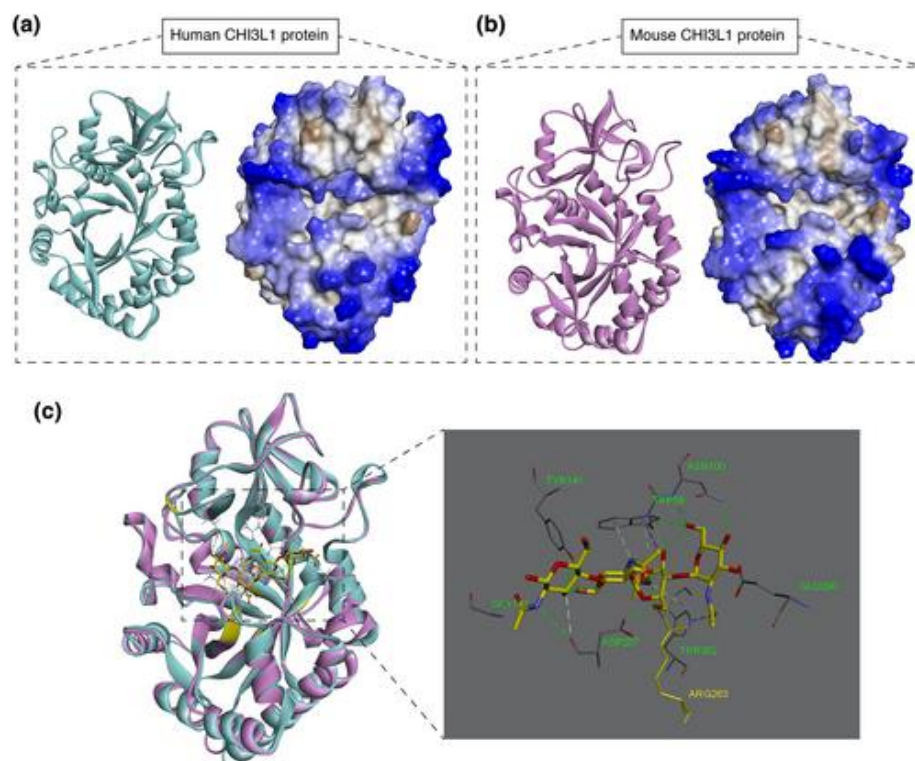


Figure (1.6) Human and mouse CHI3L1 crystal structures (a, b). (Li, 2023). The groove (c) displays an overlay of these two proteins together with their chitotetraose binding. CHI3L1: chitinase-3-like protein 1.

Chitinase-3-like protein 1 (YKL-40) is a new biomarker for endothelial dysfunction and inflammation (Tatar1ABE, 2013). A potential urinary biomarker for AKI has recently been found to be urine chitinase 3-like protein 1 (uCHI3L1) (Hoste, 2020). Urine chitinase 3-like protein 1, as opposed to urine neutrophil gelatinase-associated lipocalin (uNGAL), is a potential AKI biomarker in intensive care unit patients, as demonstrated recently in a single-centre prospective cohort research (De Loor, 2016).

1.10.3 Marker of Progression of kidney inflammation:

Neutrophil gelatinase-associated lipocalin (NGAL):

Neutrophil gelatinase-associated lipocalin (NGAL), also known as siderocalin, lipocalin-2 (LCN2), or lipocalin, is a 21–25 kDa iron-carrying protein that is widely expressed in the loop of Henle tubular epithelium and collecting ducts, structure of Neutrophil gelatinase was presented in Figure (1.7), and the molecular structure was shown in Figure (1.8)

It belongs to the lipocalin superfamily (Guo, 2020). It is first separated from the neutrophils (Kjeldsen, 1993), subsequently, researchers discovered that organs including the kidney, liver, and epithelial cells also express it (Friedl, 1999) .

It was discovered to be among the first and most powerfully activated genes and proteins in the distal nephron's tubular epithelium, and it was released from tubular epithelial cells after tissue damage, such as ischemia renal injury, which is why clinical investigators were interested in it (Mishra, 2003) .Subsequent research revealed that neutrophils create the monomeric type of urine, whereas kidney tubular epithelial cells produce the dimeric form (Cai, 2010) . The specificity of NGAL as a renal biomarker may be enhanced by this variation, it is not specific as mentioned above (Guo, 2020).



Figure (1.7) Crystal structure of NGAL (Goetz, 2000).

The crystal structure of NGAL shows an internal ligand-binding site surrounded by a single, eight-stranded, continuously hydrogen-bonded antiparallel β -barrel. β -strands are depicted as arrows with a smooth curve, whereas α -helices are represented as spiral ribbons. The depiction of fatty acid ligand molecules is an all-atom picture that is coloured. (Goetz, 2000). NGAL: Neutrophil gelatinase-associated lipocalin

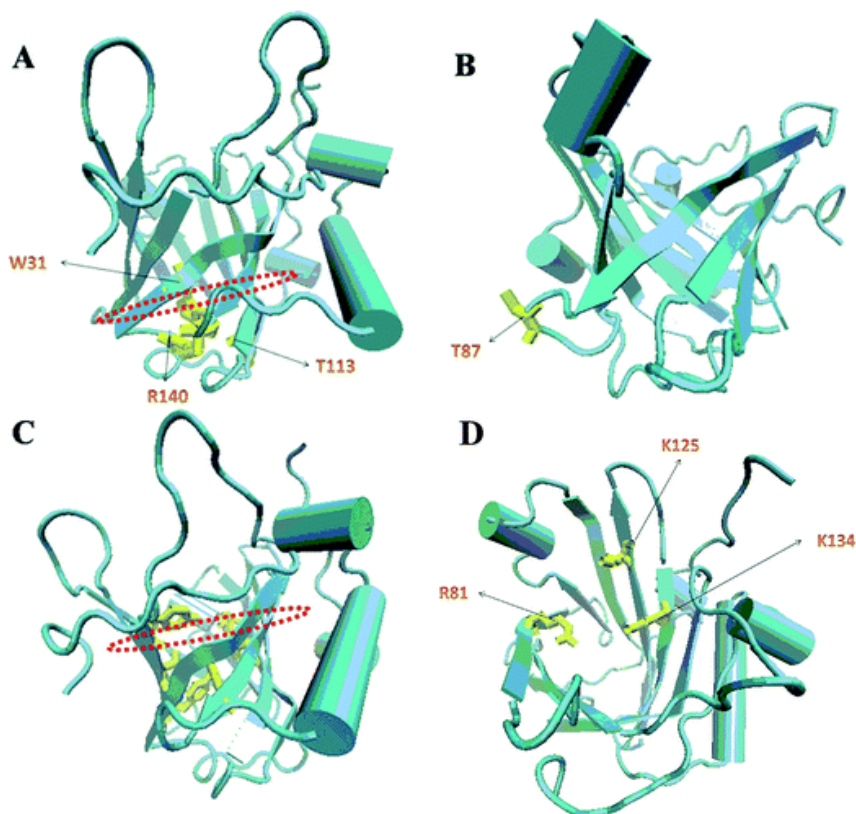


Figure (1.8) molecular structure of NGAL. (Bao, 2015)

(A) The 310-helix and the side chains cluster of the conserved residues W31, T113, and R140 (yellow) closed the barrel's smaller end at the calyx's bottom. (B) At the closed end of the calyx, the free SH group of residues C87 (yellow), which was linked to MMP-9, was located in an interstrand loop. (C) Hydrophobic aromatic and aliphatic residues, such as W31 and V33 (β 1), V66 (β 3), F83 (β 4), F92 and L94 (β 5), V108 and V110 (β 6), and V121 and F123 (β 7) (yellow) near the base of the barrel, were hypothesized to be the binding sites for lipophilic ligands. (D) The positively charged side chains of R81, K125, and K134 lysine residues were pushed into the upper open end of barrel, where they bind hydrophilic siderophores like catecholates. (Bao, 2015). *NGAL*: Neutrophil gelatinase-associated lipocalin.

It is well known that NGAL is a siderophoric protein that controls iron activity (Xiao, 2017). The iron molecule that contains NGAL interacts with cell surface receptors. After that, it is moved within the cell and releases iron (Goetz, 2002). Additionally, unbound NGAL interacts with cell surface receptors to cause an intracellular transport of iron out of the cell (Marakala, 2022).

Neutrophil gelatinase-associated lipocalin interacts with certain receptors (24p3R or megalin) either alone (Apo-NGAL) or in a compound with iron-siderophores (Holo-NGAL). Following internalization, the iron that Holo-NGAL carries is released into the cytoplasm, causing a buildup of iron and controlling certain gene pathways that are dependent on iron. NGAL can then be recycled outside of the cell as Apo-NGAL or destroyed inside the cell. This mechanism most likely explains the majority of the protective properties attributed to this protein (Bolignano, 2008).

On the other hand, the cell might lose its iron stores if Apo-NGAL manages to seize internal iron-siderophores and transfer them to the extracellular area. This most likely illustrates how NGAL has potent antimicrobial effects and, under some situations, may encourage cellular death (Bolignano, 2008).

Following injury, tubular epithelial cells produce NGAL early (Guo, 2020), (Hosohata, 2020). The degree of kidney damage is correlated with the expression of NGAL, which may assist distinguish people who are more likely to experience a quicker deterioration in renal function (Rysz, 2017).

Based on the activation of particular iron-dependent pathways, the increase in NGAL production and release from tubular cells in response to various harmful stimuli may have a self-defensive purpose.

These pathways most likely also represent the mechanism by which NGAL promotes kidney growth and differentiation. With regard to clinical nephrology and other fields, NGAL has the potential to be among the most promising next-generation biomarkers. (Bolignano, 2008)

There is a strong association between NGAL and serum creatinine, cystatin C, and estimated GFR(eGFR) (Guo, 2020). Urinary NGAL is also an excellent measure of normoalbuminuric renal disease in type 2 diabetes mellitus and a good predictor of renal damage prior to observable changes in eGFR (Li, 2019). Belonging to the lipocalin family, NGAL is a tiny molecular weight stress protein. According to previously published research, NGAL has been demonstrated to be a very reliable marker of the severity of CKD in individuals with ADPKD. In these patients, levels of uNGAL and sNGAL exhibited a strong correlation with both serum Cr and residual GFR (Bolignano, 2007). In addition, patients with higher cystic development (renal length > 16 cm and > 10 cysts) exhibited higher levels of sNGAL and uNGAL than other patients, regardless of their residual renal function. This finding raises the intriguing possibility that this protein may also play a role in the process of cyst growth, in addition to its previously demonstrated involvement in tumor and epithelial cell proliferation (Bolignano, 2008).

Meijer & Co. (Messchendorp, 2019) discovered a link between tKV and uNGAL levels, which may suggest that NGAL levels in the urine only rise in advanced PKD (Pana, 2023).

1.11 Knowledge gap

Currently, markers with poor sensitivity that indicate the risk of fast disease development in individuals with ADPKD are costly and time-consuming to evaluate. Therefore, there is a need for new, simple-to-measure indicators that can forecast the rate at which a disease progresses, either by itself or in conjunction with traditional risk markers. In this work, we looked at the potential of inflammation and tubular damage markers to forecast a loss in kidney function. Several studies have used GFR and TKV evaluations to show a strong correlation between these indicators and the severity of ADPKD (Petzold, 2015). The necessity to identify novel biomarkers, or combinations of previously identified biomarkers, with strong predictive value of ADPKD development and risk of kidney damage is emphasized by the poor ability to predict htTKV in ADPKD (Segarra-Medrano, 2020).

New prognosis markers need to be developed, either alone or in combination with conventional risk markers, which can predict the rate of disease progression in ADPKD.

The ADPKD is a tubular disease with an inflammatory component. Therefore, our point of view that when measurement of urinary tubular damage KIM-1 & CHI3L1 and inflammation markers NGAL is of interest, especially because these markers are relatively inexpensive and easy to measure.

1.12 Aims of the study:

The study aims and objectives at the following:

- Estimating the serum level of KIM-1 & CHI3L1 and inflammation markers NGAL in ADPKD patients.
- Study the disease progression through ROC analysis to assess changes in KIM1 & CHI3L1, and NGAL adjusted for eGFR.
- Evaluating the correlation between serum biomarkers in ADPKD patients.

Chapter Two

Subjects, Materials

And Methods

2. Subjects Materials and Methods

2.1. The Study Design

In the cross-sectional study design, a total 85 subjects aged between 7 and 84 years, all diagnosed with ADPKD based on the established diagnostic criteria. A questionnaire was used to collect patient data, including age, sex, address, family history of ADPKD and other diseases, height, weight, body mass index (BMI), blood pressure, history of antihypertensive therapy, history of cardiovascular disease, history of kidney replacement surgery, history of dialysis, and other relevant medical information. The study was conducted at the kidney diseases consultant of Al-Hassan Al-Mujtaba teaching hospital & Al-Saegh Center for Nephrology and Transplantation outpatient clinics in Karbala, Iraq. Study spanned from September / 2023 to August / 2024.

2.2 Ethical Approval

The College of Medicine at the University of Karbala, along with the Karbala Health Directorate, validated the ethical approval for this study.

2.3 Blood Sample Collection and Storage

Disposable syringes and needles were used for blood collection (5 mL). Blood samples were obtained from ADPKD patients via venipuncture. Each sample was placed in gel tubes and left to clot at room temperature for 10 to 15 minutes. The blood was then centrifuged at 4000 x g for 10 to 15 minutes to separate the serum. The serum was divided into two parts and stored in Eppendorf tubes at -80°C until further analysis. The levels of KIM-1,

CHI3L1, and NGAL were measured using the enzyme-linked immunosorbent assay (ELISA) technique.

2.4 The Sample Size

The study was conducted worldwide and the prevalence was 0.001 (Cornec-Le Gall, 2019).

and from this

prevalence a sample size can be calculated (Daniel & Cross, 2018):

$$n = [Z^2 \times P(1-P)] / d^2$$

$$n = [(1.96)^2 \times 0.001(1-0.001)] / (0.05)^2$$

$$n = 1.535$$

Where:

n = Sample Size

Z = Z Statistic for a level of confidence (1.96 for 95% Confidence level)

P = Expected Prevalence or Proportion

d = Precision (d is considered 0.05 to produced good precision & smaller error of estimate).

2.5 Inclusion Criteria

The patients who diagnosed with ADPKD were included in this study (Colbert, 2020) (Neumann, 2013)

2.6 Exclusion Criteria:

Patients meeting the following criteria were excluded from the study:

- Incomplete data.
- History of kidney replacement surgery.
- Currently undergoing continuous dialysis.
- Heart failure.

2.7 Diagnostic Criteria for ADPKD:

Ultrasonographic Criteria:

Individuals aged 15–39 years: At least three unilateral or bilateral kidney cysts.

Individuals aged 40–59 years: At least two cysts in each kidney.

Individuals aged 60 years or older: At least four cysts in each kidney. (Pei, 2009)

Progression of the disease was measured as changes in the eGFR and htTKV.

2.8 Ultrasound criteria for Height-Adjusted Total Kidney Volume measurement:

1. Kidney Measurements:

- The length, width, and depth of each kidney are measured using ultrasound Semens Juniper version 2023.
- Kidney length is measured in the coronal or sagittal plane, while width and depth are measured in the transverse plane.

2. Volume Calculation:

- Using the ellipsoid formula ($\text{Length} \times \text{Width} \times \text{Depth} \times \pi/6$) to estimate the volume of each kidney.
- Summing the volumes of both kidneys to obtain the total kidney volume.

The normal kidney volume is of 110 to 190 ml in men and 90 to 150 ml in women. (McGahan, 1998)

3. Height Adjustment:

- Adjustment of the TKV by dividing it by the patient's height in meters to obtain htTKV (expressed in ml/m).

2.9 Ultrasound Diagnostic Criteria for ADPKD Total Kidney Volume, and Height-Adjusted Total Kidney Volume

1. Small Kidney Volume in ADPKD:

- Less than 150 ml may indicate advanced CKD with significant cyst-induced parenchymal loss.

- Height-Adjusted Total Kidney Volume: Less than 200 ml/m².

2. Normal Kidney Volume in ADPKD:

- Total Kidney Volume: 150 to 300 ml, often seen in early-stage ADPKD before significant cystic growth.

- Height-Adjusted Total Kidney Volume: 200 to 400 ml/m².

3. Large Kidney Volume in ADPKD:

- Total Kidney Volume: Greater than 300 ml.

- Height-Adjusted Total Kidney Volume: Greater than 400 ml/m².
(ADPKD?Kidney101. ‘2024)

Ultrasound measurement of TKV typically is calculated utilizing the ellipsoid equation ($\pi/6 \times L \times W \times D$), by measuring maximum orthogonal length, width and depth of the kidney. (Hricak, 1983)

2.10 Measurement of Kidney Cysts and Biomarker Levels.

Class interval for grouping data was used to categorized the cysts into three sub-groups: small (G1: 0.7 ml - 2.2 ml), medium (G2: 2.3 ml - 3.6 ml), and large (G3: > 3.7 ml).

The magnitude of class interval depends on range and number of classes. The range is the difference between the highest and smallest values is the data series. Sturges formula to find number of classes is given below

$$K = 1 + 3.322 \log N.$$

K = No. of class

$\log N$ = Logarithm of total no. of observations

Sturges formula to find size of class interval

Size of class interval (h) = Range/ K

The study assessed the potential impact of these cyst size categories on the levels of specific kidney damage biomarkers, namely CHI3L1, KIM-1, and NGAL. The biomarker levels were reported as means \pm SD to reflect the variability within each group.

2.11 Estimated GFR is measured by CKD-EPI Equation (Chronic Kidney Disease Epidemiology Collaboration): (Matsuo, 2009)

For females: $eGFR\} = 141x (\text{serum creatinine}/0.7)^{-0.329} \times 0.993^{\text{Age}}$

For males: $eGFR\} = 141x (\text{serum creatinine}/0.9)^{-0.411} \times 0.993^{\text{Age}}$

Additional factors:

If the serum creatinine is greater than 0.7 for females or 0.9 for males, the exponent changes to -1.209.

Multiply by 1.159 if the patient is Black. (Levey, 2009)

2.12 Classification of eGFR and Biomarker Measurement.

In this study, the KDIGO (Levin, 2024) classification for estimated eGFR was utilized to categorize patients into five stages of CKD:

- G1: $eGFR \geq 90 \text{ mL}/\text{min}/1.73 \text{ m}^2$
- G2: $eGFR 60\text{-}89 \text{ mL}/\text{min}/1.73 \text{ m}^2$
- G3a: $eGFR 45\text{-}59 \text{ mL}/\text{min}/1.73 \text{ m}^2$
- G3b: $eGFR 30\text{-}44 \text{ mL}/\text{min}/1.73 \text{ m}^2$
- G4: $eGFR 15\text{-}29 \text{ mL}/\text{min}/1.73 \text{ m}^2$
- G5: $eGFR < 15 \text{ mL}/\text{min}/1.73 \text{ m}^2$

The study aimed to examine the progression of CKD by analyzing the levels of specific kidney damage biomarkers, including KIM-1, NGAL, and CHI3L1. These biomarkers were measured across the different eGFR stages to evaluate their association with the severity of kidney function decline.

Flow Chart of Study Design:

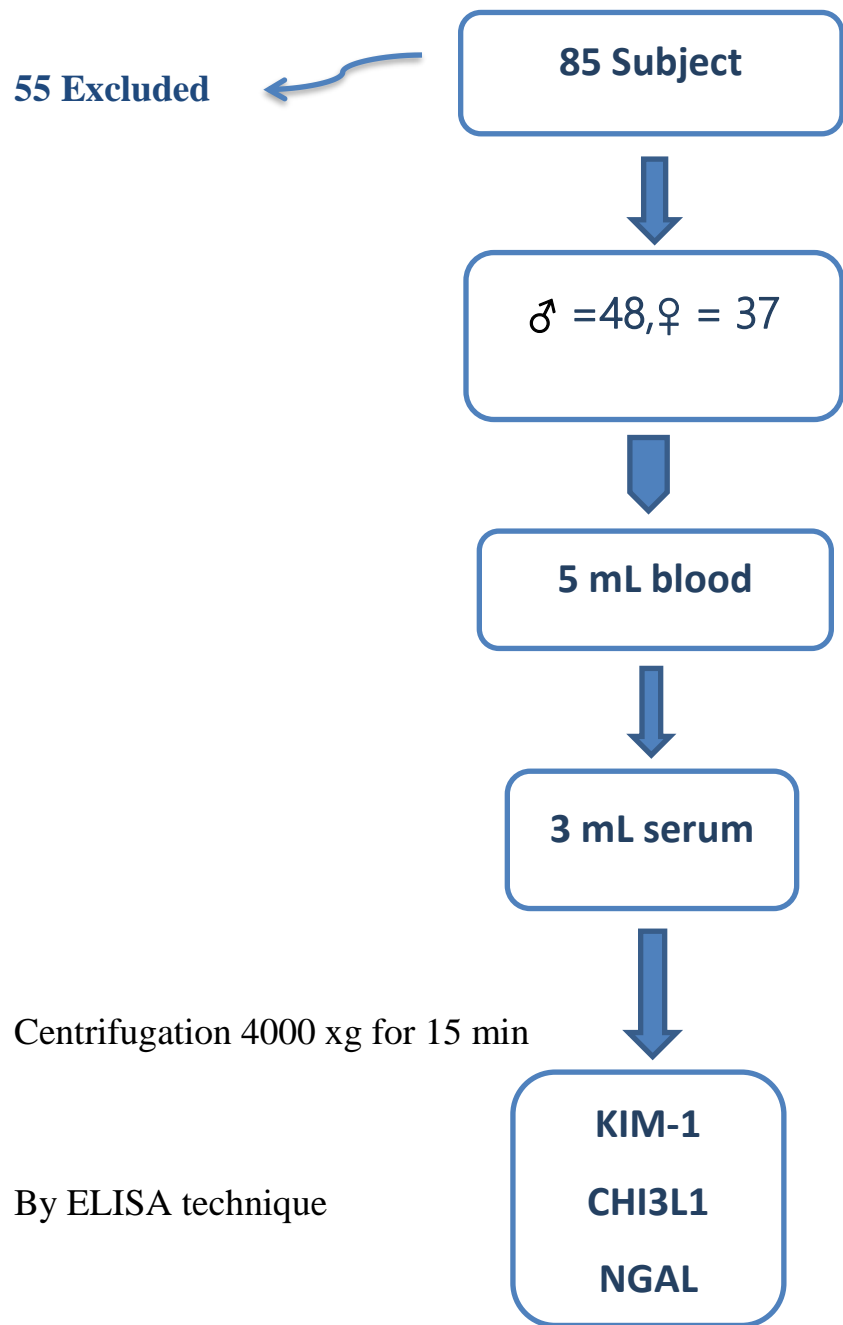


figure (2.1) flow chart of study design.

2.13 Patient Evaluation:

Serum samples from each patient were used to measure urea, creatinine, KIM-1, CHI3L1, and NGAL, as well as lipid profile components including cholesterol, triglycerides (TG), high-density lipoprotein (HDL), very low-density lipoprotein (VLDL), and low-density lipoprotein (LDL). Genetic tests were not conducted due to the high price, and the family history was taken, meaning that all patients had inherited the disease according to the fact that the disease is a dominant genetic trait.

2.14 Measurement of Body Mass Index (BMI):

Body Mass Index was calculated by dividing body weight (in kilograms) by the square of height (in meters). The formula used is:

$$\text{BMI} = \text{Weight (kg)} / \{\text{Height (m)}\}^2$$

Body Mass Index was classified according to the World Health Organization (WHO) in Table 2.1 (Seo, 2019)

Table (2.1) BMI WHO classification

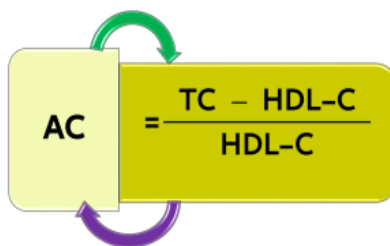
N	BMI	Unit	Classification Of BMI
1	Below 18.5	Kg/M ²	Underweight
2	18.5-24.9	Kg/M ²	Normal Weight
3	25.0 -29.9	Kg/M ²	Pre-Obesity
4	30.0 -34.9	Kg/M ²	Obesity Class-1
5	35.0 39.9	Kg/M ²	Obesity Class-2
6	Above 40	Kg/M ²	Obesity Class-3

2.15 Measurement of Atherogenic Indices

Atherogenic Coefficient (AC): The Atherogenic Coefficient (AC) is the ratio of non-high-density lipoproteins cholesterol (non-HDL-C) to high-density lipoproteins cholesterol (HDL-C) (Olamoyegun, 2016). It is used as a diagnostic tool to predict the risk of developing cardiovascular events. AC of >3 have been associated with cardiovascular disease risks. (Agu, 2024) The formula for AC is as follows:

$$AC = \text{non-HDL-C} / \text{HDL-C}$$

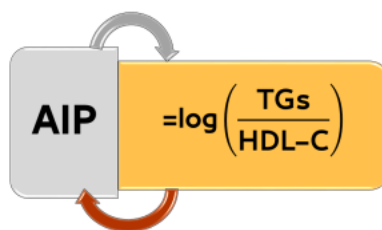
$$\text{Non-HDL-C} = \text{TC} - \text{HDL-C}$$



AC = $\frac{\text{TC} - \text{HDL-C}}{\text{HDL-C}}$

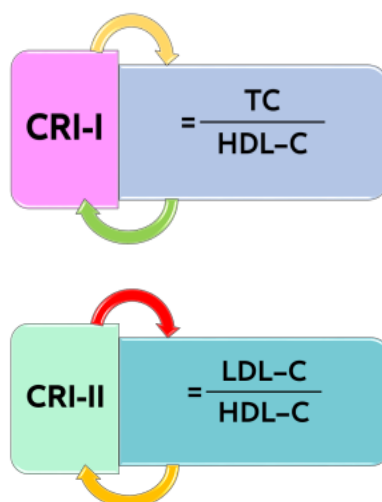
Atherogenic Index of Plasma (AIP):

The Atherogenic Index of Plasma is an unconventional lipid ratio that represents the logarithm of the molar ratio of triglycerides (TG) to HDL-C. Evidence suggests that AIP is a significant predictive index, with a positive correlation to cardiovascular disease (CVD) (Gómez-Álvarez, 2020). AIP value of < 0.1 was considered as low risk and ≥ 0.1 was considered high risk. (Sujatha, 2017)



AIP = $\log\left(\frac{\text{TGs}}{\text{HDL-C}}\right)$

- ❖ **Castelli's risk indexes (I & II) (CRI-1 and CRI-11)**, also known as cardiac risk indexes, are two lipid ratios used in this study to assess CVD risk (Igharo, 2020), (Tecer, 2019). The cut-off values for each index considered as risky were: Castelli risk index-I ≥ 5.0 , Castelli risk index-II ≥ 3.0 (Salcedo-Cifuentes, 2020)



Cholesterol index (C-index): to predict the probability of developing CAD with greater accuracy than the other indices. (Ulusoy, 2013) The cutoff to determine whether patients need further investigation and assessment is between 200 and 240 mg/dL. (Chen, 2016)



2.16 The Materials & Tools

The materials & Tools used in this study ,along with their respective suppliers ,are listed in Table (2.2).

Table (2.2) The Materials, Tools ,and Their Suppliers used in This Study

N	name	Company	Country
1	Distilled Water & washing bottle		Iraq
2	Eppendorf Tubes (1.5 mL)	Kang Gia	China
3	Gel tubes (6mL)	EZ Medical lab	China
4	Gloves	MedTech	Malaysia
5	Graduated Cylinder (1500 mL)	Eterna Duration	Germany
6	Hard Ice Gels Packs	Hepo International	China
7	Laboratory Stopwatches & Timers	Spectrum	USA
8	Micropipette (10-100 µl)	Slamed®	Germany
9	Multichannel pipette	Slamed®	China
10	Pipette Rack Stand	Slamed®	Germany
11	Pipette Tips-100µl (blue)	Slamed®	China
12	Pipette Tips-100µl (yellow)	Kirgen®	China
13	Pipette(100-1000µl)	Slamed®	Germany
14	Plate Sealer	BT Lab	China
15	Pre-Coated ELISA Plate (96-well)	BT Lab	China
16	Specimen Transport Bag	Hepo International	China
17	Surgical Spirit	Ameya Fze	UAE
18	Syringe (5 mL/cc)	Yuandong,Medical	China

2.17 The Laboratory Kits

Laboratory kits with highest purity used in this study are listed in Table (2.3) below with their suppliers: -

Table (2.3) The Laboratory Kits used in this study

N	Name	Company	Country	No. of Kits
1	Human Kidney Injury Molecule 1 Elisa KIT	BT Lab	China	1
2	Human Chitinase-3-Like Protein 1 Elisa KIT	BT Lab	China	1
3	Human neutrophil gelatinase-associated lipocalin, NGAL ELISA KIT	BT Lab	China	1
4	Lipid profile kits	Abbott laboratories	USA	1

2.18 The Instruments

All the instruments and tools used in this study are listed in Table 2.4

Table (2.4) Instruments and tools used in this study

N	Name	Company	Country
1	Architect c4000	Abbott Laboratories	USA
2	Centrifuge	Hettich	Germany
3	Deep freezer (-80 c°)	ALS	UK
4	ELISA Dia Reader	Dia-lab	Austria
5	ELISA Dia Washer	Dia-lab	Austria
6	Refrigerator (-2-8 c°)	Dia-lab	Denmark

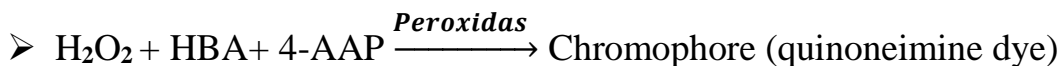
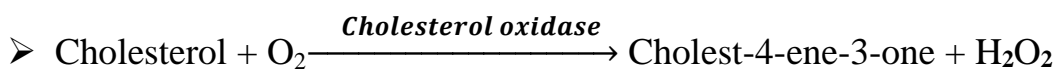
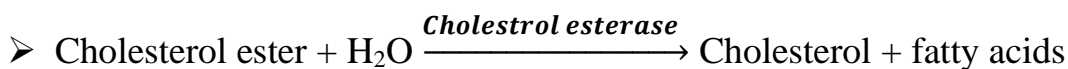
2.19 The methods

2.19.1 Measurement of Serum Cholesterol:

❖ Enzymatic Methodology

❖ Principle of Assay

- The cholesterol assay is used for the quantitation of cholesterol in human serum.



- The chromophore (a quinonimine dye) was quantitated at 500 nm.

❖ Normal Value: in serum according to (Cleeman, (2001).)

- $< 200 \text{ mg/dL} \text{-----} > \text{Desirable}$

- $200\text{-}239 \text{ mg/dL} \text{-----} > \text{Borderline}$

- $\geq 240 \text{ mg/dL} \text{-----} > \text{High}$

❖ Procedure of Assay

The Architect Abbott Laboratories device measures the Cholesterol level.

(Appendix-3)

2.19.2 Measurement of Serum Triglyceride:

❖ Methodology by Enzymatic

❖ Principle of Assay

- The Triglyceride (TG) assay is used to quantify TG in human serum.
- Triglycerides $\xrightarrow{\text{Lipase}}$ Free Fatty Acids + Glycerol
- Glycerol + ATP $\xrightarrow{\text{glycerol kinase}}$ Glycerol-3-Phosphate + ADP
- Glycerol-3-Phosphate $\xrightarrow{\text{glycerol phosphate oxidase}}$ DAP + H₂O₂
- H₂O₂ + 4-AAP + 4-CP $\xrightarrow{\text{Peroxidase}}$ Red Colored Dye
- The absorbance of this dye is proportional to the triglyceride concentration present in the sample.

❖ Normal Value: in serum according to (Cleeman, (2001).)

- < 150 mg/dL----- > **Normal**
- 150-199 mg/dL-----> **Borderline High**
- 200-499 mg/dL-----> **High**
- ≥ 500 mg/dL-----> **Very High**

❖ Procedure of Assay

The Architect Abbott Laboratories device measures the Triglyceride level.
(Appendix-4)

2.19.3 Measurement of Serum High-Density Lipoprotein:

❖ **The methodology** by Accelerator Selective Detergent.

❖ **Principle of Assay**

- The Ultra High-Density Lipoprotein (UHDL) assay is used to quantify HDL in human serum.
- The UHDL assay is a homogeneous method for directly measuring HDL cholesterol concentrations in serum.
- The method uses a 2-reagent format & properties of a special detergent.
- This method is based on accelerating the reaction of cholesterol oxidase (CO) with non-HDL un-esterified Cholesterol and dissolving HDL Cholesterol selectively using a specific detergent.
- The first reagent, Non-HDL un-esterified cholesterol, is subject to an enzyme reaction, and a peroxidase reaction consumes the peroxide generated with DSBMT, yielding a colorless product.
- the second reagent consists of a detergent (capable of solubilizing HDL cholesterol), cholesterol esterase (CE), and a chromogenic coupler to developer for the quantitative determination of HDL cholesterol.

❖ **Normal Value:** in serum according to (Cleeman, (2001).)

- $< 40 \text{ mg/dL}$ -----> **Major Risk Factor For Heart Disease.**
- $\geq 60 \text{ mg/dL}$ -----> **Negative Risk Factor For Heart Disease.**

❖ Procedure of Assay

The Architect Abbott Laboratories device measures the HDL cholesterol level. (**Appendix-5**)

2.19.4 Measurement of Serum Very Low-Density Lipoprotein-Cholesterol:

The Architect Abbott Laboratories device calculated the VLDL-C level according to Friedewald Equation. (**Friedewald, Levy & Fredrickson, 1972**).

$$\text{VLDL-C} = \text{Triglycerides}(mg/dL) / 5$$

❖ **Normal Value:** Less Than 20 mg/Dl

2.19.5 Measurement of Serum Low-Density Lipoprotein-Cholesterol :

The Architect Abbott Laboratories device calculated the LDL-C level according to Friedewald Equation. (**Friedewald, Levy & Fredrickson, 1972**).

$$\text{LDL-C} = \text{Total Cholesterol}(mg/dL) - (\text{HDL-VLDL}) mg/dL$$

Normal Value: Up to 160 mg/dL

2.19.6 Determination of Serum Creatinine Level:

Principle:

At an alkaline pH, creatinine in the sample reacts with picrate to form a creatinine-picrate complex. the rate of increase in absorbance at 500 nm due to formation of this complex is directly proportional to the concentration of creatinine in the sample (Wong, (1999).)Creatinine is the end product of creatine and creatine phosphate metabolism. Creatine is a nitrogenous organic acid that is generated predominantly in the kidney and liver, and some extent in the pancreas, using three amino acids, glycine, arginine, methionine (Kashani, 2020)

Methodology: kinetic alkaline picrate

Normal range: male (0.72-1.25mg/dl), female (0.57-1.11 mg/dl).

Table (2.5) reactive ingredients of serum creatinine level (Abbott, USA).

Reactive ingredients	Concentration
R1 sodium hydroxide	0.8 mol/L
R2 picric acid	24 mmol/L

❖ Measurement of Serum Creatinine Level

Creatinine + picric acid $\xrightarrow{\text{Alkaline ph}}$ yellow-orange complex

Procedure: 100 microliter of separated serum was placed in cuvate to be analyzed.

Calculations

The concentration of the serum creatinine is measured automatically by using architect Abbott c4000 chemistry analyzer.

2.19.7 Determination of Serum Urea Level

Principle:

The urea nitrogen assay is a modification of a totally enzymatic procedure first described by Talke and Schubert (Talke, (1965).)

The test is performed as a kinetic assay in which the initial rate of the reaction is linear for a limited period of time. Urea in the sample is hydrolyzed by urease to ammonia and carbon dioxide.

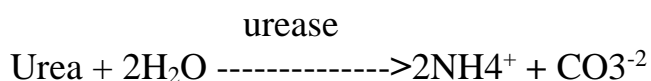
The second reaction, catalyzed by glutamate dehydrogenase (GLD) converts ammonia and α -ketoglutarate to glutamate and

water with the concurrent oxidation of reduced nicotinamide adenine dinucleotide (NADH) to nicotinamide adenine dinucleotide (NAD). Two moles of NADH are oxidized for each mole of urea present. The initial rate of decrease in absorbance at 340 nm is proportional to the urea concentration in the sample (Abbott, USA).

Table (2.6) Reactive ingredients of serum urea level (Abbott, USA).

Reactive ingredients	Concentration
R1 NADH	2.95mmol/L
R2 α -ketoglutaric acid	99.8 mmol/L
urease (jack bean)	23.5KU/L
GLD (beef liver)	63.5 KU/L
Adenosine diphosphate	7.6 mmol/L

❖ Measurement of Serum Urea Level



The rate of decrease in the NADH concentrations is directly proportional to the urea concentration in the specimen. It is determined by measuring the absorbance at 340 nm.

Procedure:

100 μ L of separated serum was putted in cuvate to be analyzed.

Calculations

The concentration of the serum urea measured automatically by using architect Abbott c4000 chemistry analyzer.

Normal range: male (17-53mg/dl), female (15-42.8mg/dl).

2.19.8 Measurement of Serum CHI3L1

❖ Principle of Assay

Here's a revised version of the text:

1. This sandwich ELISA kit is designed for the precise quantitative detection of human CHI3L1 in serum.
2. The kit employs an enzyme-linked immunosorbent assay (ELISA) technique.
3. The plate comes pre-coated with human CHI3L1 antibodies.
4. When CHI3L1 is present in the sample, it binds to the antibodies on the wells.
5. A biotinylated anti-human CHI3L1 antibody is then added, which binds to the captured CHI3L1 in the sample.
6. Streptavidin-HRP is added, which links to the biotinylated CHI3L1 antibody.
7. The plate is incubated to allow the binding reactions to occur.
8. Any unbound Streptavidin-HRP is washed away during a washing step.
9. A substrate solution is added, causing a color change proportional to the amount of CHI3L1 present in the sample.
10. The reaction is terminated by adding an acidic stop solution, and the absorbance is measured at 450 nm.

❖ Preparation of Reagent

Here's a revised version of the text:

1. Before use, all reagents (samples and standards) are brought to room temperature.
2. Reconstitution of 120 μL of the standard (480 ng/mL) with 120 μL of standard diluent to create a 240 ng/mL standard solution. Allow the solution to sit for 15 minutes with gentle agitation before further dilution.
3. Creation of duplicate standard points by serially diluting the stock standard solution (240 ng/mL) in a 1:2 ratio with standard diluent to produce concentrations of 120 ng/mL, 60 ng/mL, 30 ng/mL, and 15 ng/mL. The standard diluent serves as the zero standard (0 ng/mL).
4. Storing any residual solution at -20°C and use it within one month.

The dilution of standard solutions suggested are as follows :

Table (2.7) Serial dilution of Standard CHI3L1

240ng/ml	Standard No.5	120 μl Original Standard + 120 μl Standard Diluent
120ng/ml	Standard No.4	120 μl Standard No.5 + 120 μl Standard Diluent
60ng/ml	Standard No.3	120 μl Standard No.4 + 120 μl Standard Diluent
30ng/ml	Standard No.2	120 μl Standard No.3 + 120 μl Standard Diluent
15ng/ml	Standard No.1	120 μl Standard No.2 + 120 μl Standard Diluent

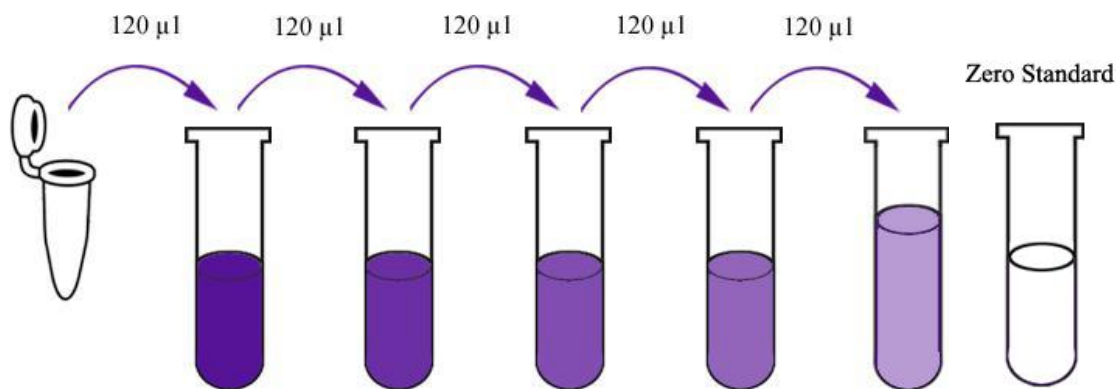


Fig (2.2) Serial dilution of Standard CHI3L1

❖ **Wash Buffer**

- 20 mL of wash buffer concentrate 25x was added into Graduated Cylinder.
- 480 mL of distilled water (D.W) was added into Graduated Cylinder to yield 500 mL wash buffer dilute.
- 500 mL of wash buffer dilute in a Graduated Cylinder was added into the washing bottle ELISA.

❖ **Procedure of Assay**

- 50µl of standard (St1– St6) was added to standard well (A1–F1) only.
- 40µl of sample (S1–S90) was added to sample wells (G1–H12) only.
- 10µl of anti-CHI3L1 antibody was added to sample wells.
- 50µl of streptavidin-HRP was added to sample & standard wells.
- Mix wells.
- The plate was covered with a new sealer.
- The plate was incubated at 37 °C for 60 minutes.
- The sealer was removed from the plate.
- The plate was washed with the wash buffer five times & blot the plate onto paper towels.
- 50µl of the substrate solution A & 50µl of the substrate solution B was added into each well.

- The plate was covered with a new sealer.
- The plate remained incubated in the dark at 37 °C for 10 minutes.
- 50 μ l of the stop solution in each well, the blue colour will change into yellow immediately.
- The plate was directly added to a microplate reader ELISA & set to 450nm.
- Optical density (O.D value) is to be read to determine the absorption level of each well.
- The results with the graphic curve stander was to be printed.

❖ **Calculation of the result:**

The concentration of serum CHI3L1, as well as the absorption and concentration of the standard, are evaluated using a standard curve generated by the ELISA Dia Reader, as shown in Table 2.8

The standard curve is created by plotting the average optical density (O.D) for each standard on the vertical (Y) axis versus the concentration on the horizontal (X) axis. A best-fit curve is then drawn through the data points.

Table (2.8) The standard curve of Human CHI3L1

No. of Standard (st)	Concentration Of Standard Curve	Optical Density (O.D)
St ₁	0 ng/ml	0.064
St ₂	15 ng/ml	0.884
St ₃	30 ng/ml	0.377
St ₄	60ng/ml	0.577
St ₅	120 ng/ml	1.111
St ₆	240 ng/ml	2.017

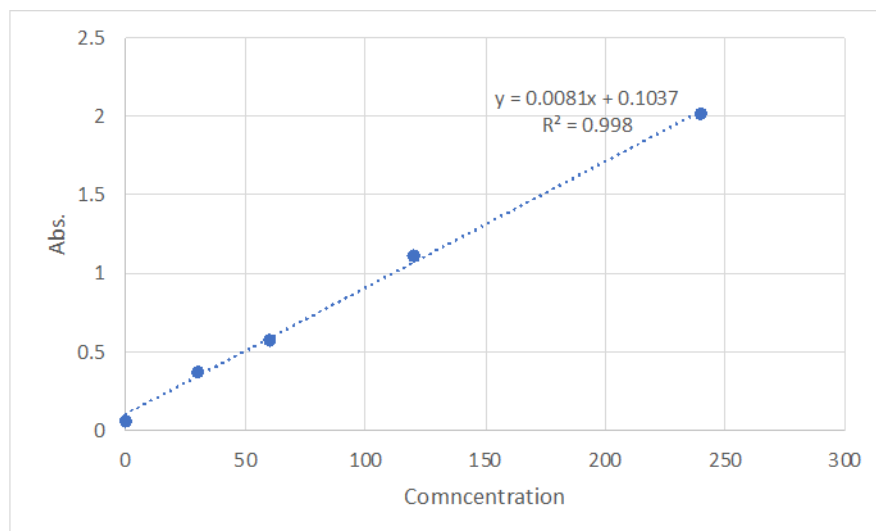


Figure (2.3) The standard curve of Human CHI3L1

Appendix-6

2.19.9 Measurement of Serum KIM 1

Principle of the Assay:

Here's a revised version of the text:

- This sandwich kit is designed for the precise quantitative detection of human KIM-1 in serum.
- The ELISA kit uses an enzyme-linked immunosorbent assay.
- The plate is pre-coated with human KIM-1 antibodies.
- KIM-1 in the sample binds to the antibodies on the wells.
- A biotinylated anti-human KIM-1 antibody is added, which binds to the captured KIM-1 in the sample.
- Streptavidin-HRP is added and links to the biotinylated KIM-1 antibody.
- The plate is incubated to allow binding reactions to occur.
- Unbound Streptavidin-HRP is washed away during the washing step.

- A substrate solution is added, resulting in a color change proportional to the amount of KIM-1 present in the sample.
- The reaction is terminated by adding an acidic stop solution, and the absorbance is recorded at 450 nm.

Preparation of Reagents:

Here's a revised version of the text:

- Before use, bring all reagents (samples and standards) to room temperature.
- Reconstitute 120 μ L of the standard (12.8 ng/mL) with 120 μ L of standard diluent to create a 6.4 ng/mL standard stock solution. Allow the solution to sit for 15 minutes with gentle agitation before further dilution.
- Create duplicate standard points by serially diluting the stock standard solution (6.4 ng/mL) in a 1:2 ratio with standard diluent to produce concentrations of 3.2 ng/mL, 1.6 ng/mL, 0.8 ng/mL, and 0.4 ng/ml. The standard diluent serves as the zero standard (0 ng/mL).
- Store any residual solution at -20°C and use it within one month.

The dilution of standard solutions suggested are as follows :

Table (2.9) Serial dilution of Standard KIM 1

6.4ng/ml	Standard No.5	120 μ l Original Standard + 120 μ l Standard Diluent
3.2ng/ml	Standard No.4	120 μ l Standard No.5 + 120 μ l Standard Diluent
1.6ng/ml	Standard No.3	120 μ l Standard No.4 + 120 μ l Standard Diluent
0.8ng/ml	Standard No.2	120 μ l Standard No.3 + 120 μ l Standard Diluent
0.4ng/ml	Standard No.1	120 μ l Standard No.2 + 120 μ l Standard Diluent

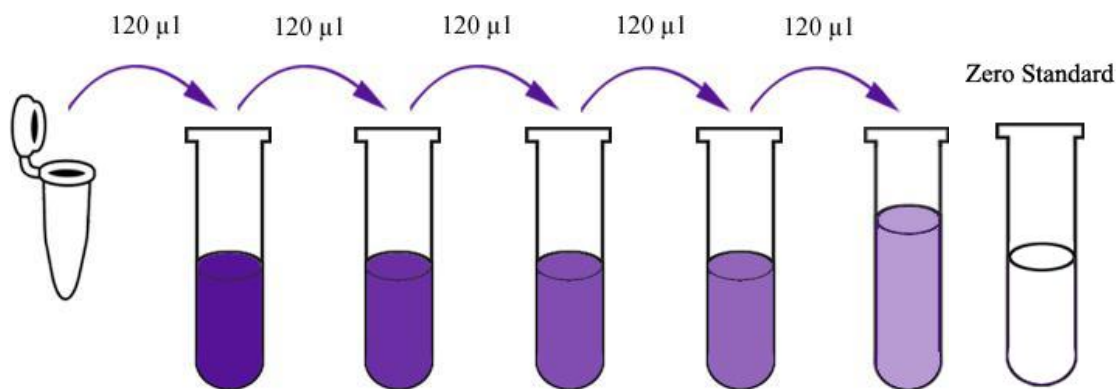


Fig (2.4) Serial dilution of Standard KIM 1

❖ **Wash Buffer**

- 20 mL of wash buffer concentrate 25x was added into Graduated Cylinder.
- 480 mL of distilled water (D.W) was added into Graduated Cylinder to yield 500 mL wash buffer dilute.
- 500 mL of wash buffer dilute in a Graduated Cylinder was added into the washing bottle ELISA.

❖ **Procedure of Assay**

- 50µl of standard (St1– St6) was added to standard well (A1–F1) only.
- 40µl of sample (S1–S90) was added to sample wells (G1–H12) only.
- 10µl of anti-KIM 1 antibody was added to sample wells.
- 50µl of streptavidin-HRP was added to sample & standard wells.
- Mix wells.
- The plate was covered with a new sealer.
- The plate was incubated at 37 °C for 60 minutes.
- The sealer was removed from the plate.
- The plate was washed with the wash buffer five times & blot the plate onto paper towels.

- 50 μ l of the substrate solution A & 50 μ l of the substrate solution B was added into each well.
- The plate was covered with a new sealer.
- The plate remained incubated in the dark at 37 °C for 10 minutes.
- 50 μ l of the stop solution in each well, the blue colour will change into yellow immediately.
- The plate was directly added to a microplate reader ELISA & set to 450nm.
- The optical density (O.D value) is to be read to determine the absorption level of each well.
- The results with the graphic curve stander is to be printed.

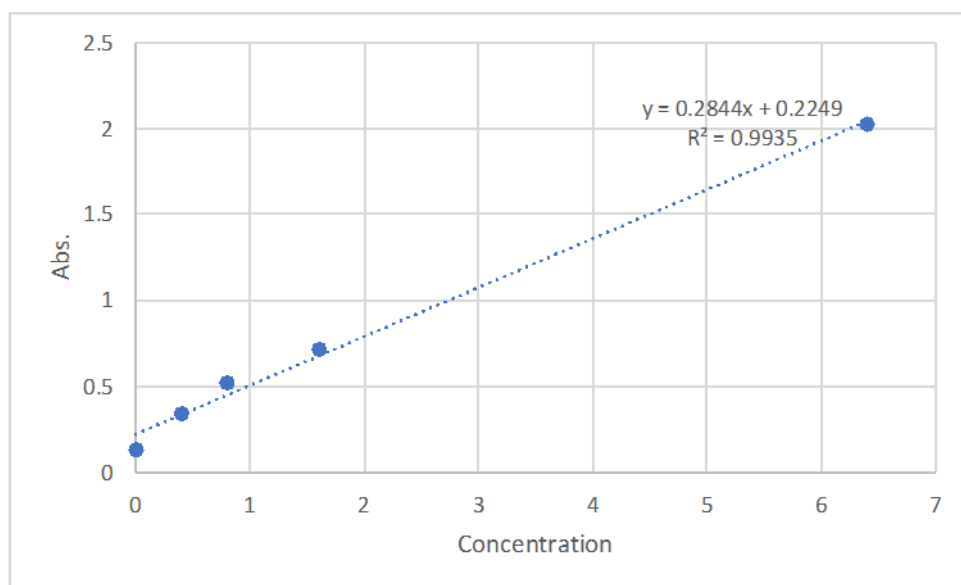
❖ Calculation of the result

The concentration of serum KIM 1 and absorption & concentration of standard is evaluated by a standard curve by the ELISA Dia Reader as shown in the table 2.10

The standard curve is calculated by graphing the average O.D for every standard on the vertical (Y) line versus the concentration on the horizontal (X) line & draw a best-fit curve through the points

Table (2.10) The standard curve of Human KIM 1

No. of Standard (st)	Concentration Of Standard Curve	Optical Density (O.D)
St ₁	0 ng/ml	0.135
St ₂	0.4 ng/ml	0.341
St ₃	0.8 ng/ml	0.521
St ₄	1.6 ng/ml	0.917
St ₅	3.2 ng/ml	1.451
St ₆	6.4 ng/ml	2.027

**Figure (2.5) The standard curve of Human KIM 1****Appendix-7**

2.19.10 Measurement of Serum NGAL

❖ Principle of Assay

Here's a revised version of the text:

- ❖ This sandwich kit is intended for the precise quantitative detection of Human NGAL in serum.
- ❖ The ELISA kit is an enzyme-linked immunosorbent assay.
- ❖ The Human NGAL antibody has been pre-coated on the plate.
- ❖ The NGAL in the sample is added and binds to antibodies coated on the wells.
- ❖ A biotinylated human NGAL Antibody is added and binds to NGAL in the sample.
- ❖ Streptavidin-HRP was added & linked to the biotinylated NGAL antibody.
- ❖ The plate was incubated.
- ❖ Unbound Streptavidin-HRP has washed away during a washing step.
- ❖ A substrate solution was added, and colour developed proportionately to the amount of human NGAL.
- ❖ The reaction is terminated by adding an acidic stop solution, and 450 nm absorbance is recorded.

Preparation of Reagent

Here's a revised version of the text:

- ❖ Before use, all reagents (sample and standard) are brought to room temperature.
- ❖ Reconstitution of 120 μ L of the standard (640ng/ml) plus 120 μ l of standard diluent to form an 320ng/ml Standard stock solution. Leaving the standard to sit for 15 minutes with gentle agitation before diluting. Creating duplicate

standard points by serially diluting the stock standard solution (320ng/ml) 1:2 with standard diluent to produce 160ng/ml, 80ng/ml, 40ng/ml and 20ng/ml solutions. The standard diluent acts as the zero standards (0 ng/mL) Fig.2.6. Any residual solution is refrigerated at -20 degrees Celsius and utilized within one month.

The dilution of standard solutions suggested are as follows :

Table (2.11) Serial dilution of Standard NGAL

320ng/ml	Standard No.5	120µl Original Standard + 120µl Standard Diluent
160ng/ml	Standard No.4	120µl Standard No.5 + 120µl Standard Diluent
80ng/ml	Standard No.3	120µl Standard No.4 + 120µl Standard Diluent
40ng/ml	Standard No.2	120µl Standard No.3 + 120µl Standard Diluent
20ng/ml	Standard No.1	120µl Standard No.2 + 120µl Standard Diluent

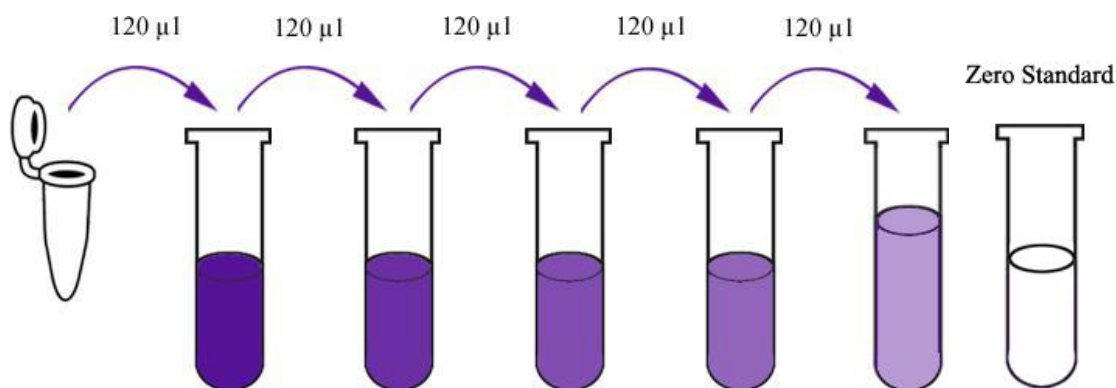


Fig (2.6) Serial dilution of Standard NGAL

❖ Wash Buffer

- 20 mL of wash buffer concentrate 25x was added into Graduated Cylinder.
- 480 mL of distilled water (D.W) was added into Graduated Cylinder to yield 500 mL wash buffer dilute.
- 500 mL of wash buffer dilute in a Graduated Cylinder was added into the washing bottle ELISA.

❖ Procedure of Assay

- 50 μ l of standard (St1– St6) was added to standard well (A1–F1) only.
- 40 μ l of sample (S1–S90) was added to sample wells (G1–H12) only.
- 10 μ l of anti-KIM 1 antibody was added to sample wells.
- 50 μ l of streptavidin-HRP was added to sample & standard wells.
- Mix wells.
- The plate was covered with a new sealer.
- The plate was incubated at 37 °C for 60 minutes.
- The sealer was removed from the plate.
- The plate was washed with the wash buffer five times & blot the plate onto paper towels.
- 50 μ l of the substrate solution A & 50 μ l of the substrate solution B was added into each well.
- The plate was covered with a new sealer.
- The plate remained incubated in the dark at 37 °C for 10 minutes.
- 50 μ l of the stop solution in each well, the blue colour will change into yellow immediately.
- The plate was directly added to a microplate reader ELISA & set to 450nm.
- The optical density (O.D value) is to be read to determine the absorption level of each well.
- The results with the graphic curve stander is to be printed.

Calculation of the Result:

The concentration of serum NGAL, as well as the absorption, and concentration of the standard, are evaluated using a standard curve generated by the ELISA Dia Reader as shown in the table 2.12.

The standard curve is created by plotting the average O.D. for every standard on the vertical (Y) line versus the concentration on the horizontal (X) line axis. A best-fit curve is then drawn through the data points.

Table (2.12) The standard curve of Human NGAL

No. of Standard (st)	Concentration Of Standard Curve	Optical Density (O.D)
St ₁	0	0.077
St ₂	20	0.115
St ₃	40	0.121
St ₄	80	0.204
St ₅	160	0.296
St ₆	320	0.624

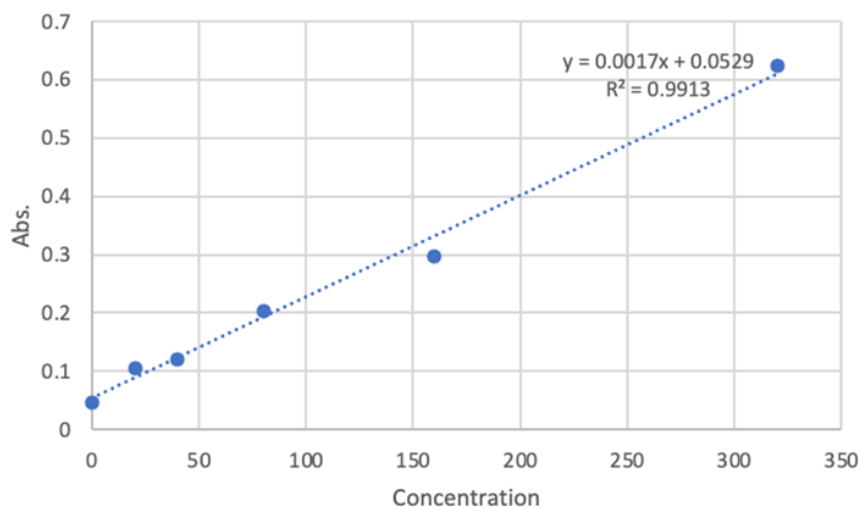


Figure (2.7) The standard curve of Human NGAL (Appendix-8)

2.20 Statistical Analysis

Information from the questionnaire and all test results from the study group samples were entered into a data sheet. The data analysis was performed using GraphPad Prism.

Descriptive statistics were conducted on the data from each group. Values were illustrated as n (%) for categorical variables. For scale variables, the mean \pm standard deviation (mean \pm SD) was used for normal data. The normality of the data distribution was assessed using the Shapiro-Wilk test.

Significant differences in categorical variables among the parameters were confirmed through analytical statistical tests. Hypothesis tests with p-values < 0.05 (two-sided) were considered statistically significant.

The simultaneous confidence level for each of the confidence intervals was calculated using Fisher's LSD technique. This simultaneous confidence level represents the probability that all confidence intervals contain the true difference.

The optimal threshold, with high specificity and sensitivity for the study cases, was determined using Receiver Operating Characteristic (ROC) analysis.

Chapter Three

Results

and

Discussion

Results and Discussion :**3.1. Demographics of patients group with Autosomal Dominant Polycystic Kidney Disease (ADPKD).**

We studied the demographic characteristics of the study group, which included 36 females (42.4%) and 49 males (57.6%). The median age of the participants was 60 years, with an age range spanning from 8 to 84 years. The mean age was recorded as 55.4 years.

The median BMI was 29.06 cm/kg, with values ranging from 16.5 to 47.7 cm/kg, and the mean BMI was 29.7 cm/kg, suggesting a prevalence of overweight or obesity within the group. The median systolic blood pressure was 130 mmHg, and the median diastolic blood pressure was 80 mmHg.

Regarding kidney cysts, the median size of the largest right kidney cyst was 2.8ml, with a range of 0.5 to 15 ml, and the mean size was 3.57 ml. For the left kidney, the median size of the largest cyst was 2.9 ml, with a range of 0.7 to 11 ml, and the mean size was 3.29 ml.

In terms of kidney function, the median urea level was 52.5 mg/dl, with a wide range from 1.23 mg/dl to 205 mg/dl. The mean urea level was 68.1 mg/dl. The median creatinine level was 1.57 mg/dl, with a range from 0.57 mg/dl to 8.09 mg/dl, and the mean creatinine level was 2.32 mg/dl. The median estimated glomerular filtration rate (eGFR) was 35.7 ml/min/1.73 m², with values ranging from 5.94 to 171.1 ml/min/1.73 m², and the mean eGFR was 40.1 ml/min/1.73 m². Table 3.1 provides a detailed overview of the demographic characteristics of the study group .

Table (3.1) Demographic characteristic of the study group

Variable	Median	Minimum	Maximum	Mean \pm2SD
Age (years)	60	8	84	55.4 \pm 19.2
BMI (Kg/cm)	29.06	16.5	47.7	29.7 \pm 6.68
SBP (mmhg)	130	80	180	128.7 \pm 19.7
DBP (mmhg)	80	50	110	81.2 \pm 13.5
Largest Rt kidney cyst (ml)	2.8	0.5	15	3.57 \pm 2.84
Largest Lt kidney cyst (ml)	2.9	0.7	11	3.29 \pm 2.28
Urea mg/dl	52.5	1.23	205	68.1 \pm 47.0
Creatinine mg/dl	1.57	0.57	8.09	2.32 \pm 1.89
eGFR (ml/min/1.73 m²)	35.737	5.9457	171.11	40.1 \pm 31.7
Sex No. of patients (%)	Female	36 (42.4%)		
	Male	49 (57.6%)		

BMI: body mass index, SBP: systolic blood pressure, DBP: diastolic blood pressure, Rt: right, Lt: left.

The demographic and clinical findings in this study on ADPKD align closely with existing literature. The observed median age, slight male predominance, high BMI indicating obesity, and the prevalence of hypertension are consistent with studies like the CRISP study (Consortium for Radiologic Imaging Studies of Polycystic Kidney Disease) (Bae, 2024) and those by (Schrier, 2014) and (Johnson, 2011). These factors are well-documented in ADPKD patients, highlighting the common challenges in

managing this disease. Kidney cyst sizes and the wide variability in renal function markers (urea, creatinine, eGFR) also align with findings from (Grantham, 2006) and (Irazabal, 2015), reflecting the heterogeneity of ADPKD. However, the slight male predominance and the variability in eGFR ranges observed in this study may differ from some global studies, such as those by (Peter and torres, 2014), which could be due to regional or sample-specific factors. Overall, this study supports the broader understanding of ADPKD, particularly in the regional context, emphasizing the importance of managing hypertension and monitoring renal function to mitigate disease progression. Further research could explore these regional differences and their implications for patient care.

3.2. Medical History of the Study Group

Regarding medical history of the study group, a significant portion of the participants (65.9%) reported a family history of autosomal dominant polycystic kidney disease (ADPKD). Additionally, 36.5% of the group had at least one chronic disease. Regarding kidney function, 16.5% of participants had undergone kidney surgery, including procedures such as nephrectomy, stone and cyst removal, or stone removal alone. Only 8.2% had previously undergone dialysis. Organomegaly, affecting the liver and spleen, was observed in 10.6% of the participants, while 18.8% had cysts in the liver and pancreas. A substantial proportion (71.8%) were on anti-hypertensive therapy, indicating a high prevalence of hypertension within the group. Interestingly, 10.6% of participants were being treated with Tolvaptan, a medication specifically used to manage kidney cysts in ADPKD. These findings suggest that Tolvaptan may be an emerging treatment option for some individuals with this condition.

This study, found that 65.9% of participants had a family history of ADPKD, consistent with findings by Torres et al. (2007), underscoring its genetic nature. Hypertension was prevalent in 71.8% of the group, aligning with (Schrier, 2014), highlighting the need for blood pressure management. A smaller proportion (16.5%) underwent kidney surgery, and 8.2% had prior dialysis, suggesting earlier stages of the disease, consistent with (Irazabal, 2015). The presence of organomegaly and other cysts (10.6% and 18.8%) aligns with (Chapman, 2015), while 10.6% treated with Tolvaptan mirrors findings by (Peter and torres, 2014)

Kidney stones were present in 44.7% of right kidneys and 51.8% of left kidneys, exceeding the prevalence reported by (Peter and torres, 2014), Nephrectomy was performed in 3.5% of right kidneys and 7% of left kidneys, reflecting advanced disease stages, consistent with surgical interventions noted by (Chapman, 2015). Agenesis (failure of kidney to develop during embryonic growth) was observed in one participant (1%) of left kidneys.

Table (3.2) Medical history among 85 patient with Autosomal Dominant Polycystic Kidney Disease (ADPKD)

Variable	No n. (%)	Yes n. (%)
Family History	29 (34.1%)	56 (65.9%)
Anti-Hypertensive Therapy	24 (28.2%)	61 (71.8%)
Chronic Disease	54 (63.5%)	31 (36.5%)
Kidney Surgery	71 (83.5%)	14 (16.5%)
Previously Dialysis	78 (91.8%)	7 (8.2%)
Organomegaly	76 (89.4%)	9 (10.6%)
Other Cysts	69 (81.2%)	16 (18.8%)
Treated with Tolvaptan(30-60mg/day)	63 (74.1%)	9 (10.6%)
Previously treated	13 (15.3%)	
Left kidney stones		
Agenesis	1 (1 %)	
Nephrectomy	6 (7 %)	
No	34 (40%)	
Yes	44 (51.8%)	
Right kidney stones		
Nephrectomy	3 (3.5%)	
No	44 (51.8%)	
Yes	38 (44.7%)	

*No represent number of patients

3.3. Study the Kidney Characteristics ADPKD

Regarding height-adjusted total kidney volume (htTKV) among patients with ADPKD, the patients were classified into three groups: increased (>400 ml/m²), decreased (<200 ml/m²), and normal (200-400 ml/m²). The findings show that 18.8% and 17.6% of patients had increased right and left kidney volumes, respectively, while 22% had increased htTKV. The majority, 63.5% for the right kidney, 64.7% for the left kidney, and 61% for htTKV, fell within the normal range. A smaller percentage, 17.6% for the right kidney, 18.8% for the left kidney, and 16% for htTKV, had decreased volumes.

The findings suggest that the majority of ADPKD patients maintain normal kidney volumes, consistent with studies such as (Irazabal, 2015). The presence of increased kidney volumes in approximately 18% of patients aligns with the understanding that as ADPKD progresses, cyst growth leads to kidney enlargement, as supported by (Peter and torres, 2014), The relatively small percentage of patients with decreased kidney volumes may indicate early-stage ADPKD or slower disease progression, as noted in studies by (Grantham, 2006). The htTKV findings closely reflect individual kidney volumes, underscoring its importance as a predictive metric for disease progression.

Table 3.3 categorizes the kidney volume and height-adjusted total kidney volume (htTKV) among patients with ADPKD

The rationale for categorizing kidney volumes and htTKV is based on the need to assess disease progression in ADPKD effectively. htTKV, which adjusts kidney volume for patient height, offers a more individualized metric for monitoring disease burden, as recommended by (Chapman, 2015). The distribution of increased, normal, and decreased kidney volumes in this study provides insights into the stages of ADPKD among patients. Monitoring htTKV alongside kidney volume allows for a more comprehensive understanding of disease severity and potential progression, aiding in better clinical decision-making and potentially guiding interventions to slow the progression of ADPKD.

Table (3.3) Categories of patients based on their htTKV.

Category of kidney volume	Right kidney volume*	Left kidney volume*	htTKV*
Increased	16(18.8%) (>190 ml men, >150 m female)	15(17.6%) (>190 ml men, >150 m female)	19(22%) (>400ml/m ²)
Decreased	15(17.6%) (<110 ml men, <90 ml female)	16(1%) (<110 ml men, <90 ml female)	14(16%) <200ml/m ²)
Normal	54(61%) (110- 190 ml men,90- 150 m female)	55(64.7%) (110- 190 ml men, 90- 150 m female)	52(61%) (200-400ml/m ²)

Numbers represents patients number for each category

The mean eGFR and standard deviation for each group (of the three htTKV groups) are presented, alongside the 95% confidence intervals and the p-value from the ANOVA test. The p-value of 0.04 indicates a statistically significant difference in eGFR across the htTKV categories, suggesting that htTKV has a significant impact on kidney function, as measured by eGFR, with lower htTKV associated with better kidney function.

Table 3.4 summarizes the relationship between htTKV categories and eGFR values.

The table demonstrates a clear association between htTKV and eGFR, indicating that patients with higher htTKV levels tend to have lower eGFR values, reflecting poorer kidney function. The significant p-value (0.04) supports the hypothesis that these differences are not due to chance, but rather represent a real effect of htTKV on kidney function. The confidence intervals suggest that there is some variability in eGFR within each group, particularly in the Normal and Increased htTKV categories, but the overall trend remains consistent with the expected pathophysiological relationship.

Table (3.4) The relation between eGFR and normal, increased, and decreased htTKV

htTKV Category	eGFR (ml/min/ 1.73 m ²) Mean± SD	95% CI (Lower - Upper)	P value
Increased htTKV >400 ml/m ²	39.06±14.92	22.9 (16.1-62.1)	0.04
Decreased htTKV <200 ml/m ²	24.93±12.4	11.7 (13.2-36.7)	
Normal htTKV (200-400) ml/m ²	43.06±19.1	8.19 (34.9-51.3)	

htTKV: height adjusted total kidney volume, eGFR: estimated glomerular filtration rate, CI: confidence interval.

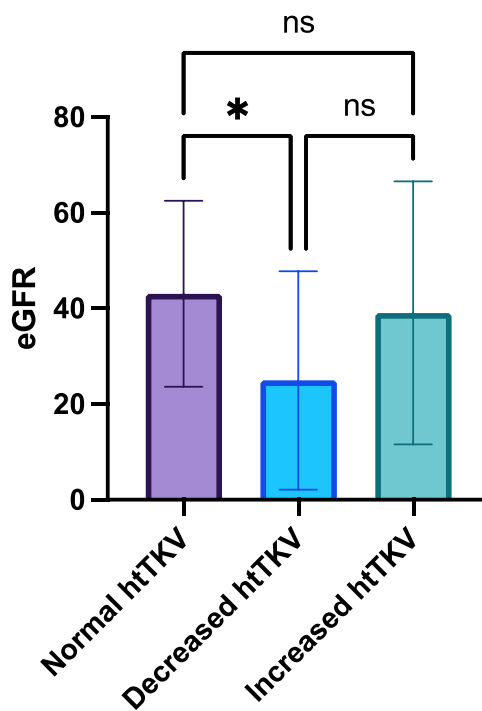


Figure (3.1) Mean Differences of the eGFR in patients groups of ADPKD based on their height adjusted total kidney volume.

htTKV: height adjusted total kidney volume, eGFR: estimated glomerular filtration rate

3.4. Study of Lipid Profile in ADPKD Patients

In aim to study the lipid profile of the study group we found that the mean triglyceride (TG) level was 151.18 mg/dl, indicating a potential elevation. The mean HDL level was 38.69 mg/dl, showing moderate variability, while the mean LDL and VLDL levels were 73.18 mg/dl and 30.32 mg/dl, respectively. Non-HDL cholesterol had a mean of 104.48 mg/dl. These findings align with research suggesting that dyslipidemia frequently coexists with ADPKD, potentially influencing disease progression (Fliszkiewicz, 2019) (Torres, 2011) (Mallett, 2015) (Ecdler, 2016).

Table 3.5 presents the mean lipid profile levels in a group of patients with ADPKD.

Table (3.5) Mean \pm Standard deviation of the lipid profile of the studied patients

	TG(mg/dl)	HDL(mg/dl)	LDL(mg/dl)	VLDL(mg/dl)	nonHDL-c (mg/dl)
Mean\pm2SD	151.18 \pm 48.	38.69 \pm 6.86	73.18 \pm 31.4	30.32 \pm 9.81	104.48 \pm 29.40

SD: standard deviation, TG: triglyceride, HDL: high density lipoprotein, LDL: low density lipoprotein, VLDL: very low density lipoprotein, nonHDL-c: non-high density lipoprotein cholesterol.

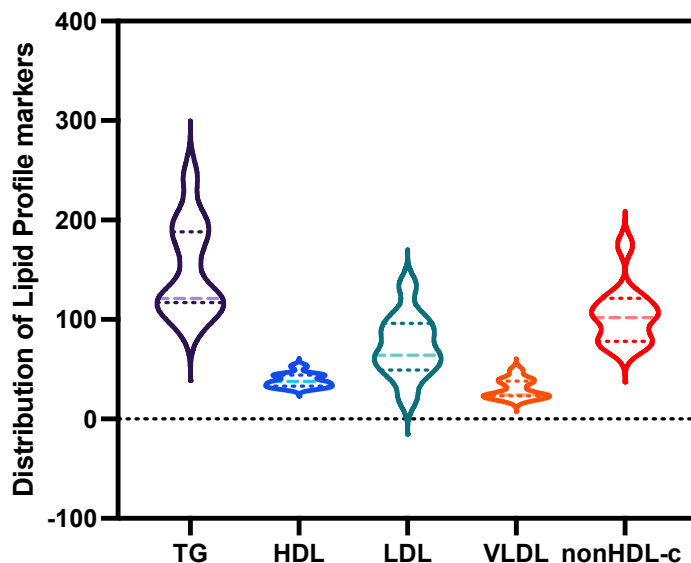


Figure (3.2) Violin boxplot to demonstrate the density of Lipid profile Levels among the studied patients

TG: triglyceride, HDL: high density lipoprotein, LDL: low density lipoprotein, VLDL: very low density lipoprotein, nonHDL-c: non-high density lipoprotein cholesterol.

3.5. Study the Atherogenic Indices in ADPKD

We studied the atherogenic indices in the study group and the results showed that the mean AC level was 2.80, The mean of AIP level was 0.57, A higher AC and AIP both indicates a greater risk of atherosclerosis.

CRI-I & CRI-II which used to estimate the 10-year risk of coronary heart disease were also calculated, the mean level of CRI-I was 3.80 and CRI-II mean was 1.97 with an 2SD of 1.01.

Table 3.6 summarizes the mean values of various atherogenic indices in a group of patients with ADPKD.

Table (3.6) Mean differences of atherogenic indices Levels among the studied patients

	(AC)	(AIP)	CRI-I	CRI-II
Mean \pm2SD	2.80 \pm 1.03	0.57 \pm 0.15	3.80 \pm 1.03	1.97 \pm 1.01

SD: standard deviation, AC: atherogenic coefficient, AIP: Atherogenic index of plasma, CRI-I: Castelli's risk index 1, CRI-II: Castelli's risk index 2.

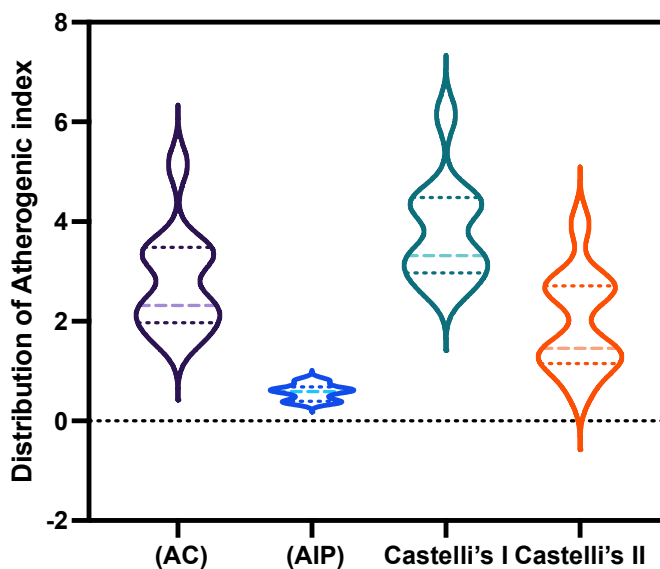


Figure (3.3) Violin boxplot to demonstrated the density of atherogenic indices among the studied patients

AC: atherogenic coefficient, AIP: Atherogenic index of plasma, CRI-I: Castelli's risk index 1, CRI-II: Castelli's risk index 2.

Only a few studies were reported the mean difference of atherogenic indices among patients group of kidney disease, but neither them were mention their role in ADPKD

According to (Oh, 2023) AIP was also connected to a lipid-related complication in cases of nephrotic syndrome.

AIP is a predictor of subclinical renal impairment, which is defined as an eGFR between 30 and 60 mL/min/1.73 m², according to recent research. (Huang, 2021) Additionally, the ratio of non-HDL-C to HDL-C is known as the atherogenic coefficient (AC). It is an alternate diagnostic method that has been applied to forecast the likelihood of experiencing cardiovascular events. (Olamoyegun, 2016)

Additionally, there are two lipid ratios known as Castelli's risk indexes (I & II) termed cardiac risk indexes. The CRI-I is the ratio of TC to HDL-C, while the CRI-II is the ratio of LDL-C to HDL-C. Both have notably favourable relationships with CVD. (Igharo, 2020). Numerous studies evaluated and verified their favourable association with 85, Chapter Four Discussion CVD (Tecer, 2019). Conversely, C-index, has been described as a straightforward indicator that more accurately predicts the likelihood of getting CAD than any other indicator. (Ulusoy, 2013)

In general, it is yet unknown how dyslipidaemia can potentially hasten the course of renal illness. One theory is that dyslipidaemia is linked to an increase in tubular epithelial cells' reabsorption of cholesterol and phospholipids. Tissue damage, foam cell production, and tubulointerstitial inflammation may all be triggered by this reabsorption. Furthermore, elevated lipoprotein levels may promote the production of proinflammatory cytokines, which would lead to glomerulosclerosis. (Keane, 1993)

It was initially hypothesized that PKD progression and aberrant lipid metabolism were related, using rat models as evidence. In a non-orthologous ADPKD model, eating a lot of fat increased the size of the kidneys and the scores for cysts and renal fluid. (Jayapalan S, 2000). In mice lacking Pkd1 and Pkd2, aberrant lipid metabolism has also been seen.

Significantly, apolipoprotein levels were elevated in cystic kidneys due to upregulation of genes governing apolipoprotein synthesis and transport; these modifications were linked to changes in the activation of the nuclear hormone receptor, hepatocyte nuclear factor-4. (Allen E, 2006) On the other hand, it was demonstrated that the polycystic kidneys had a markedly reduced level of apoA1, a critical component of the high-density lipoprotein complex. (Yoo KH, 2009) In the Consortium for Radiologic Imaging Studies of Polycystic Kidney Disease (CRISP) cohort research, clinical observations during a 6-year follow-up period revealed an inverse association between blood HDL-cholesterol levels and the pace of kidney expansion as well as the drop-in glomerular filtration rate (GFR). (Torres VE, 2011) It is unknown how having greater HDL levels provides protection. Due to its involvement in reverse cholesterol transfer, HDL possesses strong anti-atherogenic properties. Through its recognized interactions with the Class B Type 1 scavenger receptor and the sphingosine-1-phosphate receptor family, it may also have anti-inflammatory effects. Regardless of the exact mechanism, HDL is a theoretically modifiable component that slows the development of the kidney and the deterioration of renal function. (Schrier RW, 2010)

3.6. Study the Kidney damage Biomarkers in ADPKD

By studying the kidney damage biomarkers in the study group, our study found that the mean Kidney Injury Molecule-1 (KIM-1) level was 2.4 ± 1.9 ng/ml, indicating damage to the proximal tubules. The mean Neutrophil Gelatinase-Associated Lipocalin (NGAL) level was 117.3 ± 43.4 ng/ml, reflecting ongoing inflammation in the kidneys. The mean Chitinase-3-like protein 1 (CHI3L1) level was 451.3 ± 200.0 ng/ml, indicating damage to the distal tubules.

Table 3.7 presents the mean values and standard deviations of three kidney damage biomarkers in a group of ADPKD patients.

These biomarkers collectively highlight the extent of kidney injury and inflammation in the ADPKD patient population.

The elevated levels of KIM-1, NGAL, and CHI3L1 in this study align with findings from (Huang, 2020), who identified NGAL as a marker of subclinical renal impairment in nephrotic syndrome, suggesting its relevance in ADPKD as well. The higher NGAL levels observed here are consistent with the inflammatory state associated with cystic kidney diseases, as reported by (Zhiguo Mao, 2015), who highlighted the role of oxidative stress in kidney damage.

Similarly, elevated KIM-1 levels in this study support the findings of (Schrier, 2010), who reported increased oxidative stress and subsequent tubular injury in early ADPKD. The higher CHI3L1 levels are consistent with the observations of (Jayapalan, 2000), who demonstrated that lipid dysregulation and inflammation contribute to distal tubular damage.

However, this study's NGAL and CHI3L1 levels are somewhat higher than those reported by (Brookes, 2013), possibly due to differences in patient population or disease stage. The variation in biomarker levels could reflect the degree of kidney involvement and the severity of cystic disease in the studied cohort. Overall, these biomarkers provide valuable insights into the underlying mechanisms of kidney damage in ADPKD and reinforce the importance of monitoring these indicators in clinical practice.

Table (3.7) Mean differences of KIM-1, NGAL and CHI3L1 Levels among the studied patients

	KIM-1 (ng/ml)	NGAL (ng/ml)	CHI3L1 (ng/ml)
Mean ±2SD	2.4 ±1.9	117.3 ±43.4	451.3 ±200.0

SD: standard deviation, NGAL: Neutrophil gelatinase-associated lipocalin, KIM-1: kidney injury molecule1, CHI3L1: chitinase3 like protein1.

Table 3.8 presents the mean values and standard deviations of kidney damage biomarkers (KIM-1, NGAL, and CHI3L1) among ADPKD patients, stratified by sex. The mean KIM-1 level was 2.2 ± 1.2 ng/ml in females and 3.1 ± 2.3 ng/ml in males, indicating greater proximal tubular damage in males. The mean NGAL level was 115.48 ± 38.6 ng/ml in females and 157.24 ± 50.11 ng/ml in males, suggesting more significant inflammation in males. The mean CHI3L1 level was 445.94 ± 150.3 ng/ml in females and 455.78 ± 145.5 ng/ml in males, reflecting comparable levels of distal tubular damage between sexes.

Table (3.8) Mean differences of KIM-1, NGAL and CHI3L1 Levels among the studied patients of ADPKD based on their sex

Mean ±2SD	Female	Male
KIM-1(ng/ml)	2.2 ±1.2	3.1±2.3
NGA(ng/ml)	115.48±38.6	157.24±50.11
CHI3L1(ng/ml)	445.94 ±150.3	455.78 ± 145.5

NGAL: Neutrophil gelatinase-associated lipocalin, KIM-1: kidney injury molecule1, CHI3L1: chitinase3 like protein1.

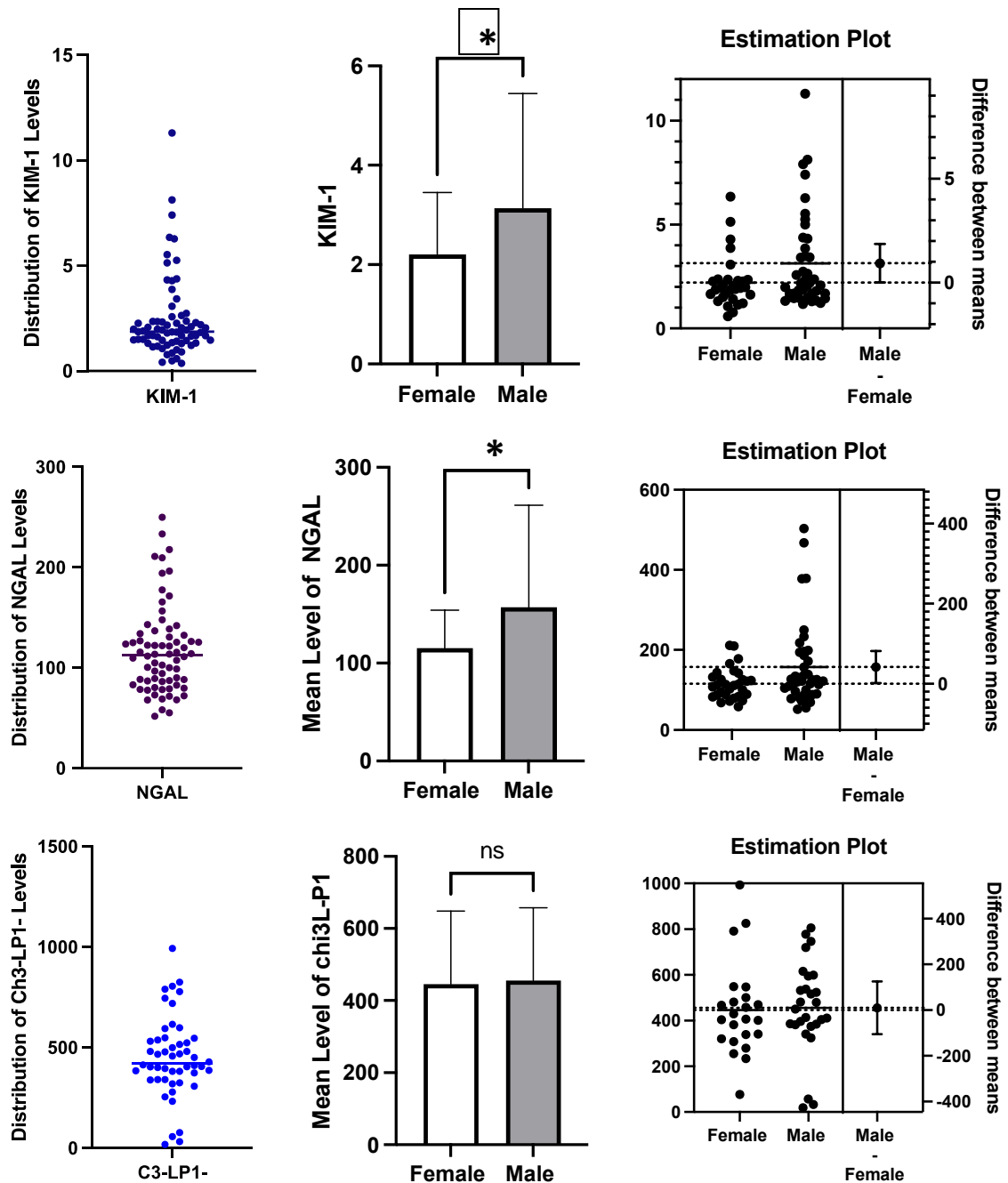


Figure (3.4) Mean differences of (KIM-1), (NGAL) and (CHI3L1) Levels among the studied patients of ADPKD based on their sex. (t-test was *:

significant at $p \leq 0.05$, **: significant at $p \leq 0.01$, *: significant at $p \leq 0.001$)**

NGAL: Neutrophil gelatinase-associated lipocalin, KIM-1: kidney injury molecule1, CHI3L1: chitinase3 like protein1.

The findings in this study show that male ADPKD patients had higher mean levels of KIM-1 and NGAL compared to females, suggesting a greater degree of kidney damage and inflammation. This aligns with findings by (Schrier, 2010), who reported that male sex is often associated with more severe disease progression in ADPKD. The higher KIM-1 levels in males indicate increased proximal tubular injury, which may be linked to the greater susceptibility of males to oxidative stress and lipid dysregulation, as highlighted by (Zhiguo, 2015).

The elevated NGAL levels in males suggest more pronounced inflammatory processes, consistent with (Huang, 2020), who demonstrated that NGAL is a reliable marker of renal inflammation. The similar CHI3L1 levels between sexes imply that distal tubular damage might be influenced by factors other than sex, possibly related to the overall burden of cystic disease.

These sex differences in kidney damage biomarkers underscore the importance of tailored monitoring and intervention strategies in managing ADPKD, with a particular focus on mitigating the more severe disease progression typically observed in male patients. KIM-1, NGAL, and CHI3L1 are biomarkers reflecting tubular injury and inflammation in ADPKD. KIM-1, which is undetectable in healthy kidneys, increases significantly with tubular damage, potentially indicating disease progression (Formica, 2020) (Griffin, 2020) NGAL, produced by damaged tubules and inflammatory cells, is a reliable marker of acute kidney injury (Mishra, 2004) (Schmidt-Ott, 2006). CHI3L1 has been studied as a biomarker for acute kidney injury (AKI), providing insights into kidney damage and healing processes (De Loor, 2016)_(Conroy, 2018). Sex differences in these biomarkers were observed, with males exhibiting higher levels of KIM-1, NGAL, and CHI3L1, suggesting potential variations in disease severity or

biological responses (Griffin, 2020). Further research is needed to clarify the role of these biomarkers in ADPKD and their sex-specific implications.

3.7. Study the Kidney damage Biomarkers based on the eGFR Stage in ADPKD

By classifying patients according to the GFR stages ,our study found that the mean KIM-1 level progressively increases across GFR stages, with the highest level observed in G4 (4.3 ± 1.5 ng/ml) and the lowest in G1 (1.7 ± 0.5 ng/ml). This suggests a potential association between higher KIM-1 levels and more severe kidney dysfunction (lower GFR).

Similar to KIM-1, NGAL shown that the highest level was in G4 (5.2 ± 2.6 ng/ml), but there is a substantial drop to G3b (1.8 ± 0.6 ng/ml).

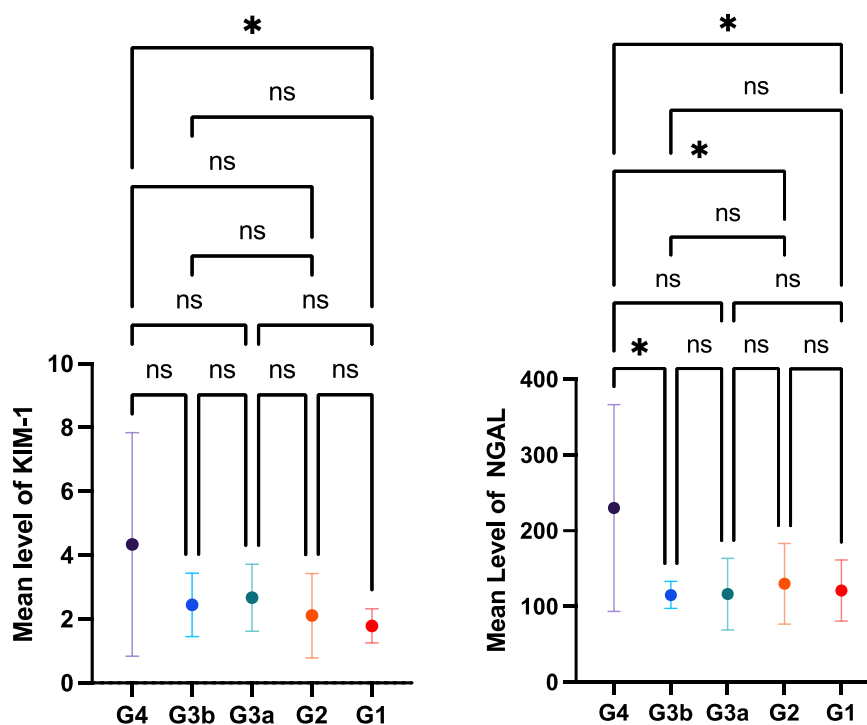
For CHI3L1 : the results were shown that the levels appear to be relatively increased across all GFR stages (around 1.7 - 4.7 ng/ml)

Table 3.9 demonstrated the mean levels and standard deviations of KIM-1, NGAL, and CHI3L1 based on the GFR stages in a group with ADPKD.

Table (3.9) Mean differences of (KIM-1), (NGAL) and (CHI3L1) Levels among the studied patients of ADPKD based on their GFR.

eGFR stages (ml/min/1.73m ²)	G4 NO:20	G3b NO:23	G3a NO:6	G2 NO:15	G1 NO:7
KIM-1					
Mean ±2SD	4.3±1.5	2.4±1.0	2.7±1.1	2.1±1.2	1.7±0.5
NGAL					
Mean ±2SD	5.2±2.6	1.8±0.6	4.3±1.6	2.4±1.1	2.0±0.7
CHI3L1					
Mean ±2SD	4.7±1.2	1.6±0.7	1.9±1.2	1.8±0.4	1.7±0.7

NGAL: Neutrophil gelatinase-associated lipocalin, KIM-1: kidney injury molecule1, CHI3L1: chitinase3 like protein1.



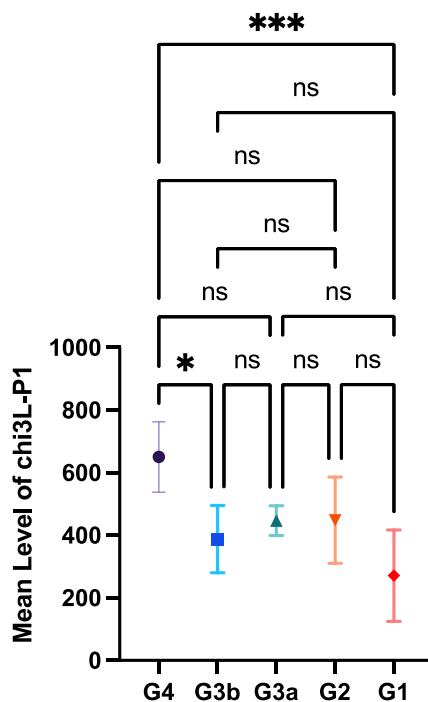


Figure (3.5) Mean differences of KIM-1, NGAL and CHI3L1 Levels among the studied patients of ADPKD based on their GFR. (Post Hoc ANOVA test was *: significant at $p \leq 0.05$, **: significant at $p \leq 0.01$, *: significant at $p \leq 0.001$)**

NGAL: Neutrophil gelatinase-associated lipocalin, KIM-1: kidney injury molecule1, CHI3L1: chitinase3 like protein1.

In the current study, the mean KIM-1 level progressively increased across GFR stages, with the highest level observed in G4 (severely reduced GFR) and the lowest in G1 (normal or high GFR). This suggests a strong correlation between higher KIM-1 levels and more severe kidney dysfunction. One indicator of renal tubule damage is KIM-1. More tubular damage may develop when ADPKD worsens and GFR drops, which would raise KIM-1 levels.

A tenable mechanism for KIM-1 overexpression in ADPKD has been described, and new research indicates that KIM-1 can forecast the course of

CKD in non-cystic illnesses. (Schrier, 2014) , The goal of the current investigation was to ascertain if KIM-1 predicts the advancement of kidney disease in ADPKD. reported comparable findings, who also showed that KIM-1 correlated with baseline kidney volume, but not with baseline eGFR (Petzold, 2015).

Similar to KIM-1, NGAL showed the highest level in G4, but there was a substantial drop in G3b (moderately reduced GFR) compared to G4. This indicates NGAL might also be a good indicator of severe kidney dysfunction in ADPKD, but the pattern might be less linear across all stages. NGAL is associated with inflammation. In later stages of ADPKD with severe kidney damage, inflammation might be more pronounced, contributing to higher NGAL levels.

The levels of CHI3L1 appeared to be relatively constant across all GFR stages (around 1.7 - 4.7/1.73 m²). This suggests a weaker association between CHI3L1 and GFR decline in ADPKD compared to KIM-1 and NGAL. CHI3L1 might have roles beyond just kidney function. Its relatively constant levels across GFR stages suggest it might be influenced by other factors besides GFR in ADPKD.

3.8. Study the Kidney Damage Biomarkers based on Left Kidney Cyst Size in ADPKD

In aim to search for a potential associations between left kidney cyst size and the levels of three kidney damage biomarkers (KIM-1, NGAL, and CHI3L1) in ADPKD patients, the cysts were categorized into three groups: small (G1: 0.7 - 2.2 ml), medium (G2: 2.3 - 3.3.ml), and large (G3: > 3.7 ml). The mean KIM-1 levels increased progressively with cyst size, from 1.9 ± 0.8 ng/ml in G1 to 3.2 ± 1.6 ng/ml in G3. NGAL levels showed a marked increase in the largest cyst group (G3: 169.5 ± 87.1 ng/ml) compared to smaller cysts. CHI3L1 levels also peaked in the G3 group (533.7 ± 173.9 ng/ml), although there was significant variability within each group.

The progressive increase in KIM-1 levels with larger cyst sizes aligns with studies by (Petzold, 2015), who demonstrated that KIM-1 is a reliable marker of proximal tubular injury in ADPKD, with levels correlating with cyst burden. This suggests that larger cysts may exert more mechanical stress on the renal tubules, leading to increased KIM-1 expression.

Table 3.10 illustrates the potential associations between left kidney cyst size and the levels of three kidney damage biomarkers (KIM-1, NGAL, and CHI3L1) in ADPKD patients.

NGAL's less consistent pattern, with a significant rise only in the largest cyst group, may indicate its role in more advanced disease stages, where inflammation and tubular damage are more pronounced (Mishra, 2004). The substantial increase in NGAL levels in G3 supports its potential as a marker for severe kidney damage in ADPKD.

The variability in CHI3L1 levels, despite an overall increase in the largest cyst group, suggests that while CHI3L1 may be associated with cyst size, it is influenced by additional factors beyond cyst burden (De Loor, 2016).

The marked increase in both NGAL and CHI3L1 levels in the largest cyst group highlights their potential utility as biomarkers for monitoring disease progression, particularly when used in combination with traditional markers such as KIM-1. These findings suggest that integrating these biomarkers into clinical practice could improve the assessment of disease severity and progression in ADPKD patients.

Table (3.10) Mean differences of KIM-1, NGAL and CHI3L1 Levels among the studied patients of ADPKD based on their the largest size of Left Kidney cysts

Lt Kidney(ml)	G1 (0.7_2.2)	G2 (2.3_3.6)	G3 (>3.7)
KIM-1			
Mean \pm 2SD	1.9 \pm 0.8	2.7 \pm 1.2	3.2 \pm 1.6
NGAL			
Mean \pm 2SD	112.0 \pm 33.3	118.8 \pm 36.3	169.5 \pm 87.1
CHI3L1			
Mean \pm 2SD	392.1 \pm 44.5	350.4 \pm 217.2	533.7 \pm 173.9

Lt: left, SD: standard deviation, NGAL: Neutrophil gelatinase-associated lipocalin, KIM-1: kidney injury molecule1, CHI3L1: chitinase3 like protein1.

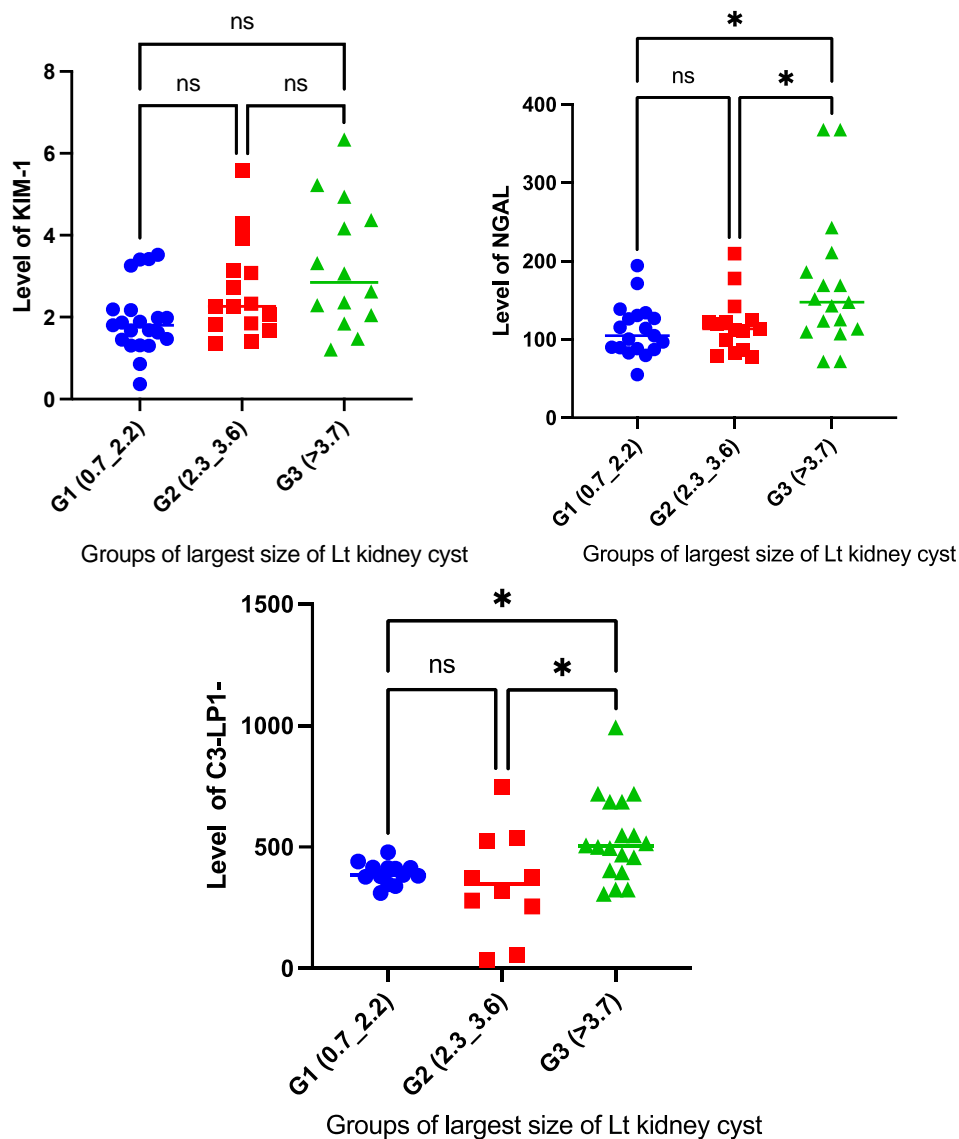


Figure (3.6) Mean differences of KIM-1, NGAL and CHI3L1 Levels among the studied patients of ADPKD based on their largest size of Left Kidney cysts.

(Post Hoc ANOVA test was *: significant at $p \leq 0.05$, **: significant at $p \leq 0.01$, *: significant at $p \leq 0.001$).**

Lt: left, SD: standard deviation, NGAL: Neutrophil gelatinase-associated lipocalin, KIM-1: kidney injury molecule1, CHI3L1: chitinase3 like protein1.

3.9. Study the Kidney damage Biomarkers by Right Kidney Cyst Size in ADPKD

Table 3.11 presents the mean levels and standard deviations we also studied for a potential association between the three kidney damage biomarkers (KIM-1, NGAL, and CHI3L1) and the size of right kidney cysts in ADPKD patients. The cysts were categorized into three groups: small (G1: 0.5 cm - 2.5 cm), medium (G2: 2.6 cm – 4.5 cm), and large (G3: > 4.6 cm). KIM-1 levels showed an increasing trend with cyst size, with the highest level in G3 (3.2 ± 1.9) and a relatively high level in G1 (2.7 ± 0.9) compared to G2 (1.7 ± 0.6). NGAL levels followed a similar pattern, peaking in G3 (183.5 ± 84.7) but dropping significantly in G2 (107.1 ± 28.7). CHI3L1 levels were highest in G3 (556.2 ± 198.4), with a decrease in G2 (403.3 ± 63.6) and G1 (396.2 ± 92.3).

Table 3.11 illustrates the potential associations between right kidney cyst size and the levels of three kidney damage biomarkers (KIM-1, NGAL, and CHI3L1) in ADPKD patients.

Table (3.11) Mean differences of KIM-1, NGAL and CHI3L1 Levels among the studied patients of ADPKD based on their largest size of right Kidney cysts

Rt Kidney(ml)	G1 (0.5_2.5)	G2 (2.6_4.5)	G3 (>4.6)
KIM-1			
Mean \pm 2S (ng/ml)	2.7 \pm 0.9	1.7 \pm 0.6	3.2 \pm 1.9
NGAL			
Mean \pm 2SD (ng/ml)	121.7 \pm 46.0	107.1 \pm 28.7	183.5 \pm 84.7
CHI3L1			
Mean \pm 2SD(ng/ml)	396.2 \pm 92.3	403.3 \pm 63.6	556.2 \pm 198.4

Rt: right, SD: standard deviation, NGAL: Neutrophil gelatinase-associated lipocalin, KIM-1: kidney injury molecule1, CHI3L1: chitinase3 like protein1.

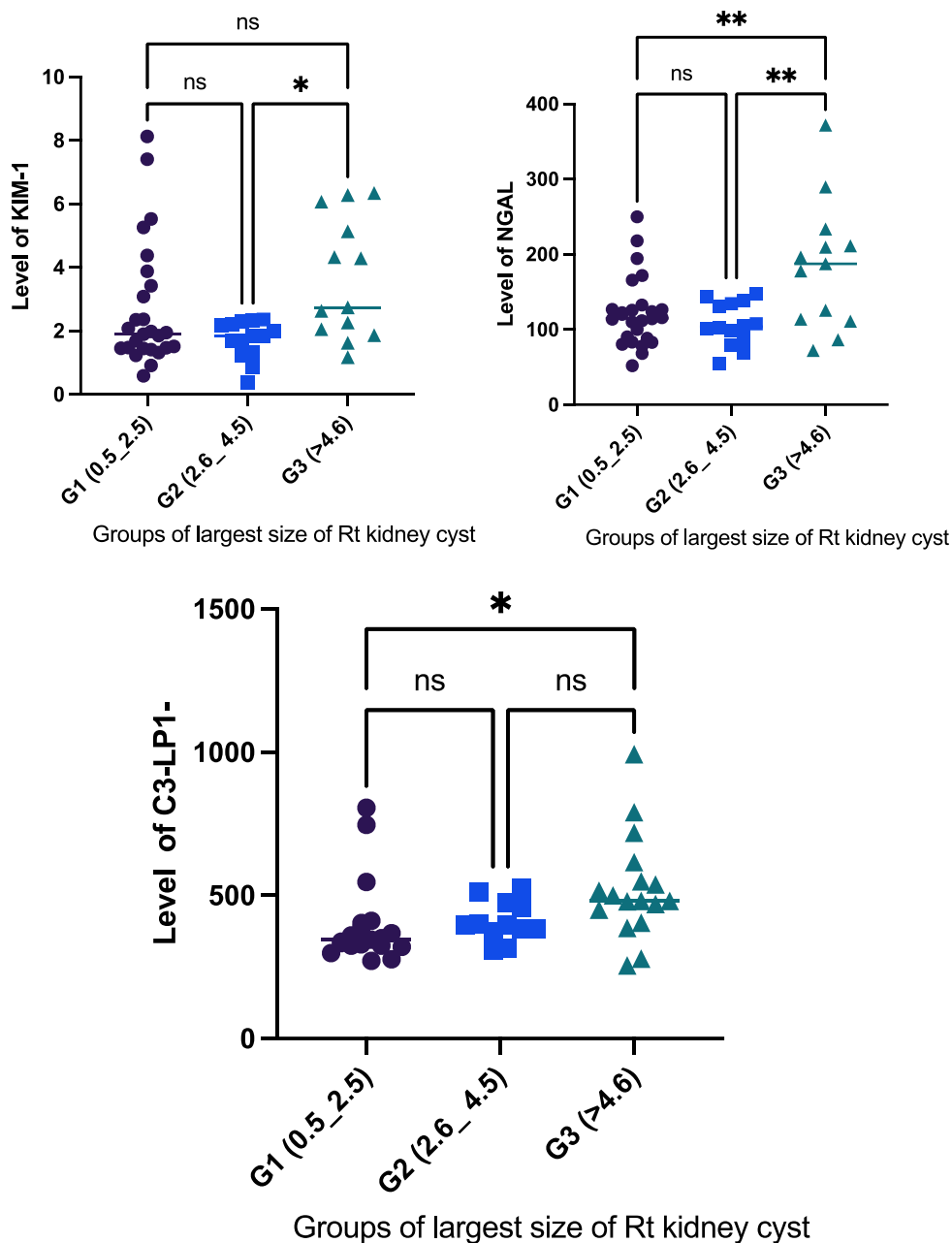


Figure (3.7) Mean differences of KIM-1, NGAL and CHI3L1 Levels among the studied patients of ADPKD based on their largest size of right Kidney cysts. (Post Hoc ANOVA test was *: significant at $p \leq 0.05$, **: significant at $p \leq 0.01$, *: significant at $p \leq 0.001$)**

Rt: right, SD: standard deviation, NGAL: Neutrophil gelatinase-associated lipocalin, KIM-1: kidney injury molecule1, CHI3L1: chitinase3 like protein1.

The progressive increase in KIM-1 levels with larger right kidney cysts supports findings by (Petzold, 2015), where KIM-1 is recognized as a marker of proximal tubular injury in ADPKD, correlating with cyst burden. The higher levels in both G1 and G3 suggest that even smaller cysts can significantly impact tubular function, possibly due to their location within the kidney.

NGAL levels, which peak in G3 and decrease in G2, may reflect the complex interplay between cyst size, inflammation, and kidney damage. This pattern aligns with (Mishra, 2004), who noted NGAL's role in inflammatory responses, particularly in cases of severe kidney damage. The significant increase in NGAL in the largest cyst group indicates its potential as a marker for advanced disease stages.

Similarly, CHI3L1 levels show the highest increase in G3, consistent with its role in kidney injury and repair processes (De Loor, 2016). However, the variability in CHI3L1 levels between cyst sizes suggests that other factors, such as cyst location or the overall kidney environment, might influence this biomarker's levels. The observed differences in biomarker levels between G1 and G3 underscore the potential utility of these markers for assessing disease severity and progression in ADPKD, emphasizing the need for a comprehensive approach that considers both cyst size and other influencing factors. This study presents preliminary evidence linking kidney cyst size with specific kidney damage biomarkers in ADPKD. KIM-1 levels progressively increased with larger cysts ($G1 < G2 < G3$), suggesting a direct correlation between cyst size and proximal tubule injury. NGAL and CHI3L1 levels also significantly increased in the largest cyst group (G3), indicating their potential as markers of advanced kidney damage.

While KIM-1 and NGAL are established indicators of tubular injury, particularly in AKI, their role in ADPKD remains less explored. KIM-1 has been correlated with kidney volume and tubular injury in ADPKD (Kuehn, 2002) (Meijer, 2010), whereas NGAL's results have been inconsistent, reflecting its complex role in inflammation (Virzì, 2015). Despite their widespread use in AKI, the application of these biomarkers in CKD, particularly ADPKD, warrants further investigation (Seibert, 2021). These findings suggest that KIM-1, NGAL, and CHI3L1 may be useful for identifying patients with more severe kidney damage in ADPKD, with a particular focus on their correlation with cyst size and associated complications.

3.10. Receiver operating characteristics (ROC) curve

When we tried to study which biomarkers are efficient in predicting stage 4 CKD among patients with ADPKD, we found that both biomarkers demonstrated good overall performance, as indicated by their Area Under the Curve (AUC) values, with NGAL having a slightly higher AUC (80.5%) compared to KIM-1 (79.1%). NGAL exhibited higher sensitivity (71.4%) than KIM-1 (57.1%), indicating that NGAL is more likely to correctly identify patients with stage 4 CKD. However, KIM-1 showed higher specificity (99%) compared to NGAL (91%), suggesting that KIM-1 is more effective at correctly identifying patients without stage 4 CKD. The optimal cut-off points for both biomarkers were provided, and results were validated using Youden's J statistics, with NGAL showing a higher index (0.623) than KIM-1 (0.561), further supporting NGAL's slightly better performance in ruling in CKD. Table 3.12 summarizes the performance of KIM-1 and NGAL levels in predicting stage 4 CKD among patients with ADPKD.

Table (3.12) AUC, optimal threshold, Sensitivity and specificity of KIM-1 and NGAL levels for predicting stage 4 of CKD among the studied patients of ADPKD.

Variable	AUC	Sensitivity %	Specificity %	Cut-off points	Youden index	CI (95%)
KIM-1	79.1%	57.1%	99%	3.0165	0.561	0.568-1.000
NGAL	80.5%	71.4%	91%	163.8335	0.623	0.580-1.000

NGAL: Neutrophil gelatinase-associated lipocalin, KIM-1: kidney injury molecule1, AUC: area under curve.

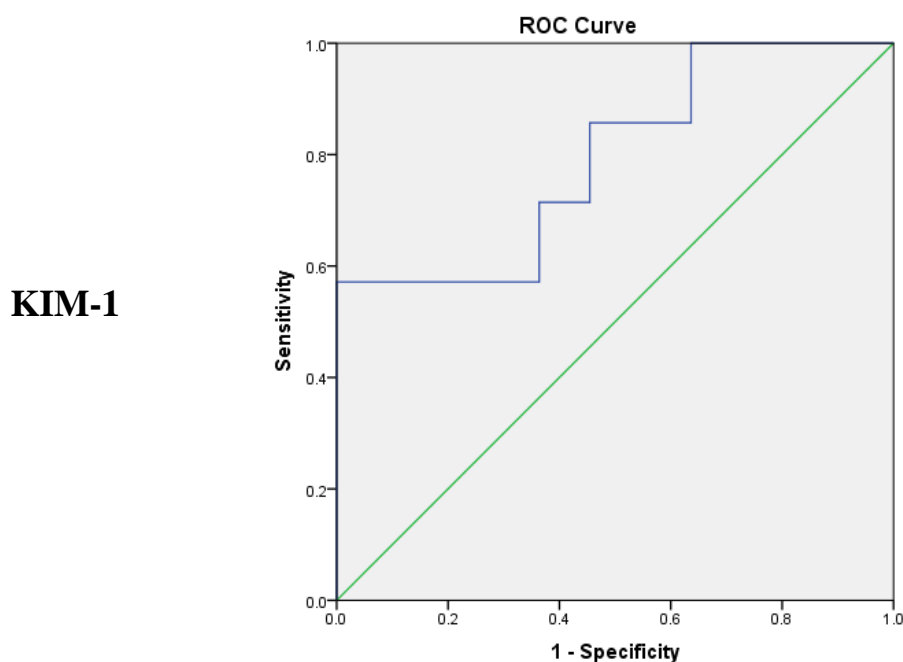


Figure (3.8):A: ROC curves for KIM-1 among the studied patients of ADPKD to analyze the optimal diagnostic points for predicting disease progression (stage 4) based on eGFR. KIM-1: kidney injury molecule1.

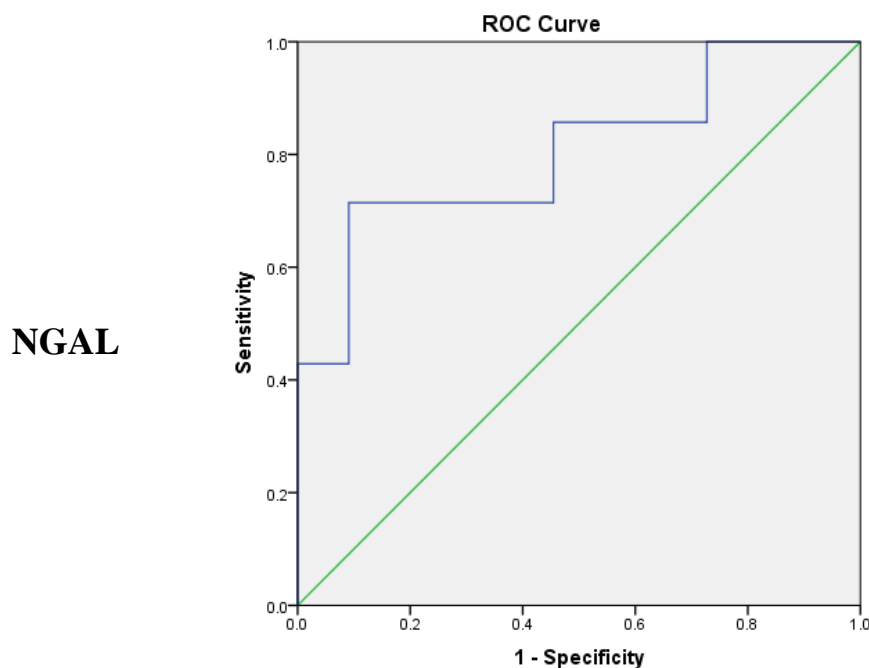


Figure (3.8):B: ROC curves for NGAL among the studied patients of ADPKD to analyze the optimal diagnostic points for predicting disease progression (stage 4) based on eGFR. NGAL: Neutrophil gelatinase-associated lipocalin.

The findings from this study indicate that both KIM-1 and NGAL are valuable biomarkers for predicting stage 4 CKD in ADPKD patients, with each having distinct strengths. NGAL's higher AUC (80.5%) and sensitivity (71.4%) suggest it is more effective in correctly identifying patients who have progressed to stage 4 CKD, making it a potentially useful marker for early intervention in more severe cases. This aligns with previous studies, such as those by (Mishra, 2004) and (Schrier, 2014), which identified NGAL as a reliable marker for detecting kidney injury and inflammation.

On the other hand, KIM-1's higher specificity (99%) indicates its strength in correctly ruling out patients who have not yet progressed to stage 4 CKD, which is crucial for avoiding false positives. This high specificity aligns with

research by (Meijer, 2010), which demonstrated KIM-1's effectiveness in reflecting tubular injury and its correlation with disease progression in ADPKD. The optimal cut-off points identified in this study provide practical thresholds for clinicians to classify patients based on their risk of progressing to stage 4 CKD. The higher Youden's J index for NGAL (0.623) compared to KIM-1 (0.561) suggests that NGAL may be slightly more suitable for ruling in CKD, although both biomarkers offer significant value in clinical decision-making for ADPKD management. Both KIM-1 and NGAL have been identified as biomarkers for predicting the risk of developing stage 3 CKD in patients with ADPKD.

The ROC for CH13L1 levels, AUC, optimal threshold, Sensitivity and specificity for predicting stage 4 of CKD among the studied patients of ADPKD was very low and therefore neglected.

In table 3.12 KIM-1 shows a very high specificity (99%), indicating a strong ability to correctly identify patients who do not have stage 3 CKD. However, KIM-1's sensitivity is lower (36.6%), suggesting it may miss some patients who are at risk. In contrast, NGAL has a lower specificity (92.3%) but a higher Youden Index (0.561) compared to KIM-1 (0.354), suggesting that NGAL may provide a better overall balance between sensitivity and specificity for identifying patients at risk for stage 3 CKD.

Table (3.13) AUC, optimal threshold, Sensitivity and specificity of KIM-1 and NGAL levels for predicting stage 3 of CKD among the studied patients of ADPKD.

Variable	AUC	Specificity %	Sensitivity %	Cut-off points	Youden index	CI (95%)
KIM-1	70%	99%	36.6%	1.3765	0.354	0.476-0.909
NGAL	60.8%	92.3%	36.4%	140.475	0.561	0.291-0.786

NGAL: Neutrophil gelatinase-associated lipocalin, KIM-1: kidney injury molecule1, AUC: area under curve, CI: confidence interval.

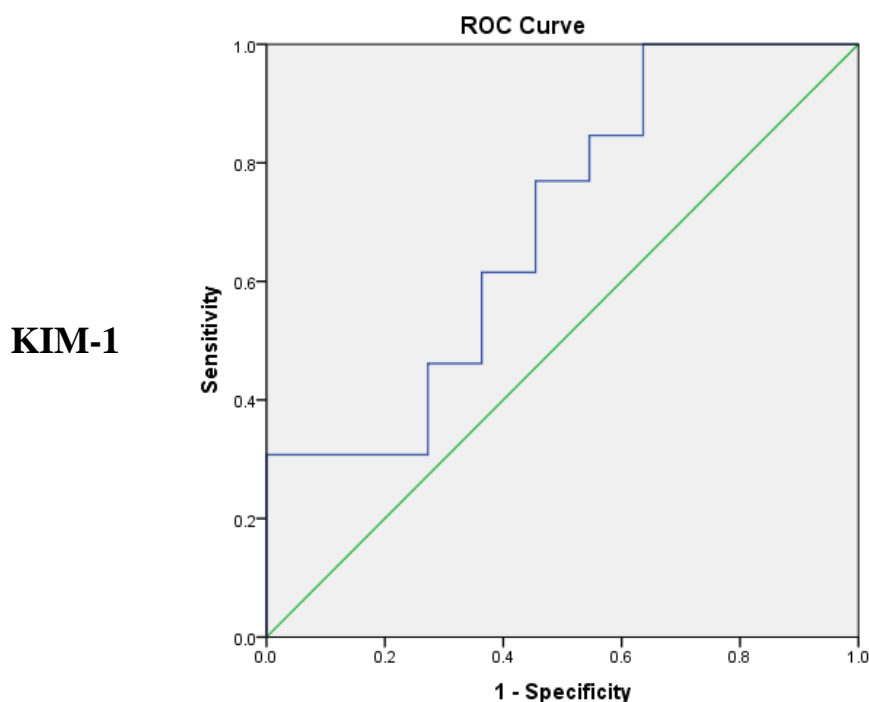


Figure (3.9):A: ROC curves for KIM-1 among the studied patients of ADPKD to analyze the optimal diagnostic points for predicting disease progression (stage 3) based on the eGFR. KIM-1: kidney injury molecule1.

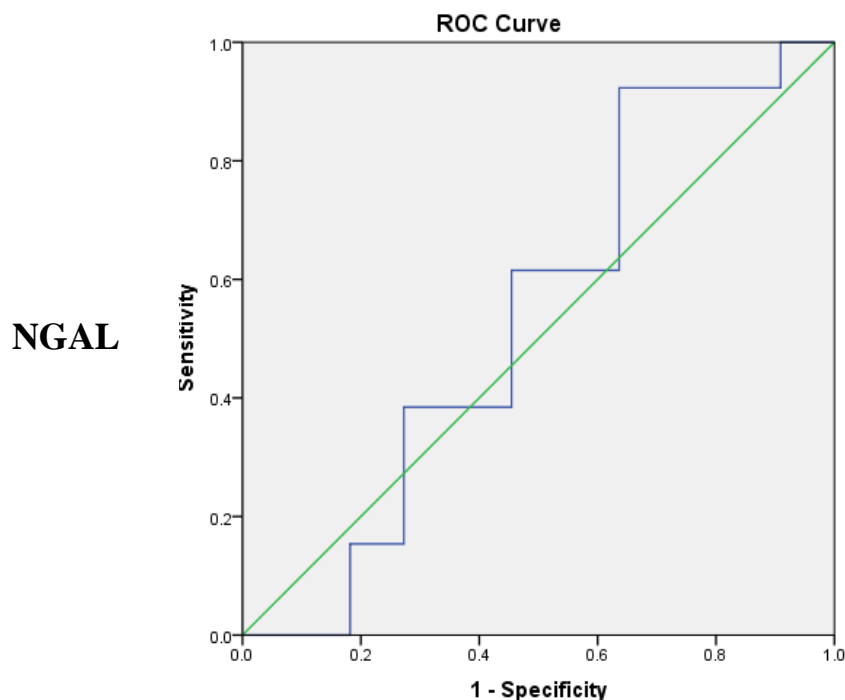


Figure (3.9):B: ROC curves for NGAL among the studied patients of ADPKD to analyze the optimal diagnostic points for predicting disease progression (stage 3) based on the eGFR. NGAL: Neutrophil gelatinase-associated lipocalin.

In the context of predicting stage 3 CKD in ADPKD, both KIM-1 and NGAL demonstrate utility, though with differing strengths. KIM-1's very high specificity (99%) indicates its strong potential to rule out patients who are not at risk of progressing to stage 3 CKD. This high specificity aligns with findings from (Meijer, 2010), reinforcing KIM-1's role in accurately identifying those without significant kidney damage. However, its lower sensitivity (36.6%) suggests that KIM-1 may not be as effective in detecting early or developing cases of stage 3 CKD. On the other hand, NGAL offers a more balanced approach with a higher Youden Index (0.561) compared to KIM-1 (0.354), indicating that NGAL may be more effective overall in identifying patients at risk for stage 3 CKD. The higher sensitivity of

NGAL, despite slightly lower specificity, makes it a potentially better biomarker for early detection and intervention, which is critical in managing the progression of CKD in ADPKD patients. These findings are consistent with previous research that highlights NGAL's role in early kidney injury detection (Mishra, 2004), making it a valuable tool in the early identification of at-risk patients.

For CHI3L1, it was appeared to be a promising biomarker for identifying patients with ADPKD who are at risk of developing stage 3 CKD. It has a good AUC (80%) and a Youden Index (0.583), indicating a good balance between sensitivity (75%) and specificity (83.3%). This means CHI3-LP1 can effectively identify both patients with stage 3 CKD.

Table (3.14) AUC, optimal threshold, Sensitivity and specificity of CHI3L1 levels for predicting stage 3 of CKD among the studied patients of ADPKD.

Variable	AUC	Sensitivity %	Specificity %	Cut-off points	Youden index	CI (95%)
CHI3L1	80%	75%	83.3%	402.6543	0.583	0.534-1.000

CHI3L1: chitinase 3 like protein1, AUC: area under curve, CI: confidence interval.

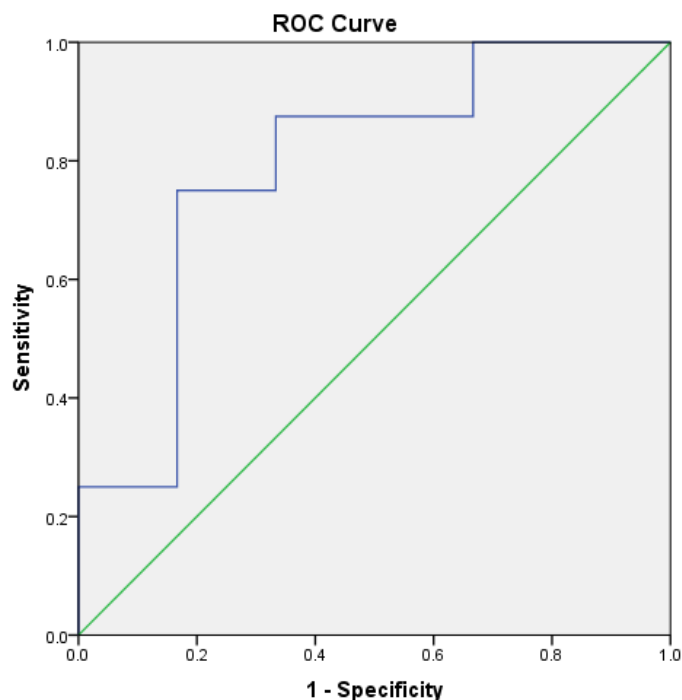


Figure (3.10) ROC curves for CHI3L1 among the studied patients of ADPKD to analyze the optimal diagnostic points for predicting disease progression (stage 3) based on the eGFR. CHI3L1: chitinase 3 like protein1

Table 3.15 presents the performance of KIM-1 and NGAL levels in predicting stage 2 CKD among patients with ADPKD. Both biomarkers showed relatively low Area Under the Curve (AUC) values, with KIM-1 at 51.5% and NGAL at 52.5%, indicating limited effectiveness in distinguishing patients with stage 2 CKD. KIM-1 exhibited very high sensitivity (99%) but low specificity (36.4%), suggesting it can identify nearly all patients with stage 2 CKD but also produces many false positives. In contrast, NGAL showed much higher specificity (91%) but lower sensitivity (33.3%), making it better at ruling out stage 2 CKD. The cut-off points for both biomarkers were provided, and the Youden Index was low for both KIM-1 (0.354) and NGAL (0.242), indicating that neither biomarker is ideal for diagnosing stage 2 CKD in this population.

Table (3.15) AUC, optimal threshold, Sensitivity and specificity of KIM-1 and NGAL levels for predicting stage 2 of CKD among the studied patients of ADPKD.

Variable	AUC	Sensitivity %	Specificity %	Cut-off points	Youden index	CI (95%)
KIM-1	51.5%	99%	36.4%	1.3045	0.354	0.246-0.784
NGAL	52.5%	33.3%	91%	160.7455	0.242	0.250-0.800

NGAL: Neutrophil gelatinase-associated lipocalin, KIM-1: kidney injury molecule1, AUC: area under curve, CI: confidence interval.

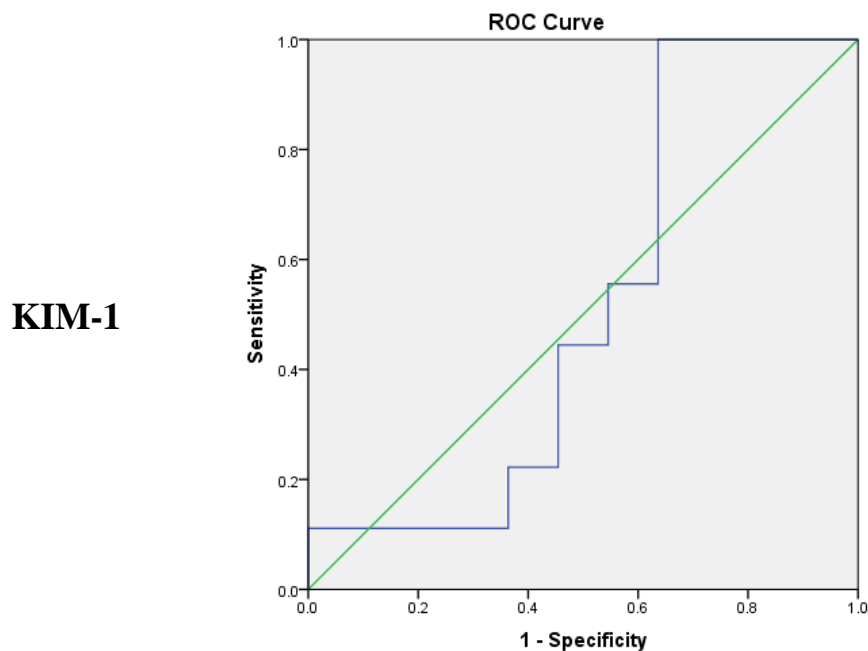


Figure (3.11):A: ROC curves for KIM among the studied patients of ADPKD to analyze the optimal diagnostic points for predicting disease progression (stage 2) based on the eGFR KIM-1: kidney injury molecule1.

NGAL

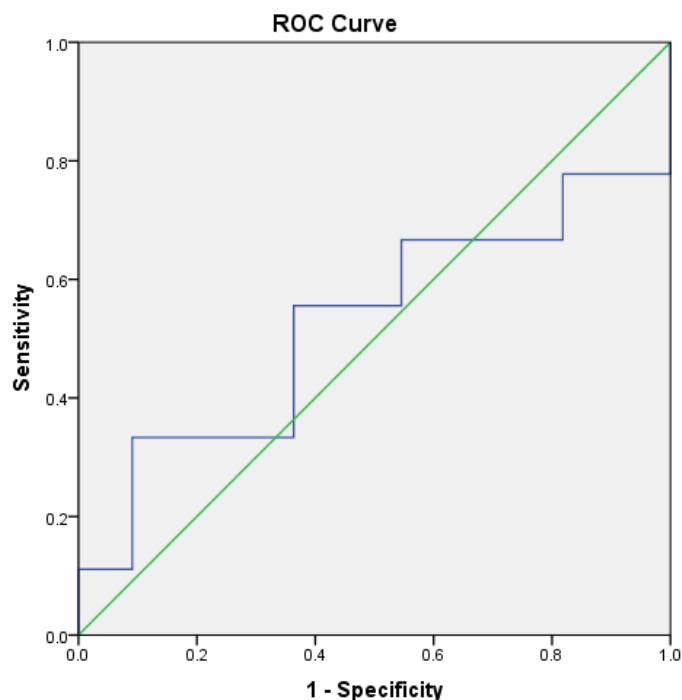


Figure (3.11):B: ROC curves for NGAL among the studied patients of ADPKD to analyze the optimal diagnostic points for predicting disease progression (stage 2) based on the eGFR NGAL: Neutrophil gelatinase-associated lipocalin.

The low AUC values for both KIM-1 (51.5%) and NGAL (52.5%) suggest that these biomarkers have limited utility in differentiating patients with stage 2 CKD in ADPKD. KIM-1's very high sensitivity (99%) means it can detect almost all cases of stage 2 CKD, but its low specificity (36.4%) results in a high rate of false positives, limiting its practical application. This indicates that while KIM-1 may be useful in ensuring that stage 2 CKD cases are not missed, it is not effective at accurately identifying those without the condition.

NGAL, on the other hand, with a specificity of 91%, is more reliable in ruling out stage 2 CKD but fails to detect a significant number of true

positives due to its low sensitivity (33.3%). This makes NGAL less useful as a standalone marker for diagnosing stage 2 CKD in ADPKD.

The low Youden Index values for both KIM-1 (0.354) and NGAL (0.242) further support the conclusion that neither biomarker is ideal for diagnosing stage 2 CKD in this context. These findings suggest that while KIM-1 and NGAL have roles in identifying more advanced stages of CKD, their application in early-stage (stage 2) CKD is limited, and alternative or additional biomarkers may be needed to improve diagnostic accuracy in this patient population.

The ROC for CH13L1 levels, AUC, optimal threshold, Sensitivity and specificity for predicting stage 2 of CKD among the studied patients of ADPKD was very low and therefore neglected.

The ROC for KIM-1, NGAL, CH13L1 levels, AUC, optimal threshold, Sensitivity and specificity for predicting stage 1 of CKD among the studied patients of ADPKD were neglected for their very low results.

Conclusions

- KIM-1, NGAL, and htTKV are key markers for monitoring kidney function decline in ADPKD.
- NGAL offers better sensitivity, while KIM-1 has higher specificity for predicting CKD progression.
- KIM-1, CHI3L1 and NGAL are less effective in diagnosing early-stage CKD (stage 2).
- CHI3L1 appear to be a promising biomarker for identifying patients with ADPKD who are at risk of developing stage 3 CKD.
- htTKV remains a crucial predictor of disease progression and kidney function decline in ADPKD.
- Monitoring metabolic abnormalities and lipid profiles is essential to manage cardiovascular risks in ADPKD.

Recommendations

1. Use ultra sonographic htTKV as a key predictor of kidney function decline.
2. Regularly assess metabolic and lipid profiles to mitigate cardiovascular risks.

Future work should compare biomarker findings, explore correlations with ADPKD severity, assess therapeutic impacts, consider sex-specific ranges, and investigate biomarker combinations for improved kidney function assessment.

References

References:

- Agu, P. U., Egbugara, M. N., Ogboi, J. S., Ajah, L. O., Nwagha, U. I., Ugwu, E. O., & Ezugwu, E. C. (2024). Atherogenic Index, Cardiovascular Risk Ratio, and Atherogenic Coefficient as Risk Factors for Cardiovascular Disease in Pre-eclampsia in Southeast Nigeria: A Cross-Sectional Study. *Nigerian Journal of Clinical Practice*, 27(2), 221-227.
- Alguire, P. C. (2006). MKSAP 18: medical knowledge self-assessment program. (*No Title*).
- Allen, E., Piontek, K. B., Garrett-Mayer, E., Garcia-Gonzalez, M., Gorelick, K. L., & Germino, G. G. (2006). Loss of polycystin-1 or polycystin-2 results in dysregulated apolipoprotein expression in murine tissues via alterations in nuclear hormone receptors. *Human molecular genetics*, 15(1), 11-21.
- Anyatonwu, G. I., Estrada, M., Tian, X., Somlo, S., & Ehrlich, B. E. (2007). Regulation of ryanodine receptor-dependent calcium signaling by polycystin-2. *Proceedings of the National Academy of Sciences*, 104(15), 6454-6459.
- Lavu, S., Vaughan, L. E., Senum, S. R., Kline, T. L., Chapman, A. B., Perrone, R. D., ... & Harris, P. C. (2020). The value of genotypic and imaging information to predict functional and structural outcomes in ADPKD. *JCI insight*, 5(15).
- Bae, Kyongtae (2024). Consortium for Radiologic Imaging Studies of Polycystic Kidney Disease (V9) [Dataset]. NIDDK Central Repository. <https://doi.org/10.58020/956q-m463>
- Bao, G. H., Ho, C. T., & Barasch, J. (2015). The ligands of neutrophil gelatinase-associated lipocalin. *RSC advances*, 5(126), 104363-104374.
- Benedetto, R., Ousingawat, J., Cabrita, I., Pinto, M., Lérias, J. R., Wanitchakool, P., ... & Kunzelmann, K. (2019). Plasma membrane-localized TMEM16 proteins are indispensable for expression of CFTR. *Journal of Molecular Medicine*, 97, 711-722.
- Bergmann, C., Guay-Woodford, L. M., Harris, P. C., Horie, S., Peters, D. J., & Torres, V. E. (2018). Polycystic kidney disease. *Nature reviews Disease primers*,
- Besse, W., Roosendaal, C., Tuccillo, L., Roy, S. G., Gallagher, A. R., & Somlo, S. (2020). Adult inactivation of the recessive polycystic kidney disease gene causes polycystic liver disease. *Kidney360*, 1(10), 1068-1076.

- Blazer-Yost, B. L., & Wallace, D. P. (2020). The Polycystins and Polycystic Kidney Disease. *Studies of Epithelial Transporters and Ion Channels: Ion Channels and Transporters of Epithelia in Health and Disease-Vol. 3*, 1149-1186.
- Bolignano, D., Coppolino, G., Campo, S., Aloisi, C., Nicocia, G., Frisina, N., & Buemi, M. (2007). Neutrophil gelatinase-associated lipocalin in patients with autosomal-dominant polycystic kidney disease. *American journal of nephrology*, 27(4), 373-378.
- Bolignano, D., Donato, V., Coppolino, G., Campo, S., Buemi, A., Lacquaniti, A., & Buemi, M. (2008). Neutrophil gelatinase-associated lipocalin (NGAL) as a marker of kidney damage. *American journal of kidney diseases*, 52(3), 595-605.
- Brilland, B., Boud'hors, C., Wacrenier, S., Blanchard, S., Cayon, J., Blanchet, O., ... & Augusto, J. F. (2023). Kidney injury molecule 1 (KIM-1): A potential biomarker of acute kidney injury and tubulointerstitial injury in patients with ANCA-glomerulonephritis. *Clinical Kidney Journal*, 16(9), 1521-1533.
- Brookes, Z. L., Ruff, L., Upadhyay, V. S., Huang, L., Prasad, S., Solanky, T., ... & Ong, A. C. (2013). Pkd2 mesenteric vessels exhibit a primary defect in endothelium-dependent vasodilatation restored by rosiglitazone. *American Journal of Physiology-Heart and Circulatory Physiology*, 304(1), H33-H41.
- Cai, L., Rubin, J., Han, W., Venge, P., & Xu, S. (2010). The origin of multiple molecular forms in urine of HNL/NGAL. *Clinical Journal of the American Society of Nephrology*, 5(12), 2229-2235.
- Calvet, J. P. (2008). Strategies to inhibit cyst formation in ADPKD. *Clinical Journal of the American Society of Nephrology*, 3(4), 1205-1211.
- Canki, E., Kho, E., & Hoenderop, J. G. (2024). Urinary biomarkers in kidney disease. *Clinica Chimica Acta*, 117798.
- Chapman, A. B., Devuyst, O., Eckardt, K. U., Gansevoort, R. T., Harris, T., Horie, S., ... & Participants, C. (2015). Autosomal-dominant polycystic kidney disease (ADPKD): executive summary from a Kidney Disease: Improving Global Outcomes (KDIGO) Controversies Conference. *Kidney international*, 88(1), 17-27.
- Chen, Q. J., Lai, H. M., Chen, B. D., Li, X. M., Zhai, H., He, C. H., ... & Yang, Y. N. (2016). Appropriate LDL-C-to-HDL-C ratio cutoffs for categorization of cardiovascular disease risk factors among Uygur adults in

Xinjiang, China. *International journal of environmental research and public health*, 13(2), 235.

- Cleeman, J. I. (2001). Executive summary of the third report of the National Cholesterol Education Program (NCEP) expert panel on detection, evaluation, and treatment of high blood cholesterol in adults (Adult Treatment Panel III).
- Colbert, G. B., Elrggal, M. E., Gaur, L., & Lerma, E. V. (2020). Update and review of adult polycystic kidney disease. *Disease-a-Month*, 66(5), 100887.
- Conroy, A. L., Hawkes, M. T., Elphinstone, R., Opoka, R. O., Namasopo, S., Miller, C., ... & Kain, K. C. (2018). Chitinase-3-like 1 is a biomarker of acute kidney injury and mortality in paediatric severe malaria. *Malaria journal*, 17, 1-11.
- Cornec-Le Gall, E., Alam, A., & Perrone, R. D. (2019). Autosomal dominant polycystic kidney disease. *The Lancet*, 393(10174), 919-935.
- Daniel, W. W., & Cross, C. L. (2018). *Biostatistics: a foundation for analysis in the health sciences*. Wiley.
- De Loor, J., Decruyenaere, J., Demeyere, K., Nuytinck, L., Hoste, E. A., & Meyer, E. (2016). Urinary chitinase 3-like protein 1 for early diagnosis of acute kidney injury: a prospective cohort study in adult critically ill patients. *Critical care*, 20, 1-14.
- Ecker, T. (2016). Statins in the treatment of autosomal dominant polycystic kidney disease. *Nephrology Dialysis Transplantation*, 31(8), 1194-1196.
- Feather, A., Randall, D., & Waterhouse, M. (Eds.). (2020). *Kumar and Clark's Clinical Medicine E-Book: Kumar and Clark's Clinical Medicine E-Book*. Elsevier Health Sciences.
- Fliszkiewicz, M., Niemczyk, M., Kulesza, A., Łabuś, A., & Pączek, L. (2019). Glucose and lipid metabolism abnormalities among patients with autosomal dominant polycystic kidney disease. *Kidney and Blood Pressure Research*, 44(6), 1416-1422.
- Formica, C., & Peters, D. J. (2020). Molecular pathways involved in injury-repair and ADPKD progression. *Cellular Signalling*, 72, 109648.
- Friedl, A., Stoesz, S. P., Buckley, P., & Gould, M. N. (1999). Neutrophil gelatinase-associated lipocalin in normal and neoplastic human tissues. Cell type-specific pattern of expression. *The Histochemical Journal*, 31, 433-441.
- Friedewald, W. T., Levy, R. I., & Fredrickson, D. S. (1972). Estimation of the concentration of low-density lipoprotein cholesterol in plasma, without use of the preparative ultracentrifuge. *Clinical chemistry*, 18(6), 499-502.

- Gallagher, A. R., Germino, G. G., & Somlo, S. (2010). Molecular advances in autosomal dominant polycystic kidney disease. *Advances in chronic kidney disease*, 17(2), 118-130.
- Gauer, S., Urbschat, A., Gretz, N., Hoffmann, S. C., Kränzlin, B., Geiger, H., & Obermüller, N. (2016). Kidney injury molecule-1 is specifically expressed in cystically-transformed proximal tubules of the PKD/Mhm (cy/+) rat model of polycystic kidney disease. *International Journal of Molecular Sciences*, 17(6), 802.
- Goetz, D. H., Holmes, M. A., Borregaard, N., Bluhm, M. E., Raymond, K. N., & Strong, R. K. (2002). The neutrophil lipocalin NGAL is a bacteriostatic agent that interferes with siderophore-mediated iron acquisition. *Molecular cell*, 10(5), 1033-1043.
- Goetz, D. H., Willie, S. T., Armen, R. S., Bratt, T., Borregaard, N., & Strong, R. K. (2000). Ligand preference inferred from the structure of neutrophil gelatinase associated lipocalin. *Biochemistry*, 39(8), 1935-1941.
- Gómez-Álvarez, E., Verdejo, J., Ocampo, S., Ponte-Negretti, C. I., Ruíz, E., & Ríos, M. M. (2020). The CNIC-polypill improves atherogenic dyslipidemia markers in patients at high risk or with cardiovascular disease: results from a real-world setting in Mexico. *IJC Heart & Vasculature*, 29, 100545.
- Grantham, J. J. (2003). Lillian Jean Kaplan International Prize for advancement in the understanding of polycystic kidney disease: understanding polycystic kidney disease: a systems biology approach. *Kidney international*, 64(4), 1157-1162.
- Grantham, J. J., Geiser, J. L., & Evan, A. P. (1987). Cyst formation and growth in autosomal dominant polycystic kidney disease. *Kidney international*, 31(5), 1145-1152.
- Grantham, J. J., Mulamalla, S., & Swenson-Fields, K. I. (2011). Why kidneys fail in autosomal dominant polycystic kidney disease. *Nature Reviews Nephrology*, 7(10), 556-566.
- Grantham, J. J., Torres, V. E., Chapman, A. B., Guay-Woodford, L. M., Bae, K. T., King Jr, B. F., ... & Miller, J. P. (2006). Volume progression in polycystic kidney disease. *New England Journal of Medicine*, 354(20), 2122-2130.
- Grantham, J. J. (2015). Rationale for early treatment of polycystic kidney disease. *Pediatric nephrology*, 30, 1053-1062.

- Griffin, B. R., Faubel, S., & Edelstein, C. L. (2019). Biomarkers of drug-induced kidney toxicity. *Therapeutic drug monitoring*, 41(2), 213-226.
- Griffin, B. R., You, Z., Nouredine, L., Gitomer, B., Perrenoud, L., Wang, W., ... & HALT Investigators. (2020). KIM-1 and kidney disease progression in autosomal dominant polycystic kidney disease: HALT-PKD results. *American journal of nephrology*, 51(6), 473-479.
- Guo, L., Zhu, B., Yuan, H., & Zhao, W. (2020). Evaluation of serum neutrophil gelatinase-associated lipocalin in older patients with chronic kidney disease. *Aging Medicine*, 3(1), 35-42.
- Halvorson, C. R., Bremmer, M. S., & Jacobs, S. C. (2010). Polycystic kidney disease: inheritance, pathophysiology, prognosis, and treatment. *International journal of nephrology and renovascular disease*, 69-83.
- Han, W. K., Bailly, V., Abichandani, R., Thadhani, R., & Bonventre, J. V. (2002). Kidney Injury Molecule-1 (KIM-1): a novel biomarker for human renal proximal tubule injury. *Kidney international*, 62(1), 237-244.
- Hardy, E., & Tsiokas, L. (2020). Polycystins as components of large multiprotein complexes of polycystin interactors. *Cellular signalling*, 72, 109640.
- Harris, P. C., & Torres, V. E. (2014). Genetic mechanisms and signaling pathways in autosomal dominant polycystic kidney disease. *The Journal of clinical investigation*, 124(6), 2315-2324.
- Hricak, H., & Lieto, R. P. (1983). Sonographic determination of renal volume. *Radiology*, 148(1), 311-312.
- Hofherr, A., & Köttgen, M. (2011). TRPP channels and polycystins. *Transient Receptor Potential Channels*, 287-313.
- Horie, S., Mochizuki, T., Muto, S., Hanaoka, K., Fukushima, Y., Narita, I., ... & Matsuo, S. (2016). Evidence-based clinical practice guidelines for polycystic kidney disease 2014. *Clinical and experimental nephrology*, 20, 493-509.
- Hosohata, K., Matsuoka, H., Iwanaga, K., & Kumagai, E. (2020). Urinary vanin-1 associated with chronic kidney disease in hypertensive patients: A pilot study. *The Journal of Clinical Hypertension*, 22(8), 1458-1465.
- Hoste, E. A., Vaara, S. T., De Loor, J., Haapio, M., Nuytinck, L., Demeyere, K., ... & Meyer, E. (2020). Urinary cell cycle arrest biomarkers and chitinase 3-like protein 1 (CHI3L1) to detect acute kidney injury in the critically ill: a

post hoc laboratory analysis on the FINNAKI cohort. *Critical Care*, 24, 1-10.

- Huang, F., Wang, L., Zhang, Q., Wan, Z., Hu, L., Xu, R., ... & Liu, Q. (2021). Elevated atherogenic index and higher triglyceride increase risk of kidney function decline: a 7-year cohort study in Chinese adults. *Renal Failure*, 43(1), 32-39.
- Igharo, O. G., Akinfenwa, Y., Alphonsus, R., Idomeh, F. A., Nwobi, N. L., Anetor, J. I., & Osibanjo, O. (2020). Lipid profile and atherogenic indices in nigerians occupationally exposed to e-waste: a cardiovascular risk assessment study. *Maedica*, 15(2), 196.
- Iliuta, I. A., Kalatharan, V., Wang, K., Cornec-Le Gall, E., Conklin, J., Pourafkari, M., ... & Pei, Y. (2017). Polycystic kidney disease without an apparent family history. *Journal of the American Society of Nephrology*, 28(9), 2768-2776.
- Irazabal, M. V., Rangel, L. J., Bergstralh, E. J., Osborn, S. L., Harmon, A. J., Sundsbak, J. L., ... & Crisp Investigators. (2015). Imaging classification of autosomal dominant polycystic kidney disease: a simple model for selecting patients for clinical trials. *Journal of the American Society of Nephrology*, 26(1), 160-172.
- Jayapalan, S., Saboorian, M. H., Edmunds, J. W., & Aukema, H. M. (2000). High dietary fat intake increases renal cyst disease progression in Han: SPRD-cy rats. *The Journal of nutrition*, 130(9), 2356-2360.
- Johnson, R. J., Feehally, J., & Floege, J. (2014). *Comprehensive clinical nephrology E-Book*. Elsevier Health Sciences.
- Karmakova, T. A., Sergeeva, N. S., Kanukoev, K. Y., Alekseev, B. Y., & Kaprin, A. D. (2021). Kidney injury molecule 1 (KIM-1): a multifunctional glycoprotein and biological marker. *Современные технологии в медицине*, 13(3 (eng)), 64-78.
- Kashani, K., Rosner, M. H., & Ostermann, M. (2020). Creatinine: from physiology to clinical application. *European journal of internal medicine*, 72, 9-14.
- Keane, W. F., O'Donnell, M. P., Kasiske, B. L., & Kim, Y. (1993). Oxidative modification of low-density lipoproteins by mesangial cells. *Journal of the American Society of Nephrology*, 4(2), 187-194.
- Kjeldsen, L., Johnsen, A. H., Sengeløv, H., & Borregaard, N. (1993). Isolation and primary structure of NGAL, a novel protein associated with

- human neutrophil gelatinase. *Journal of Biological Chemistry*, 268(14), 10425-10432.
- Köttgen, M., Buchholz, B., Garcia-Gonzalez, M. A., Kotsis, F., Fu, X., Doerken, M., ... & Walz, G. (2008). TRPP2 and TRPV4 form a polymodal sensory channel complex. *The Journal of cell biology*, 182(3), 437.
 - Kuehn, E. W., Park, K. M., Somlo, S., & Bonventre, J. V. (2002). Kidney injury molecule-1 expression in murine polycystic kidney disease. *American Journal of Physiology-Renal Physiology*, 283(6), F1326-F1336.
 - Lanktree, M. B., Haghghi, A., di Bari, I., Song, X., & Pei, Y. (2021). Insights into autosomal dominant polycystic kidney disease from genetic studies. *Clinical journal of the American Society of Nephrology*, 16(5), 790-799.
 - Levey, A. S., Stevens, L. A., Schmid, C. H., Zhang, Y., Castro III, A. F., Feldman, H. I., ... & CKD-EPI (Chronic Kidney Disease Epidemiology Collaboration)*. (2009). A new equation to estimate glomerular filtration rate. *Annals of internal medicine*, 150(9), 604-612.
 - Levin, A., Ahmed, S. B., Carrero, J. J., Foster, B., Francis, A., Hall, R. K., ... & Stevens, P. E. (2024). Executive summary of the KDIGO 2024 Clinical Practice Guideline for the Evaluation and Management of Chronic Kidney Disease: known knowns and known unknowns. *Kidney international*, 105(4), 684-701.
 - Li, A., Yi, B., Liu, Y., Wang, J., Dai, Q., Huang, Y., ... & Zhang, H. (2019). Urinary NGAL and RBP are biomarkers of normoalbuminuric renal insufficiency in type 2 diabetes mellitus. *Journal of immunology research*, 2019(1), 5063089.
 - Magayr, T. A., Song, X., Streets, A. J., Vergoz, L., Chang, L., Valluru, M. K., ... & Ong, A. C. (2020). Global microRNA profiling in human urinary exosomes reveals novel disease biomarkers and cellular pathways for autosomal dominant polycystic kidney disease. *Kidney international*, 98(2), 420-435.
 - Mallawaarachchi, A. C., Lundie, B., Hort, Y., Schonrock, N., Senum, S. R., Gayevskiy, V., ... & Furlong, T. J. (2021). Genomic diagnostics in polycystic kidney disease: an assessment of real-world use of whole-genome sequencing. *European Journal of Human Genetics*, 29(5), 760-770.
 - Mallett, A., Patel, M., Tunnicliffe, D. J., & Rangan, G. K. (2015, November). KHA-CARI autosomal dominant polycystic kidney disease

guideline: management of renal stone disease. In *Seminars in nephrology* (Vol. 35, No. 6, pp. 603-606). Elsevier.

- Ma, M. (2021, February). Cilia and polycystic kidney disease. In *Seminars in Cell & Developmental Biology* (Vol. 110, pp. 139-148). Academic Press.
- Marakala, V. (2022). Neutrophil gelatinase-associated lipocalin (NGAL) in kidney injury—A systematic review. *Clinica chimica acta*, 536, 135-141.
- McGahan, J. P., & Goldberg, B. B. (1998). Diagnostic ultrasound: a logical approach.
- Mei, C. L., Xue, C., Yu, S. Q., Dai, B., Chen, J. H., Li, Y., ... & ADPKD Clinical Guideline Working Group. (2020). Executive summary: clinical practice guideline for autosomal dominant polycystic kidney disease in China. *Kidney Diseases*, 6(3), 144-149.
- Meijer, E., Boertien, W. E., Nauta, F. L., Bakker, S. J., van Oeveren, W., Rook, M., ... & Gansevoort, R. T. (2010). Association of urinary biomarkers with disease severity in patients with autosomal dominant polycystic kidney disease: a cross-sectional analysis. *American Journal of Kidney Diseases*, 56(5), 883-895.
- Messchendorp, A. L., Meijer, E., Visser, F. W., Engels, G. E., Kappert, P., Losekoot, M., ... & DIPAK-1 Study Investigators. (2019). Rapid progression of autosomal dominant polycystic kidney disease: urinary biomarkers as predictors. *American journal of nephrology*, 50(5), 375-385.
- Mishra, J., Mori, K., Ma, Q., Kelly, C., Yang, J., Mitsnefes, M., ... & Devarajan, P. (2004). Amelioration of ischemic acute renal injury by neutrophil gelatinase-associated lipocalin. *Journal of the American Society of Nephrology*, 15(12), 3073-3082.
- Mishra, J., Ma, Q., Prada, A., Mitsnefes, M., Zahedi, K., Yang, J., ... & Devarajan, P. (2003). Identification of neutrophil gelatinase-associated lipocalin as a novel early urinary biomarker for ischemic renal injury. *Journal of the American Society of Nephrology*, 14(10), 2534-2543.
- Mosetti, M. A., Leonardou, P., Motohara, T., Kanematsu, M., Armao, D., & Semelka, R. C. (2003). Autosomal dominant polycystic kidney disease: MR imaging evaluation using current techniques. *Journal of Magnetic Resonance Imaging: An Official Journal of the International Society for Magnetic Resonance in Medicine*, 18(2), 210-215.
- Nauta, F. L., Scheven, L., Meijer, E., van Oeveren, W., de Jong, P. E., Bakker, S. J., & Gansevoort, R. T. (2013). Glomerular and tubular damage

- markers in individuals with progressive albuminuria. *Clinical Journal of the American Society of Nephrology*, 8(7), 1106-1114.
- Neumann, H. P., Jilg, C., Bacher, J., Nabulsi, Z., Malinoc, A., Hummel, B., ... & Else-Kroener-Fresenius-ADPKD-Registry. (2013). Epidemiology of autosomal-dominant polycystic kidney disease: an in-depth clinical study for south-western Germany. *Nephrology Dialysis Transplantation*, 28(6), 1472-1487.
 - Noce, E. M. (2022). Considerations for genetic testing in individuals with autosomal dominant polycystic kidney disease. *Journal of the American Association of Nurse Practitioners*, 34(12), 1249-1251.
 - Norman, J. (2011). Fibrosis and progression of autosomal dominant polycystic kidney disease (ADPKD). *Biochimica et Biophysica Acta (BBA)-Molecular Basis of Disease*, 1812(10), 1327-1336.
 - Oh, D., Lee, S., Yang, E., Choi, H. Y., Park, H. C., & Jhee, J. H. (2023). Atherogenic indices and risk of chronic kidney disease in metabolic derangements: Gangnam Severance Medical Cohort. *Kidney Research and Clinical Practice*.
 - Olamoyegun, M. A., Oluyombo, R., & Asaolu, S. O. (2016). Evaluation of dyslipidemia, lipid ratios, and atherogenic index as cardiovascular risk factors among semi-urban dwellers in Nigeria. *Annals of African medicine*, 15(4), 194-199.
 - Ong, A. C., Ward, C. J., Butler, R. J., Biddolph, S., Bowker, C., Torra, R., ... & Harris, P. C. (1999). Coordinate expression of the autosomal dominant polycystic kidney disease proteins, polycystin-2 and polycystin-1, in normal and cystic tissue. *The American journal of pathology*, 154(6), 1721-1729.
 - Pana, C., Stanigut, A. M., Cimpineanu, B., Alexandru, A., Salim, C., Nicoara, A. D., ... & Tuta, L. A. (2023). Urinary Biomarkers in Monitoring the Progression and Treatment of Autosomal Dominant Polycystic Kidney Disease—The Promised Land?. *Medicina*, 59(5), 915.
 - Pei, Y. (2001). A ‘two-hit’ model of cystogenesis in autosomal dominant polycystic kidney disease?. *Trends in molecular medicine*, 7(4), 151-156.
 - Pei, Y. (2006). Diagnostic approach in autosomal dominant polycystic kidney disease. *Clinical Journal of the American Society of Nephrology*, 1(5), 1108-1114.
 - Pei, Y., Obaji, J., Dupuis, A., Paterson, A. D., Magistroni, R., Dicks, E., ... & Ravine, D. (2009). Unified criteria for ultrasonographic diagnosis of ADPKD. *Journal of the American Society of Nephrology*, 20(1), 205-212.

- Petzold, K., Poster, D., Krauer, F., Spanaus, K., Andreisek, G., Nguyen-Kim, T. D. L., ... & Rotar, L. (2015). Urinary biomarkers at early ADPKD disease stage. *PloS one*, *10*(4), e0123555.
- Polycystic Kidney Disease Foundation. (n.d.). What is ADPKD? Kidney 101. Retrieved August 18, 2024, from <https://pkdcure.org/what-is-adpkd/kidney-101/>
- Qiu, J., Germino, G. G., & Menezes, L. F. (2023). Mechanisms of cyst development in polycystic kidney disease. *Advances in kidney disease and health*, *30*(3), 209-219.
- Reiterová, J., & Tesař, V. (2022). Autosomal dominant polycystic kidney disease: from pathophysiology of cystogenesis to advances in the treatment. *International Journal of Molecular Sciences*, *23*(6), 3317.
- Rossetti, S., Kubly, V. J., Consugar, M. B., Hopp, K., Roy, S., Horsley, S. W., ... & Harris, P. C. (2009). Incompletely penetrant PKD1 alleles suggest a role for gene dosage in cyst initiation in polycystic kidney disease. *Kidney international*, *75*(8), 848-855.
- Rysz, J., Gluba-Brzózka, A., Franczyk, B., Jabłonowski, Z., & Ciałkowska-Rysz, A. (2017). Novel biomarkers in the diagnosis of chronic kidney disease and the prediction of its outcome. *International journal of molecular sciences*, *18*(8), 1702.
- Salcedo-Cifuentes, M., Belalcazar, S., Acosta, E. Y., & Medina-Murillo, J. J. (2020). Conventional biomarkers for cardiovascular risks and their correlation with the Castelli Risk Index-Indices and TG/HDL-C. *Archivos de Medicina (Manizales)*, *20*(1), 11-22.
- Schirrer, L., Marín-García, P. J., & Llobat, L. (2021). Feline polycystic kidney disease: an update. *Veterinary Sciences*, *8*(11), 269.
- Schmidt-Ott, K. M., Mori, K., Kalandadze, A., Li, J. Y., Paragas, N., Nicholas, T., ... & Barasch, J. (2006). Neutrophil gelatinase-associated lipocalin-mediated iron traffic in kidney epithelia. *Current opinion in nephrology and hypertension*, *15*(4), 442-449.
- Schrier, R. W., & Levi, M. (2010). Lipids and renal cystic disease. *Nephrology Dialysis Transplantation*, *25*(11), 3490-3492.
- Schrier, R. W., Abebe, K. Z., Perrone, R. D., Torres, V. E., Braun, W. E., Steinman, T. I., ... & Chapman, A. B. (2014). Blood pressure in early autosomal dominant polycystic kidney disease. *New England Journal of Medicine*, *371*(24), 2255-2266.

- Schulz, C. A., Engström, G., Nilsson, J., Almgren, P., Petkovic, M., Christensson, A., ... & Orho-Melander, M. (2020). Plasma kidney injury molecule-1 (p-KIM-1) levels and deterioration of kidney function over 16 years. *Nephrology Dialysis Transplantation*, 35(2), 265-273.
- Segarra-Medrano, A., Martin, M., Agraz, I., Vilapriñó, M., Chamoun, B., Jatem, E., ... & Roche, S. (2020). Association between urinary biomarkers and disease progression in adults with autosomal dominant polycystic kidney disease. *Clinical Kidney Journal*, 13(4), 607-612.
- Seibert, F. S., Sitz, M., Passfall, J., Haesner, M., Laschinski, P., Buhl, M., ... & Westhoff, T. H. (2021). Urinary calprotectin, NGAL, and KIM-1 in the differentiation of primarily inflammatory vs. non-inflammatory stable chronic kidney diseases. *Renal Failure*, 43(1), 417-424.
- Seo, M. H., Lee, W. Y., Kim, S. S., Kang, J. H., Kang, J. H., Kim, K. K., ... & Committee of Clinical Practice Guidelines. (2019). 2018 Korean society for the study of obesity guideline for the management of obesity in Korea. *Journal of obesity & metabolic syndrome*, 28(1), 40.
- Spithoven, E. M., Kramer, A., Meijer, E., Orskov, B., Wanner, C., Abad, J. M., ... & Schaefer, F. (2014). Renal replacement therapy for autosomal dominant polycystic kidney disease (ADPKD) in Europe: prevalence and survival—an analysis of data from the ERA-EDTA Registry. *Nephrology Dialysis Transplantation*, 29(suppl_4), iv15-iv25.
- Sujatha, R., & Kavitha, S. (2017). Atherogenic indices in stroke patients: a retrospective study. *Iranian journal of neurology*, 16(2), 78.
- Sussman, C. R., Ward, C. J., Leightner, A. C., Smith, J. L., Agarwal, R., Harris, P. C., & Torres, V. E. (2014). Phosphodiesterase 1A modulates cystogenesis in zebrafish. *Journal of the American Society of Nephrology*, 25(10), 2222-2230.
- Szánthó, A. (2020). Boala polichistică renală autozomal-dominantă. *Medic. ro*, 133(1).
- Talke, H. S. G. E., & Schubert, G. E. (1965). Enzymatic urea determination in the blood and serum in the Warburg optical test. *Klinische Wochenschrift*, 43, 174-175.
- Tatar1ABE, E., Gungor2BE, O., Celtik2E, A., Sisman3D, A. R., Yaprak2B, M., Asci2C, G., ... & Toz2ACD, H. (2013). Correlation between serum YKL-40 (chitinase-3-like protein 1) level and proteinuria in renal transplant recipients. *Ann Transplant*, 18, 95-100.

- Tecer, D., Sunar, I., Ozdemirel, A. E., Tural, R., Kucuksahin, O., Dincel, A. S., & Ataman, S. (2019). Usefulness of atherogenic indices and Ca-LDL level to predict subclinical atherosclerosis in patients with psoriatic arthritis?. *Advances in Rheumatology*, 59, 49.
- TEMPO 3: 4 Investigators Gansevoort Ron T. rt.gansevoort@umcg.nl Meijer Esther Chapman Arlene B. Czerwiec Frank S. Devuyst Olivier Grantham Jared J. Higashihara Eiji Krasa Holly B. Ouyang John Perrone Ronald D. Torres Vicente E. (2016). Albuminuria and tolvaptan in autosomal-dominant polycystic kidney disease: results of the TEMPO 3: 4 Trial. *Nephrology Dialysis Transplantation*, 31(11), 1887-1894.
- Torres, V. E., & Bennett, W. M. (2020). Autosomal dominant polycystic kidney disease (ADPKD) in adults: Epidemiology, clinical presentation, and diagnosis. *Wolter Kluwer*, 1(2), 7-21.
- Torres, V. E., Grantham, J. J., Chapman, A. B., Mrug, M., Bae, K. T., King Jr, B. F., ... & Consortium for Radiologic Imaging Studies of Polycystic Kidney Disease (CRISP). (2011). Potentially modifiable factors affecting the progression of autosomal dominant polycystic kidney disease. *Clinical Journal of the American Society of Nephrology*, 6(3), 640-647.
- Torres, V. E., Gansevoort, R. T., Perrone, R. D., Chapman, A. B., Ouyang, J., Lee, J., ... & Wang, T. (2021). Tolvaptan in ADPKD patients with very low kidney function. *Kidney international reports*, 6(8), 2171-2178.
- Torres, V. E., Higashihara, E., Devuyst, O., Chapman, A. B., Gansevoort, R. T., Grantham, J. J., ... & TEMPO 3: 4 Trial Investigators. (2016). Effect of tolvaptan in autosomal dominant polycystic kidney disease by CKD stage: results from the TEMPO 3: 4 trial. *Clinical Journal of the American Society of Nephrology*, 11(5), 803-811.
- Turner, N. N., Lameire, N., Goldsmith, D. J., Winearls, C. G., Himmelfarb, J., & Remuzzi, G. (Eds.). (2015). *Oxford textbook of clinical nephrology*. Oxford university press.
- Ulusoy, R. E. (2013). LDL cholesterol measurement in terms of CHOLINDEX. *ANADOLU KARDIYOLOJİ DERGİSİ-THE ANATOLIAN JOURNAL OF CARDIOLOGY*, 13(6), 612-612.
- Vaidya, V. S., Niewczas, M. A., Ficociello, L. H., Johnson, A. C., Collings, F. B., Warram, J. H., ... & Bonventre, J. V. (2011). Regression of microalbuminuria in type 1 diabetes is associated with lower levels of urinary tubular injury biomarkers, kidney injury molecule-1, and N-acetyl- β -D-glucosaminidase. *Kidney international*, 79(4), 464-470.

- Vaidya, V. S., Ramirez, V., Ichimura, T., Bobadilla, N. A., & Bonventre, J. V. (2006). Urinary kidney injury molecule-1: a sensitive quantitative biomarker for early detection of kidney tubular injury. *American Journal of Physiology-Renal Physiology*, 290(2), F517-F529.
- van Timmeren, M. M., van den Heuvel, M. C., Bailly, V., Bakker, S. J., van Goor, H., & Stegeman, C. A. (2007). Tubular kidney injury molecule-1 (KIM-1) in human renal disease. *The Journal of pathology*, 212(2), 209-217.
- Vasileva, V. Y., Sultanova, R. F., Sudarikova, A. V., & Ilatovskaya, D. V. (2021). Insights into the molecular mechanisms of polycystic kidney diseases. *Frontiers in Physiology*, 12, 693130.
- Virzì, G. M., Gastaldon, F., Corradi, V., de Cal, M., Cruz, D. N., Clementi, M., & Ronco, C. (2015). Plasma NGAL and ADPKD progression. *Giornale Italiano di Nefrologia: Organo Ufficiale Della Societa Italiana di Nefrologia*, 32(3), gin-32.
- Wilson, P. D. (2004). Polycystic kidney disease. *New England Journal of Medicine*, 350(2), 151-164.
- Wong, E. (1999). *Clinical Laboratory Diagnostics: Use and Assessment of Clinical Laboratory Results*. Lothar Thomas. Frankfurt/Main, Germany: TH-Books Verlagsgesellschaft, 1998, 1727 pp., \$149.00. ISBN 3-9805215-4-0.
- Wu, Y., Su, T., Yang, L., Zhu, S. N., & Li, X. M. (2010). Urinary neutrophil gelatinase-associated lipocalin: a potential biomarker for predicting rapid progression of drug-induced chronic tubulointerstitial nephritis. *The American journal of the medical sciences*, 339(6), 537-542.
- Xiao, X., Yeoh, B. S., & Vijay-Kumar, M. (2017). Lipocalin 2: an emerging player in iron homeostasis and inflammation. *Annual review of nutrition*, 37(1), 103-130.
- Yoo, K. H., Kim, Y. N., Lee, M. J., Seong, J. K., & Park, J. H. (2009). Identification of apolipoproteinA1 reduction in the polycystic kidney by proteomics analysis of the Mx11-deficient mouse. *Proteomics*, 9(15), 3824-3832.
- Mao, Z., Xie, G., & Ong, A. C. (2015). Metabolic abnormalities in autosomal dominant polycystic kidney disease. *Nephrology Dialysis Transplantation*, 30(2), 197-203.
- Zhao, T., Su, Z., Li, Y., Zhang, X., & You, Q. (2020). Chitinase-3 like-protein-1 function and its role in diseases. *Signal transduction and targeted therapy*, 5(1), 201.

Appendixes

Appendix-1

Questionnaire

For Iraqi patient with polycystic kidney disease

Age :

Sex :

Address :

Family history :

Height :

Weight :

BMI :

Diastolic blood pressure :

Systolic blood pressure :

anti-hypertensive therapy :

Cardio vascular disease :

Kidney replacement therapy :

Kidney surgery :

Dialysis history :

Ultra sound :

Urea :

Creatinine :

Lipid profile :

CKD stage :

Tolvaptan medication :

Appendix-2



وزارة التعليم العالي و البحث العلمي
جامعة كربلاء

شهادة استيفاء

نؤيد استيفاء الطالب

ايات خضر علي عبيد

الوحدات الدراسية المطلوبة في نظام تطوير المهارات الاكاديمية لطلبة الدراسات
العليا للعام الدراسي 2023-2024

شعبية 6127

ا.د. نجم عبد الحسين نجم

مساعد رئيس الجامعة للشؤون العلمية

Appendix-3

Cholesterol

This package insert contains information to run the Cholesterol assay on the ARCHITECT c Systems™ and the AEROSET System.

INTENDED USE

The Cholesterol assay is used for the quantitation of cholesterol in human serum or plasma.

SUMMARY AND EXPLANATION OF TEST

Measurement of serum cholesterol levels can serve as an indicator of liver function, biliary function, intestinal absorption, propensity toward coronary artery disease, and thyroid function. Cholesterol levels are important in the diagnosis and classification of hyperlipoproteinemias. Stress, age, gender, hormonal balance, and pregnancy affect normal cholesterol levels.¹

The Adult Treatment Panel of the National Cholesterol Education Program (NCEP) recommends that all adults 20 years of age and over should have a fasting lipoprotein profile (total cholesterol, LDL cholesterol, HDL cholesterol, and triglyceride) once every five years to screen for coronary heart disease risk.²

PRINCIPLES OF PROCEDURE

The use of enzymes to assay cholesterol has been studied by many investigators.^{3,4} This reagent is based on the formulation of Allain,

et al.⁵ and the modification of Roeschlau⁶ with further improvements to render the reagent stable in solution.

Cholesterol esters are enzymatically hydrolyzed by cholesterol

esterase to cholesterol and free fatty acids. Free cholesterol, including that originally present, is then oxidized by cholesterol oxidase to cholest-4-ene-3-one and hydrogen peroxide. The hydrogen peroxide combines with hydroxybenzoic acid (HBA) and 4-aminoantipyrine to form a chromophore (quinoneimine dye) which is quantitated at 500 nm.

Methodology: Enzymatic

REAGENTS

Reagent Kit

REF 7D62 Cholesterol is supplied as a liquid, ready-to-use, single reagent kit which contains:

R1 10 x 84 mL

Estimated tests per kit: 3,032

Calculation is based on the minimum reagent fill volume per kit.

Reactive Ingredients ----- > Concentration

Cholesterol Oxidase (Microbial) ----- > more than 200 U/L

Cholesterol Esterase (Microbial)----- > more than 500 U/L

Peroxidase (Horseradish)----- > more than 300 U/L

4-Aminoantipyrine----- > 0.25 mmol/L

HBA----- > 10 mmol/L

The Abbott Clinical Chemistry Cholesterol reagent is certified to be traceable to the National Reference System for Cholesterol, against the Abell-Kendall reference method in a CDC-Certified Cholesterol Reference Method Laboratory Network (CRMLN).

REAGENT HANDLING AND STORAGE

Reagent Handling

Remove air bubbles, if present in the reagent cartridge, with a new applicator stick. Alternatively, allow the reagent to sit at the appropriate storage temperature to allow the bubbles to dissipate. To minimize volume depletion, do not use a transfer pipette to remove the bubbles.

CAUTION: Reagent bubbles may interfere with proper detection of reagent level in the cartridge, causing insufficient reagent aspiration which could impact results.

Reagent Storage

Unopened reagents are stable until the expiration date when stored at 2 to 8°C.

Reagent stability is 30 days if the reagent is uncapped and onboard.

SPECIMEN COLLECTION AND HANDLING

Suitable Specimens

Serum and plasma are acceptable specimens. The National Cholesterol Education Program (NCEP) recommends using fasting specimens.²

- **Serum:** Use serum collected by standard venipuncture techniques into glass or plastic tubes with or without gel barriers. Ensure complete clot formation has taken place prior to centrifugation. Separate serum from red blood cells or gel as soon after collection as possible.

Some specimens, especially those from patients receiving anticoagulant or thrombolytic therapy, may take longer to complete their clotting processes. Fibrin clots may subsequently form in these sera and the clots could cause erroneous test results.

- **Plasma:** Use plasma collected by standard venipuncture techniques into glass or plastic tubes. Acceptable anticoagulants are lithium heparin (with or without gel barrier) and sodium heparin. Ensure centrifugation is adequate to remove platelets. Separate plasma from red blood cells or gel as soon after collection as possible.

Specimen Storage Serum and plasma

<u>Temperature</u>	<u>Maximum Storage</u>
--------------------	------------------------

20 to 25°C-----	> 7 days ⁵
-----------------	-----------------------

2 to 8°C-----	> 7 days ^{5,12}
---------------	--------------------------

-20°C-----	> 3 months ⁵
------------	-------------------------

Guder et al.¹¹ suggest storage of frozen specimens at -20°C for no longer than the time interval cited above. However, limitations of laboratory equipment make it necessary in practice for clinical laboratories to establish a range around -20°C for specimen storage. This temperature range may be established from either the freezer manufacturer's specifications or your laboratory standard operating procedure(s) for specimen storage.

NOTE: Stored specimens must be inspected for particulates. If present, mix and centrifuge the specimen to remove particulates prior to testing.

BIBLIOGRAPHY

1. Burtis CA, Ashwood ER, editors. Tietz Fundamentals of Clinical Chemistry, 5th ed. Philadelphia, PA: WB Saunders; 2001:480–5.
2. Executive summary of the third report of the National Cholesterol Education Program (NCEP) Expert Panel on detection, evaluation, and treatment of high blood cholesterol in adults (Adult Treatment Panel III). JAMA 2001; 285:2486–97.
3. Flegg HM. An investigation of the determination of serum cholesterol by an enzymatic method. Ann Clin Biochem 1973; 10:79– 84.
4. Richmond W. Preparation and properties of a cholesterol oxidase from Nocardia sp. and its application to the enzymatic assay of total cholesterol in serum. Clin Chem 1973;19(12):1350–6.
5. Guder WG, Narayanan S, Wisser H, et al. List of analytes— preanalytical variables. Annex In: Samples: From the Patient to the Laboratory. Darmstadt, Germany: GIT Verlag; 1996: Annex 12–3.
6. US Pharmacopeial Convention, Inc. General notices. In: US Pharmacopeia National Formulary, 1995 ed (USP 23/NF 18). Rockville, MD: The US Pharmacopeial Convention, Inc; 1994:11.

Appendix-4

TRIGLYCERIDE

This package insert contains information to run the Triglyceride assay on the ARCHITECT c Systems™ and the AEROSET System.

INTENDED USE

The Triglyceride assay is used for the quantitation of triglyceride in human serum or plasma.

SUMMARY AND EXPLANATION OF TEST

Triglycerides are a family of lipids absorbed from the diet and produced endogenously from carbohydrates and fatty acids. Measurement of triglyceride is important in the diagnosis and management of hyperlipidemia. These diseases can be genetic or secondary to other disorders

including nephrosis, diabetes mellitus, and endocrine disturbances. The National Cholesterol Education Program (NCEP) cites evidence that triglycerides are an independent risk factor for atherosclerosis.¹ Individuals with hypertension, obesity, and/or diabetes are at greater risk than are those without these conditions.^{2,3}

The Adult Treatment Panel of the NCEP recommends that all adults 20 years of age and over should have a fasting lipoprotein profile (total cholesterol, LDL cholesterol, HDL cholesterol, and triglyceride) once every five years to screen for coronary heart disease risk.¹

PRINCIPLES OF PROCEDURE

Triglycerides are enzymatically hydrolyzed by lipase to free fatty acids and glycerol. The glycerol is phosphorylated by adenosine triphosphate (ATP) with glycerol kinase (GK) to produce glycerol-3-phosphate and adenosine diphosphate (ADP). Glycerol-3-phosphate is oxidized to dihydroxyacetone phosphate (DAP) by glycerol phosphate oxidase (GPO) producing hydrogen peroxide (H₂O₂). In a color reaction catalyzed by peroxidase, the H₂O₂ reacts with 4-aminoantipyrine (4-AAP) and 4-chlorophenol (4-CP) to produce a red colored dye. The absorbance of this dye is proportional to the concentration of triglyceride present in the sample. This analytical methodology is based on the reaction sequence described by Fossati et al.⁴ and by McGowan et al.⁵ In this reagent, 4-chlorophenol is used rather than 2-hydroxy-3,5-dichlorobenzenesulfonate, used in the Fossati and McGowan studies.

Methodology: Glycerol Phosphate Oxidase

REAGENTS

Reagent Kit

REF 7D74 Triglyceride is supplied as a liquid, ready-to-use, single reagent kit which contains:

R1 10 x 84 mL

Estimated tests per kit: 3,032

Calculation is based on the minimum reagent fill volume per kit.

Reactive Ingredients

Concentration

ATP----- > 2.5 mmol/L

Mg²⁺----- > 2.5 mmol/L

4-Aminoantipyrine ----- > 0.4 mmol/L

4-Chlorophenol ----- > 2 mmol/L

Peroxidase (Horseradish)----- > more than 2,000 U/L

GK (Microbial)----- > more than 600 U/L

GPO (Microbial)----- > more than 6,000 U/L

Lipoprotein Lipase (Microbial)-----> more than 3.000 U/L

REAGENT HANDLING AND STORAGE

Reagent Handling

Remove air bubbles, if present in the reagent cartridge, with a new applicator stick. Alternatively, allow the reagent to sit at the appropriate storage temperature to allow the bubbles to dissipate. To minimize volume depletion, do not use a transfer pipette to remove the bubbles.

CAUTION: Reagent bubbles may interfere with proper detection of reagent level in the cartridge, causing insufficient reagent aspiration which could impact results.

Reagent Storage

Unopened reagents are stable until the expiration date when stored at 2 to 8°C.

Reagent stability is 42 days if the reagent is uncapped and onboard.

SPECIMEN COLLECTION AND HANDLING

Suitable Specimens

Serum and plasma are acceptable specimens. The National Cholesterol Education Program (NCEP) recommends using fasting specimens.¹

- **Serum:** Use serum collected by standard venipuncture techniques into glass or plastic tubes with or without gel barriers. Ensure complete clot formation has taken place prior to centrifugation. Separate serum from red blood cells or gel as soon after collection as possible.

Some specimens, especially those from patients receiving anticoagulant or thrombolytic therapy, may take longer to complete their clotting processes. Fibrin clots may subsequently form in these sera and the clots could cause erroneous test results.

• **Plasma:** Use plasma collected by standard venipuncture techniques into glass or plastic tubes. Acceptable anticoagulants are lithium heparin (with or without gel barrier) and sodium heparin. Ensure centrifugation is adequate to remove platelets. Separate plasma from red blood cells or gel as soon after collection as possible.

SPECIMEN COLLECTION AND HANDLING

Specimen Storage

Serum and plasma

Temperature	Maximum Storage
--------------------	------------------------

20 to 25°C-----	> 2 days ⁵
-----------------	-----------------------

2 to 8°C-----	> 7 days ^{5,6}
---------------	-------------------------

-20°C-----	>1 year ⁵
------------	----------------------

Guder et al.¹⁰ suggest storage of frozen specimens at -20°C for no longer than the time interval cited above. However, limitations of laboratory equipment make it necessary in practice for clinical laboratories to establish a range around -20°C for specimen storage. This temperature range may be established from either the freezer manufacturer's specifications or your laboratory standard operating procedure(s) for specimen storage.

NOTE: Stored specimens must be inspected for particulates. If present, mix and centrifuge the specimen to remove particulates prior to testing.

BIBLIOGRAPHY

1. Executive summary of the third report of the National Cholesterol Education Program (NCEP) Expert Panel on detection, evaluation, and treatment of high blood cholesterol in adults (Adult Treatment Panel III). JAMA 2001; 285:2486–97.
2. Rubins HB. Triglycerides and coronary heart disease: implications of recent clinical trials. J Cardiovasc Risk 2000;7(5):339–45.

3. Forrester JS. Triglycerides: risk factor or fellow traveler? *Curr Opin Cardiol* 2001; 16:261–4.
4. Fossati P, Prencipe L. Serum triglycerides determined colorimetrically with an enzyme that produces hydrogen peroxide. *Clin Chem* 1982; 28:2077–80.
5. Guder WG, Narayanan S, Wisser H, et al. List of analytes—preanalytical variables. Annex In: *Samples: From the Patient to the Laboratory*. Darmstadt, Germany: GIT Verlag; 1996: Annex 22–3.
6. US Pharmacopeial Convention, Inc. General notices. In: *US Pharmacopeia National Formulary*, 1995 ed (USP 23/NF 18). Rockville, MD: The US Pharmacopeial Convention, Inc; 1994:11.

Appendix-5

Ultra HDL

This package insert contains information to run the Ultra HDL assay on the ARCHITECT c Systems™ and the AEROSET System.

INTENDED USE

The Ultra HDL (UHDL) assay is used for the quantitation of high-density lipoprotein (HDL) cholesterol in human serum or plasma.

SUMMARY AND EXPLANATION OF TEST

Plasma lipoproteins are spherical particles containing varying amounts of cholesterol, triglycerides, phospholipids, and proteins. Phospholipids, free cholesterol, and proteins constitute the outer surface of the lipoprotein particle, while the inner core contains mostly esterified cholesterol and triglyceride. These particles serve to solubilize and transport cholesterol and triglyceride in the bloodstream.

The relative proportions of protein and lipid determine the density of these lipoproteins and provide a basis on which to begin their classification.¹ The classes are: chylomicron, very-low-density lipoprotein (VLDL), low-density lipoprotein (LDL), and high-density lipoprotein (HDL). Numerous clinical studies have shown that the different lipoprotein classes have very distinct and varied effects on coronary heart disease risk.²

The principle role of HDL cholesterol in lipid metabolism is the uptake and transport of cholesterol from peripheral tissues to the liver through a process known as reverse cholesterol transport (a proposed cardioprotective mechanism).³ Low HDL cholesterol levels are strongly associated with an increased risk of coronary heart disease.⁴⁻⁷

Hence, the determination of serum HDL cholesterol is a useful tool in identifying high-risk patients. The Adult Treatment Panel of the National Cholesterol Education Program (NCEP) recommends that in all adults 20 years of age and over, a fasting lipoprotein profile (total cholesterol, LDL cholesterol, HDL cholesterol, and triglyceride) should be obtained once every five years to screen for coronary heart disease risk.⁸

PRINCIPLES OF PROCEDURE

The Ultra HDL assay is a homogeneous method for directly measuring HDL cholesterol concentrations in serum or plasma without the need for off-line pretreatment or centrifugation steps.

The method uses a two-reagent format and depends on the properties of a unique detergent. This method is based on accelerating the reaction of cholesterol oxidase (CO) with non-HDL unesterified cholesterol and dissolving HDL cholesterol selectively using a specific detergent. In the first reagent, non-HDL unesterified cholesterol is subject to an enzyme reaction and the peroxide generated is consumed by a peroxidase reaction with DSBmT yielding a colorless product. The second reagent consists of a detergent (capable of solubilizing HDL cholesterol), cholesterol esterase (CE), and chromagenic coupler to develop color for the quantitative determination of HDL cholesterol.

Methodology: Accelerator Selective Detergent.

REAGENTS

Reagent Kit

REF 3K33 Ultra HDL is supplied as a liquid, ready-to-use, two-reagent kit which contains:

R1 4 x 84 mL

R2 4 x 32 mL

Estimated tests per kit: 1,440

Calculation is based on the minimum reagent fill volume per kit.

<u>Reactive Ingredients</u>	<u>Concentration</u>
R1 Cholesterol oxidase (E. coli) -----	> < 1,000 U/L
Peroxidase (Horseradish)-----	> < 1,300 ppq U/L
N, N-bis (4-sulphobutyl)-m-toluidine-disodium----- (DSBmT)	> < 1.0 mmol/L
Accelerator-----	> < 1.0 mmol/L
Ascorbic oxidase (Curcubita sp.) -----	> < 3,000 U/L
R2 Cholesterol esterase (Pseudomonas sp.) -----	> < 1,500 U/L
4-Aminoantipyrine -----	> < 0.1%
Detergent-----	> < 2.0%

The Ultra HDL reagent is certified as traceable to the HDL cholesterol designated comparison method, covering the NCEP medical decision points, by the CDC-Certified Cholesterol Reference Method Laboratory Network (CRMLN).

REAGENT HANDLING AND STORAGE

Reagent Handling

Remove air bubbles, if present in the reagent cartridge, with a new applicator stick. Alternatively, allow the reagent to sit at the appropriate storage temperature to allow the bubbles to dissipate. To minimize volume depletion, do not use a transfer pipette to remove the bubbles.

CAUTION: Reagent bubbles may interfere with proper detection of reagent level in the cartridge, causing insufficient reagent aspiration which could impact results.

Reagent Storage

- Unopened reagents are stable until the expiration date when stored at 2 to 8°C.
- DO NOT FREEZE.
- Protect reagents from direct sunlight.

- Reagent stability is 28 days if the reagent is uncapped and onboard.

Indications of Deterioration

- Quality control results outside of the acceptance criteria defined by your laboratory.
- Presence of turbidity.

SPECIMEN COLLECTION AND HANDLING

Suitable Specimens

Serum and plasma are acceptable specimens. The National Cholesterol Education Program (NCEP) recommends using fasting specimens for

a lipoprotein profiles. If the specimen is nonfasting, only the values for total cholesterol and HDL cholesterol are usable.⁹

- **Serum:** Use serum collected by standard venipuncture techniques into glass or plastic tubes with or without gel barriers. Ensure complete clot formation has taken place prior to centrifugation. When processing samples, separate serum from blood cells or gel according to the specimen collection tube manufacturer's instructions.

Some specimens, especially those from patients receiving anticoagulant or thrombolytic therapy, may take longer to complete their clotting processes. Fibrin clots may subsequently form in these sera and the clots could cause erroneous test results.

- **Plasma:** Use plasma collected by standard venipuncture techniques into glass or plastic tubes. Acceptable anticoagulants are sodium heparin, lithium heparin (with or without gel barrier), and spray-dried EDTA. * Ensure centrifugation is adequate to remove platelets. When processing samples, separate plasma from blood cells or gel according to the specimen collection tube manufacturer's instructions.

***NOTE:** Lower HDL cholesterol results obtained from EDTA plasma have been attributed to an osmotic dilution effect. The NCEP has suggested multiplying EDTA plasma results by a factor of 1.03 to correct the EDTA result to a serum equivalent value.¹⁰

SPECIMEN COLLECTION AND HANDLING

Specimen Storage

Serum and Plasma

Temperature	Maximum Storage
--------------------	------------------------

20 to 25°C-----	> 2 days ⁵
-----------------	-----------------------

2 to 8°C-----	> 7 days ^{5,6}
---------------	-------------------------

-20°C-----	>1 year ⁵
------------	----------------------

Guder et al.¹⁰ suggest storage of frozen specimens at -20°C for no longer than the time interval cited above. However, limitations of laboratory equipment make it necessary in practice for clinical laboratories to establish a range around -20°C for specimen storage. This temperature range may be established from either the freezer manufacturer's specifications or your laboratory standard operating procedure(s) for specimen storage.

NOTE: Stored specimens must be inspected for particulates. If present, mix and centrifuge the specimen to remove particulates prior to testing.

BIBLIOGRAPHY

1. Gotto AM. Lipoprotein metabolism and the etiology of hyperlipidemia. *Hosp Pract* 1988;23(Suppl 1):4-13.
2. Third Report of the National Cholesterol Education Program (NCEP) Expert Panel on Detection, Evaluation, and Treatment of High Blood Cholesterol in Adults (Adult Treatment Panel III)—Final Report. National Institutes of Health. National Heart, Lung, and Blood Institute. NIH Publication No. 02-5215. September 2002; I-1-II-22.
3. Badimon JJ, Badimon L, Fuster V. Regression of atherosclerotic lesions by high density lipoprotein plasma fraction in the cholesterol-fed rabbit. *J Clin Invest* 1990;85(4):1234-41.
4. Castelli WP, Doyle JT, Gordon T, et al. HDL Cholesterol and other lipids in coronary heart disease. The cooperative lipoprotein phenotyping study. *Circulation* 1977;55(5):767-72.
5. Gordon T, Castelli WP, Hjortland MC, et al. High-density lipoprotein as a protective factor against coronary heart disease. *Am J Med* 1977;62(5):707.

6. Williams P, Robinson D, Bailey A. High density lipoprotein and coronary risk factors in normal men. *Lancet* 1979;1(8107):72–5.
7. Kannel WB, Castelli WP, Gordon T. Cholesterol in the prediction of atherosclerotic disease; New perspectives based on the Framingham study. *Ann Intern Med* 1979;90(1):85–91.
8. US Department of Labor, Occupational Safety and Health Administration. 29 CFR Part 1910.1030. Occupational Exposure to Bloodborne Pathogens.
9. Executive summary of the third report of the National Cholesterol Education Program (NCEP) Expert Panel on detection, evaluation, and treatment of high blood cholesterol in adults (Adult Treatment Panel III). *JAMA* 2001;285(19):2486–97.
10. National Cholesterol Education Program. Recommendations on Lipoprotein Measurement, from the Working Group on Lipoprotein Measurement. National Institutes of Health. National Heart, Lung, and Blood Institute. NIH Publication No. 95-3044. September 1995.

APPENDIX-6

Human Chitinase-3-like Protein 1 ELISA Kit

Cat.No E2063Hu

Standard Curve Range: 1-400ng/ml

Sensitivity: 0.61ng/ml

Size: 96 wells / 48 wells

Storage: Store the reagents at 2-8°C. For over 6-month storage refer to the expiration date keep it at -20°C.

Avoid repeated thaw cycles. If individual reagents are opened it is recommended that the kit be used within 1 month. *This product is for research use only, not for use in diagnosis procedures. It's highly recommended to read this instruction entirely before use.

Precision Intra-Assay Precision (Precision within an assay) Three samples of known concentration were tested on one plate to assess intra-assay precision. Inter-Assay Precision (Precision between assays) Three samples of known concentration were tested in separate assays to assess inter-assay precision. $CV(\%) = SD/mean \times 100$

Intra-Assay: CV<8%

Inter-Assay: CV<10%

Intended Use This sandwich kit is for the accurate quantitative detection of Human Chitinase-3-like Protein 1(also known as CHI3L1) in serum, plasma, cell culture supernates, Ascites, tissue homogenates or other biological fluids.

Reagent Provided

Components	Quantity (96T)	Quantity (48T)
Standard Solution (480ng/ml)	0.5ml x1	0.5ml x1
Pre-coated ELISA Plate	12 * 8 well strips x1	12 * 4 well strips x1
Standard Diluent	3ml x1	3ml x1
Streptavidin-HRP	6ml x1	3ml x1
Stop Solution	6ml x1	3ml x1
Substrate Solution A	6ml x1	3ml x1
Substrate Solution B	6ml x1	3ml x1
Wash Buffer Concentrate (25x)	20ml x1	20ml x1
Biotinylated Human CHI3L1 Antibody	1ml x1	1ml x1
User Instruction	1	1
Plate Sealer	2 pics	2 pics
Zipper bag	1 pic	1 pic

Material Required But Not Supplied

- 37°C±0.5°C incubator
- Absorbent paper
- Precision pipettes and disposable pipette tips
- Clean tubes
- Deionized or distilled water
- Microplate reader with 450 ± 10nm wavelength filter.

Precautions

- Prior to use, the kit and sample should be warmed naturally to room temperature 30 minutes.
- This instruction must be strictly followed in the experiment.
- Once the desired number of strips has been removed, immediately reseal the bag to protect the remain from deterioration. Cover all reagents when not in use.
- Make sure pipetting order and rate of addition from well-to-well when pipetting reagents.
- Pipette tips and plate sealer in hand should be clean and disposable to avoid cross-contamination.
- Avoid using the reagents from different batches together.
- Substrate solution B is sensitive to light, don't expose substrate solution B to light for a long time.
- Stop solution contains acid. Please wear eye, hand and skin protection when using this material. Avoid contact of skin or mucous membranes with kit reagent.
- The kit should not be used beyond.

Specimen Collection Serum Allow serum to clot for 10-20 minutes at room temperature. Centrifuge at 2000-3000 RPM for 20 minutes. Collect the supernatant without sediment. **Plasma** Collect plasma using EDTA or heparin as an anticoagulant. After mix 10-20 minutes, centrifuge samples for 20 minutes at 2000-3000 RPM. Collect the supernatant without sediment. **Urine/Ascites/ Cerebrospinal fluid** Collect by sterile tube. Centrifuge at 2000-3000 RPM for 20 minutes. Collect the supernatant without sediment. **Cell culture supernatant** Collect by sterile tubes. When detecting secrete components, centrifuge at 2000-3000 RPM for 20 minutes. Collect the supernatants. When detecting the components in the cell, use PBS (pH 7.2-7.4) to dilute cell suspension, the cell concentration of approximately 1 million/ml. Damage cells through repeated freeze-thaw cycles to let out the inside components. Centrifuge at 2000-3000 RPM for 20 minutes. Collect the supernatant without sediment. **Tissue** Rinse tissues in ice-cold PBS (pH 7.4) to remove excess blood thoroughly and weigh before homogenization. Mince tissues and homogenize them in PBS (tissue weight (g): PBS (mL) volume=1:9) with a glass homogenizer on ice. To further break down the cells, you can sonicate the suspension with an ultrasonic cell disrupter or subject it to freeze-thaw cycles. The homogenates are then centrifuged for 5 minutes at 5000×g to get the supernatant.

APPENDIX-7

Human Kidney injury molecule 1 ELISA Kit

Cat.No E1099Hu

Standard Curve Range: 0.05-10ng/ml

Sensitivity: 0.01ng/ml

Size: 96 wells / 48 wells

Storage: Store the reagents at 2-8°C. For over 6-month storage refer to the expiration date keep it at -20°C. Avoid repeated thaw cycles. If individual reagents are opened it is recommended that the kit be used within 1 month. *This product is for research use only, not for use in diagnosis procedures. It's highly recommended to read this instruction entirely before use.

Precision Intra-Assay Precision (Precision within an assay) Three samples of known concentration were tested on one plate to assess intra-assay precision. Inter-Assay Precision (Precision between assays) Three samples of known concentration were tested in separate assays to assess inter-assay precision. $CV(\%) = SD/mean \times 100$

Intra-Assay: $CV < 8\%$

Inter-Assay: $CV < 10\%$

Intended Use This sandwich kit is for the accurate quantitative detection of kidney injury molecule-1 (also known as KIM-1) in serum, plasma, cell culture supernates, Ascites, tissue homogenates or other biological fluids.

Reagent provided

Components	Quantity (96T)	Quantity (48T)
Standard Solution (12.8ng/ml)	0.5ml x1	0.5ml x1
Pre-coated ELISA Plate	12 * 8 well strips x1	12 * 4 well strips x1
Standard Diluent	3ml x1	3ml x1
Streptavidin-HRP	6ml x1	3ml x1
Stop Solution	6ml x1	3ml x1
Substrate Solution A	6ml x1	3ml x1
Substrate Solution B	6ml x1	3ml x1
Wash Buffer Concentrate (25x)	20ml x1	20ml x1
Biotinylated Human Kim-1 Antibody	1ml x1	1ml x1
User Instruction	1	1
Plate Sealer	2 pics	2 pics
Zipper bag	1 pic	1 pic

Material Required But Not Supplied

- 37°C±0.5°C incubator
- Absorbent paper
- Precision pipettes and disposable pipette tips
- Clean tubes
- Deionized or distilled water
- Microplate reader with 450 ± 10nm wavelength filter.

Precautions

- Prior to use, the kit and sample should be warmed naturally to room temperature 30 minutes.
- This instruction must be strictly followed in the experiment.
- Once the desired number of strips has been removed, immediately reseal the bag to protect the remain from deterioration. Cover all reagents when not in use.
- Make sure pipetting order and rate of addition from well-to-well when pipetting reagents.
- Pipette tips and plate sealer in hand should be clean and disposable to avoid cross-contamination.
- Avoid using the reagents from different batches together.
- Substrate solution B is sensitive to light, don't expose substrate solution B to light for a long time.
- Stop solution contains acid. Please wear eye, hand and skin protection when using this material. Avoid contact of skin or mucous membranes with kit reagent.

- The kit should not be used beyond.

Specimen Collection Serum Allow serum to clot for 10-20 minutes at room temperature. Centrifuge at 2000-3000 RPM for 20 minutes. Collect the supernatant without sediment. **Plasma** Collect plasma using EDTA or heparin as an anticoagulant. After mix 10-20 minutes, centrifuge samples for 20 minutes at 2000-3000 RPM. Collect the supernatant without sediment. **Urine/Ascites/ Cerebrospinal fluid** Collect by sterile tube. Centrifuge at 2000-3000 RPM for 20 minutes. Collect the supernatant without sediment. **Cell culture supernatant** Collect by sterile tubes. When detecting secreted components, centrifuge at 2000-3000 RPM for 20 minutes. Collect the supernatants. When detecting the components in the cell, use PBS (pH 7.2-7.4) to dilute cell suspension, the cell concentration of approximately 1 million/ml. Damage cells through repeated freeze-thaw cycles to let out the inside components. Centrifuge at 2000-3000 RPM for 20 minutes. Collect the supernatant without sediment. **Tissue** Rinse tissues in ice-cold PBS (pH 7.4) to remove excess blood thoroughly and weigh before homogenization. Mince tissues and homogenize them in PBS (tissue weight (g): PBS (mL) volume=1:9) with a glass homogenizer on ice. To further break down the cells, you can sonicate the suspension with an ultrasonic cell disrupter or subject it to freeze-thaw cycles. The homogenates are then centrifuged for 5 minutes at 5000×g to get the supernatant.

Appendix-8

Human neutrophil gelatinase-associated lipocalin ELISA Kit

Cat.No E1719Hu

Standard Curve Range: 5-600ng/ml

Sensitivity: 2.01ng/ml

Size: 96 wells / 48 wells

Storage: Store the reagents at 2-8°C. For over 6-month storage refer to the expiration date keep it at -20°C. Avoid repeated thaw cycles. If individual reagents are opened it is recommended that the kit be used within 1 month. *This product is for research use only, not for use in diagnosis procedures. It's highly recommended to read this instruction entirely before use.

Precision Intra-Assay Precision (Precision within an assay) Three samples of known concentration were tested on one plate to assess intra-assay precision. Inter-Assay Precision (Precision between assays) Three samples of known concentration were tested in separate assays to assess inter-assay precision. $CV(\%) = SD/mean \times 100$

Intra-Assay: CV<8%

Inter-Assay: CV<10%

Intended Use This sandwich kit is for the accurate quantitative detection of Human neutrophil gelatinase-associated lipocalin (also known as NGAL) in serum, plasma, cell culture supernates, Ascites, tissue homogenates or other biological fluids.

Reagent provided

Components	Quantity (96T)	Quantity (48T)
Standard Solution (640ng/ml)	0.5ml x1	0.5ml x1
Pre-coated ELISA Plate	12 * 8 well strips x1	12 * 4 well strips x1
Standard Diluent	3ml x1	3ml x1
Streptavidin-HRP	6ml x1	3ml x1
Stop Solution	6ml x1	3ml x1
Substrate Solution A	6ml x1	3ml x1
Substrate Solution B	6ml x1	3ml x1
Wash Buffer Concentrate (25x)	20ml x1	20ml x1
Biotinylated Human NGAL Antibody	1ml x1	1ml x1
User Instruction	1	1
Plate Sealer	2 pics	2 pics
Zipper bag	1 pic	1 pic

Material Required But Not Supplied

- 37°C±0.5°C incubator
- Absorbent paper
- Precision pipettes and disposable pipette tips
- Clean tubes
- Deionized or distilled water
- Microplate reader with 450 ± 10nm wavelength filter.

Precautions

- Prior to use, the kit and sample should be warmed naturally to room temperature 30 minutes.
- This instruction must be strictly followed in the experiment.
- Once the desired number of strips has been removed, immediately reseal the bag to protect the remain from deterioration. Cover all reagents when not in use.
- Make sure pipetting order and rate of addition from well-to-well when pipetting reagents.
- Pipette tips and plate sealer in hand should be clean and disposable to avoid cross-contamination.
- Avoid using the reagents from different batches together.
- Substrate solution B is sensitive to light, don't expose substrate solution B to light for a long time.
- Stop solution contains acid. Please wear eye, hand and skin protection when using this material. Avoid contact of skin or mucous membranes with kit reagent.

- The kit should not be used beyond.

Specimen Collection Serum Allow serum to clot for 10-20 minutes at room temperature. Centrifuge at 2000-3000 RPM for 20 minutes. Collect the supernatant without sediment. **Plasma** Collect plasma using EDTA or heparin as an anticoagulant. After mix 10-20 minutes, centrifuge samples for 20 minutes at 2000-3000 RPM. Collect the supernatant without sediment. **Urine/Ascites/ Cerebrospinal fluid** Collect by sterile tube. Centrifuge at 2000-3000 RPM for 20 minutes. Collect the supernatant without sediment. **Cell culture supernatant** Collect by sterile tubes. When detecting secreted components, centrifuge at 2000-3000 RPM for 20 minutes. Collect the supernatants. When detecting the components in the cell, use PBS (pH 7.2-7.4) to dilute cell suspension, the cell concentration of approximately 1 million/ml. Damage cells through repeated freeze-thaw cycles to let out the inside components. Centrifuge at 2000-3000 RPM for 20 minutes. Collect the supernatant without sediment. **Tissue** Rinse tissues in ice-cold PBS (pH 7.4) to remove excess blood thoroughly and weigh before homogenization. Mince tissues and homogenize them in PBS (tissue weight (g): PBS (mL) volume=1:9) with a glass homogenizer on ice. To further break down the cells, you can sonicate the suspension with an ultrasonic cell disrupter or subject it to freeze-thaw cycles. The homogenates are then centrifuged for 5 minutes at 5000×g to get the supernatant.

المخلص:

****الخلفية:****

ان مرض الكلى المتعدد الكيسات هو اضطراب يتميز بتطور العديد من الأكياس الكلوية الثنائية. يلعب نمو الأكياس دورًا مهمًا في تقدم مرض الكلى المتعدد الكيسات الوراثي، وقد يؤدي الضغط الذي تمارسه الأكياس المتضخمة على الأنابيب الكلوية المجاورة إلى زيادة تعبير جزيء إصابة الكلى ١.

قد يشير وجود جزيء إصابة الكلى ١ في البول إلى زيادة خطر تقدم مرض الكلى في مرض الكلى المتعدد الكيسات الوراثي. يتم التعبير عن البروتين ١ الشبيه بالكتيناز ٣ بشكل كبير في أنسجة الكلى السليمة ويتم ترشيحه بحرية عن طريق الكبيبة. يتم إفراز البروتين ١ الشبيه بالكتيناز ٣ أيضًا بواسطة البلاعم المنشطة في الكلى عند حدوث إجهاد أو تلف. يفرز الليبوكالين المرتبط بالجيلاتيناز العدلي من الخلايا الظهارية الأنبوبية بعد حدوث تلف و يرتبط مستوى التعبير عن الليبوكالين المرتبط بالجيلاتيناز العدلي بدرجة إصابة الكلى وقد يساعد في التمييز بين المرضى الذين هم في خطر أعلى لتدهور أسرع في وظيفة الكلى.

هناك حاجة لتطوير علامات تنبؤية جديدة، سواء كانت منفردة أو بالاشتراك مع العلامات التقليدية، والتي يمكن أن تتنبأ بمعدل تقدم المرض في مرض الكلى المتعدد الكيسات الوراثي، وبالتالي كان الهدف الرئيسي من هذه الدراسة تحديد ما إذا كانت هناك علاقة بين علامات التلف الأنبوبي والضرر القريب والتهاب في البول مع تقدم مرضى الكلى المتعدد الكيسات أم لا.

****الطرق:****

شملت الدراسة المقطعية خمسة وثمانين مشاركًا تتراوح أعمارهم بين سبع سنوات وأربعة وثمانين عامًا. تم تشخيص جميع المرضى بتقدم مرض الكلى المتعدد الكيسات الوراثي الذي تم التعبير عنه كتغيرات في معدل الترشيح الكبيبي أو حجم الكلى الكلي. أجريت الدراسة في مستشفى الحسن المجتبي التعليمي و مركز الصانغ لأمراض وزرع الكلى في مدينة كربلاء.

في بداية الدراسة، تم قياس العلامات الالتهابية (الليبوكالين المرتبط بالجيلاتيناز العدلي) وعلامات التلف الأنبوبي (جزيء إصابة الكلى ١ والبروتين ١ الشبيه بالكتيناز ٣) في المصل باستخدام اختبار الممتز المناعي المرتبط بالإنزيم، في حين تم تحليل الملف الدهني في المصل باستخدام جهاز من مختبرات أبوت.

تم إجراء تحليلات الفروق في المتوسطات لتقييم العلامات الحيوية مع مرض الكلى المتعدد الكيسات الوراثي والتقدم و تقييم كفاءة القيمة التنبؤية باستخدام منحنى الخصائص التشغيلية للمستقبل.

النتائج:

لوحظ أن متوسط مستوى جزيء إصابة الكلى ١ يزداد تدريجياً عبر مراحل معدل الترشيح الكبيبي، حيث لوحظ أعلى مستوى في المرحلة الرابعة (٤,٣ ± ١,٥) وأدنى مستوى في المرحلة الأولى (١,٧ ± ٠,٥). وهذا يشير إلى ارتباط محتمل بين مستويات جزيء إصابة الكلى ١ الأعلى وتدهور وظيفة الكلى الأكثر شدة (انخفاض معدل الترشيح الكبيبي).

على غرار جزيء إصابة الكلى ١، أظهر الليبوكالين المرتبط بالجيلائيناز العدلي أن أعلى مستوى كان في المرحلة الرابعة (٢,٦ ± ٥,٢)، ولكن هناك انخفاض كبير في المرحلة الثالثة ب (١,٨ ± ٠,٦). بالنسبة للبروتين ١ الشبيه بالكتيناز ٣، أظهرت النتائج أن المستويات تبدو مرتفعة نسبياً عبر جميع مراحل معدل الترشيح الكبيبي (حوالي ١,٧ - ٤,٧). يتمتع كل من جزيء إصابة الكلى ١ والليبوكالين المرتبط بالجيلائيناز العدلي بقيم عالية لمنطقة تحت المنحنى، مما يشير إلى أداء عام جيد في التمييز بين المرضى الذين يعانون من المرحلة الرابعة من مرض الكلى المزمن بين مرض الكلى المتعدد الكيسات الوراثي. يتمتع الليبوكالين المرتبط بالجيلائيناز العدلي بقيمة أعلى لمنطقة تحت المنحنى (٨٠,٥%) مقارنة بجزيء إصابة الكلى ١ (٧٩,١%). يتمتع الليبوكالين المرتبط بالجيلائيناز العدلي بحساسية أعلى (٧١,٤%) من جزيء إصابة الكلى ١ (٥٧,١%).

هذا يعني أن الليبوكالين المرتبط بالجيلائيناز العدلي أكثر احتمالاً للتعرف بشكل صحيح على المرضى الذين يعانون من المرحلة الرابعة من مرض الكلى المزمن في مرض الكلى المتعدد الكيسات الوراثي. بينما يتمتع جزيء إصابة الكلى ١ بخصوصية أعلى بكثير (٩٩%) مقارنة بالليبوكالين المرتبط بالجيلائيناز العدلي (٩١%).

تشير الخصوصية إلى احتمالية التعرف الصحيح على المرضى الذين لا يعانون من المرحلة الرابعة من مرض الكلى المزمن في مرض الكلى المتعدد الكيسات الوراثي.

الاستنتاجات:

قد يكون كل من جزيء إصابة الكلى ١ والليبوكالين المرتبط بالجيلائيناز العدلي أدوات قيمة لمراقبة وظيفة الكلى لدى مرضى مرض الكلى المتعدد الكيسات الوراثي، خاصة مع انخفاض معدل الترشيح الكبيبي.

من خلال تتبع التغيرات في مستويات جزيء إصابة الكلى ١ والليبوكالين المرتبط بالجيلائيناز العدلي، قد يتمكن العاملون في الرعاية الصحية من اكتساب رؤى حول تقدم تلف الكلى في مرض الكلى المتعدد الكيسات الوراثي.

بينما قد يكون للبروتين ١ الشبيه بالكتيناز ٣ بعض الفائدة، فإن ارتباطه الأضعف مع معدل الترشيح الكبيبي في مرض الكلى المتعدد الكيسات الوراثي يشير إلى أنه قد يكون أقل ملاءمة لمراقبة وظيفة الكلى في هذا السياق المحدد.



جمهورية العراق
وزارة التعليم العالي والبحث العلمي
جامعة كربلاء - كلية الطب
فرع الكيمياء السريرية



دور بعض المؤشرات الحيوية في تقييم تلف الأنبوب الكلوي في مرضى مرض الكلى المتعدد
الكيسات السائد

رسالة مقدمة الى

جامعة كربلاء - فرع الكيمياء الحياتية - مجلس كلية الطب

كجزء من متطلبات نيل درجة الماجستير في الكيمياء السريرية

من قبل

ايات خضر علي

بكالوريوس علوم كيمياء / جامعة كربلاء / ٢٠٢٠

بإشراف

الأستاذ المساعد

د. رنا مجيد حميد

دكتوراه كيمياء حياتية

فرع الكيمياء السريرية

كلية الطب / جامعة كربلاء

الأستاذ الدكتور

د. رياض محي الصائغ

أخصائي أمراض وزراعة الكلى

فرع الطب الباطني

كلية الطب / جامعة كربلاء